2009

Hemeproteins Bathed in Ionic Liquids;Examining the Role of Water and Protons in Redox Behavior and Catalytic Function

John Joseph Moran
Cleveland State University

HEMEPROTEINS BATHED IN IONIC LIQUIDS: EXAMINING THE ROLE OF WATER AND PROTONS IN REDOX BEHAVIOR AND CATALYTIC FUNCTION

JOHN J. MORAN

Bachelor of Arts, Chemistry
University of Akron, Akron, Ohio
May, 1991

Master of Business Administration
Keller Graduate School of Management, Chicago, Illinois
June, 2000

Master of Science, Chemistry
Cleveland State University, Cleveland, Ohio
May, 2003

submitted in partial fulfillment of requirements for the degree
DOCTOR OF PHILOSOPHY IN CLINICAL AND BIOANALYTICAL CHEMISTRY
at the
CLEVELAND STATE UNIVERSITY
MAY, 2009

This dissertation has been approved for the Department of Chemistry and the College of Graduate Studies by:

Dissertation Committee Chairperson, Dr. Mekki Bayachou
Department of Chemistry, Cleveland State University

Dissertation Committee Member, Dr. Stanley A. Duraj
Department of Chemistry, Cleveland State University

Dissertation Committee Member, Dr. Valentin Gogonea
Department of Chemistry, Cleveland State University

Dissertation Committee Member, Dr. Yan Xu
Department of Chemistry, Cleveland State University

Dissertation Committee Member, Dr.Ulrich Zurcher
Department of Physics, Cleveland State University

ACKNOWLEDGEMENTS AND DEDICATION

Early in this process, Dr. John Turner advised me to keep a journal of my time here in graduate school, just so I can look back and see what I was thinking and remember those details of the experience that tend to otherwise fade away. Just four days into my graduate school career, we all celebrated Chinese New Year with a luncheon where I first met most of my fellow graduate students from around the world. I was very taken aback with this new cultural interface and wrote, "*This is all so new to me and so much fun. I hope I will always remember the wonder, the awe, and the enthusiasm that filled me during that first week of class…*" I do remember all of the wonder and awe that filled me that week and in the weeks to come, and I hope to carry these cherished memories forever. You, my fellow graduate students, have truly made this a memorable experience. I look forward to many years of continued relationships with all of you.

To those students that worked closest with me in the Bayachou Lab, Ling, Indika, Dhanuja, Pubudu, Reshani, Charbel, Jeremiah, Noufissa, Jean, Melissa, Kerri, Bryan, Nyoka, Bhagya, and Saleem, you all contributed to my success. Thanks, bohoma stuthi, shukran gazilan, vielen dank, merci beaucoup, and xie xie!

Thanks to all of my committee members for taking the time to provide me with valuable insights and for challenging me to push myself harder in order to gain the "level of knowledge commensurate with that of a Ph.D." It is with your guidance and approval that I now go into the world and proudly represent the Cleveland State University Department of Chemistry. I won't let you down.

Thanks to all the faculty and staff in the Department of Chemistry who acted as my advisors and helped me to develop my teaching skills. My future students will thank all of you for making me a better teacher.

Thanks to Dr. Robert Wei who was always supportive of my career goals.

To Dr. Stan Duraj, who always took a personal interest in my progress and gave me the encouragement that I needed to keep pushing this to completion.

To Dr. Alan Riga, a man who has more energy and ideas in one day than I have in a year. You are a model of what I want to become, a teacher, a giver, and a man who can still take time away from it all to enjoy life.

To Dr. Lily Ng. You always take time to listen, providing sound advice and reassurance. Your support for our students and our department is greatly appreciated.

To Dr. Mekki Bayachou. If it was easy, we would all be doctors. You ensured that I didn't get it the cheap way and you made me earn everything I got. I appreciate your hard work and your insistence that nothing less than the best is acceptable. Your high standard of excellence is a blessing to this university. I will take these lessons you taught me and make my school a better place, too.

To my Mom and Dad. May God bless you for everything that you've done for me throughout the years, and for all the sacrifices you made for me and my brother and sisters while we were growing up. I was probably an ungrateful child, but you now have my undying gratitude. You always believed in my abilities, and without your love, encouragement, and support, this would not be possible.

To my son, Mack. I hope you finish college and graduate school long before you're my age, but if one day you find yourself like me, trying to make up for lost time

and lost opportunities, you now have proof that you can reignite your college career, or anything else for that matter, later in life. Work hard, demand excellence from yourself, and always keep improving yourself along the way.

To my wife Lee Ann. None of this happens without you. You are the foundation of this experience. Nobody could possibly succeed in this type of endeavor without a strong, supportive wife by their side. You pushed me to greatness, you believed in me, you shouldered the brunt of the burden to ease my mind, and you tolerated my occasional lapses of attention to the task at hand. You stand beside me and make all of my accomplishments possible, including this, my greatest achievement to date. With you by my side, I can do anything.

Finally, this thesis is dedicated to Dr. Ralph Gardner-Chavis, a man whose skill and knowledge of chemistry gave him the opportunity to work on the most important project of his generation, The Manhattan Project, alongside the greatest scientists of the time. Dr. Gardner still fondly recalls the time he met and shook the hand of Nobel Laureate Enrico Fermi as though it happened just yesterday. Dr. Gardner connects the great chemists of our past to the future scientists of tomorrow, and does so with the grace, charm, humor, and integrity that are hallmarks of his character. He continues to work tirelessly at an age when most others have long since quit, setting an example of the work ethic that makes this country great. We are all richer for the experience, Dr. Gardner. Thank you.

HEMEPROTEINS BATHED IN IONIC LIQUIDS: EXAMINING THE ROLE OF WATER AND PROTONS IN REDOX BEHAVIOR AND CATALYTIC FUNCTION

JOHN J. MORAN

ABSTRACT

We investigate the changing behaviors of myoglobin and nitric oxide synthase (NOS) in the near-absence of bulk water and/or protons by using ionic liquid *butyl methyl imidazolium tetrafluoroborate* as a non-aqueous milieu. Through direct charge transfer and metalloprotein-mediated catalytic reduction of oxygen and nitric oxide, we shed light on diverging aspects on how the two hemeproteins face the scarcity of water and/or protons in bulk. Isotopic effect investigations using D_2O further elucidates kinetic aspects of proton transfer. Finally, in the case of NOS oxygenase, pterin cofactor binding and NOS-mediated catalytic oxidation of L-arginine in ionic liquids interrogates proton and water availability as a modulating factor affecting electrochemically-driven production of nitric oxide. Overall, our results indicate that the catalytic and redox properties of NOS and other heme-proteins change in a unique way as a function of available water. The redox and catalytic behavior of each metalloprotein is rationalized in terms of its inherent structural aspects.

TABLE OF CONTENTS

LIST OF TABLES

LIST OF FIGURES

CHAPTER I

THE ROLE OF WATER IN METALLOPROTEIN FUNCTION

1.1 Introduction and Background

There is a fundamental gap between the electrochemical data that is generated in aqueous electrochemical cells and the true electrochemical characteristics of proteins and enzymes that operate in relatively hydrophobic environments such as lipid bilayers. The role of water in electron transfer cannot easily be investigated in aqueous media. In this project, we take advantage of ionic liquids to provide an essentially anhydrous, electrolytic environment to better understand the role of water in charge transfer and related catalytic activations performed by metalloproteins.

We focus our efforts on two hemeproteins that are used for comparative purposes, myoglobin and nitric oxide synthase (NOS*)*. These two proteins were chosen for this study for myriad reasons, but the short version is that myoglobin and NOS are significantly different in both structure and function, while both can offer insights on the differential redox and catalytic control of the protein around a heme as a redox center. Myoglobin is a relatively simple protein involved in oxygen transport and storage, while

NOS is an enzyme whose function involves key elemental steps where the role of water may prove pivotal. The factors that govern NOS function are also of critical importance with regard to its role in cardiovascular diseases, as will be described later.

Our goal is ultimately to get a better understanding of how the availability of water affects the catalytic function and the electron transfer properties of proteins and enzymes. To get there, we use a stepwise approach that begins with an examination of redox activity. Our experimental design allows us to accurately measure and compare the direct redox electrochemistry of these two proteins, including key indicators of electron transfer thermodynamics and kinetics, in completely anhydrous conditions and as a function of increased water levels. Redox electrochemistry of NOS in the presence of tetrahydrobiopterin (H_4B) is also examined to show if the effect of this cofactor on NOS redox properties is modulated by the hydrogen bonding network.

Next, we electrochemically drive metalloprotein-mediated catalytic reduction of oxygen and nitric oxide in this same environment to quantitatively study the kinetics of key catalytic intermediates while introducing oxygen (or nitric oxide) and water into the system at controlled levels. We replace water with deuterium oxide to monitor resulting changes on the kinetics and thermodynamics of electron transfer and the catalytic function of both proteins. Finally, we examine the function of the NOS enzyme in the presence of substrate L-arginine and cofactor tetrahydrobiopterin and compare enzyme activity in the low-water environment to that in aqueous medium.

We expect the results of this work will show how the availability of protons and/or water affects the redox and catalytic behavior of proteins. Our rationale for this study is that many proteins have a catalytic function in environments where protons and water availability is carefully controlled; measuring redox properties and catalytic efficiency in this fashion will help us gain an understanding of how water in and around the protein's environment helps to regulate its catalytic performance.

The research performed herein is significant because NOS is responsible for the production of nitric oxide (NO), which has broad importance not only as a cardiovascular signaler that helps regulate blood pressure, but also as an important neurotransmitter signaling agent, and as a powerful cytotoxic, mutagenic oxidizing agent. Our non-aqueous approach will be valuable to understanding the role of water/proton supply on the NOS-mediated activation of oxygen and production of NO.

1.2 Structure/Function Considerations of NOS and Mb

1.2.1 The Physiological Importance of NO

Nitric oxide has broad physiological function not only as a cardiovascular signaler that helps to regulate blood pressure[1], but also as a neurotransmitter, and as an agent to effect immunological defense. NO is responsible for regulating and maintaining vascular smooth muscle tone and dysfunctional NO production has been implicated as a

contributing factor in vascular diseases such as hypertension, both coronary and cerebral vasospasm, and platelet aggregation that leads to thrombosis[2, 3]. On the other hand, overproduction of this reactive agent by the immune system also been linked to cytotoxicity.

Nitric oxide has always been with us as a physiological effector, but the discovery of NO as this multi-functional molecule that is so important to so many disparate biological processes was not made until very recently, relatively speaking. It is odd that such an important and ubiquitous molecule escaped detection for so long. Perhaps this is because the first beginnings of the discovery of NO's physiological effects began with a bang, literally, when Ascanio Sobrero detonated a small amount of nitroglycerine (NG) to the amazement of the *Academia delle Scienze di Torino* in 1847[4]. Either by accident or by extremely bold scientific methodology, Sobrero tasted a small drop of his new compound and reported that it produced "a violent headache (that lasted) for several hours". The investigation of nitroglycerine as a physiological effector had begun. Despite its obvious headache-producing effect, it was speculated that nitroglycerine might actually be used to cure those who were already suffering headaches, a like-cures-like approach to curative homeopathic medicine[4].

Across the continent, Frederick Guthrie noticed a cardiovascular effect after inhalation of amyl nitrite (1859), whereupon the heart would begin to race and the face to go flush[5], though nobody initially thought to tie his findings to Sobrero's discoveries

from over a decade earlier. Guthrie's work, however, caught the interest of Thomas Lauder Brunton, who first recorded the use of amyl nitrite to relieve angina[6].

By 1876, William Murrell was using nitroglycerine for the treatment of angina, making a stable compound by blending a small aliquot of NG into chocolate bars as the preferred mode of dosage[7]. Again, the linkage between the two organonitrite compounds and their similar effects on vasodilation escaped notice. The British *Pharmacopoeia* at this time listed nitroglycerine as a remedy for hypertension.

Workers exposed to organic nitrites during the nitroglycerine manufacturing process (c. 1900) reported suffering serious "Monday morning headaches" that would dissipate as the week wore on, supposedly as they grew accustomed to the vasodilatory effects of the NG. The belief is that workers would return to their "normal state" during the course of the weekend away from the factory whereupon the headache would return again Monday morning as a new round of exposure begins[8]. This was coupled with reports of "Sunday heart attacks", a result of overcompensation by the cardiovascular system in otherwise healthy patients who were withdrawing from their regular inhaled dosages of organonitrites received at work from Monday through Friday[8]. Though not a widespread killer, these Sunday heart attacks were a source of some concern and also a source of inspiration when physicians contemplated the strength of these nitrite-containing compounds and their effects on human physiology.

Although the mechanism was not known, the effects of nitroglycerine on the cardiovascular system was well documented by the 1950s[9, 10], making nitroglycerine tablets and transdermal patches *de rigueur* for the treatment of angina and hypertension. It was not as though scientists did not try to understand, but merely that the answer eluded them.

By 1977, Ferid Murad discovered a link between nitroglycerine-released NO and vasodilation[11], which set in motion experiments by Robert Furchgott[12, 13], Louis Ignarro[14, 15] and Salvador Moncada[16, 17]. Through the course of all their individual efforts they eventually solved the puzzle. What causes amyl nitrite and nitroglycerine to have such a profound effect on the cardiovascular system?[4] The answer is NO.

By 1992, NO was heralded as Science magazine's "molecule of the year"[18] due to its multifunctional physiological roles as a vasodilator, neurotransmitter, and in the body's cytotoxic immune response[19]. Yet as recently as 1986, Furchgott had only just identified NO as the endothelium-derived relaxing factor (EDRF) responsible for mediating the action of certain vasodilators in the regulation of blood flow and blood pressure[12, 13, 16]. The combined work earned Furchgott, Ignarro, and Murad a split of the 1998 Nobel Prize in Medicine, a mere 151 years after Sobrero reported his first NO-related headache.

Though the significance of NO's role as a signaling mediator was made clear by this finding, it was not quite clear how NO was produced and by 1989 only minimal

information concerning the mechanisms and controlling factors regarding its synthesis *in vivo* via nitric oxide synthase was available[20-23].

1.2.2 The Structure and Function of NOS in the Production of NO

Through identification of differences in NOS mechanisms in different tissues[17], it was determined that NOS was not a singularity, but it rather has two or more isoforms. Since then, three distinctly different NOS isoforms have been discovered and characterized[24, 25], endothelial (eNOS), neuronal (nNOS), and inducible (iNOS), while even more possible isoforms are being proposed[26]. In the years since NOS enzymes were originally described, there has been substantial progress made to identify their precise structures[27-31], their function[20, 28, 30, 32-34], the mechanisms by which molecules such as NADPH, flavins as electron transfer relays, and the cofactor 5,6,7,8-tetrahydrobiopterin (H_4B) help to produce nitric oxide from the catalytic oxidation of the amino acid L-arginine as a substrate. The reaction takes place on a P450-type heme in a domain called NOS oxygenase (NOSoxy) and uses molecular oxygen as a co-substrate. Figure 1.1 shows a schematic of iNOS in its dimeric form.

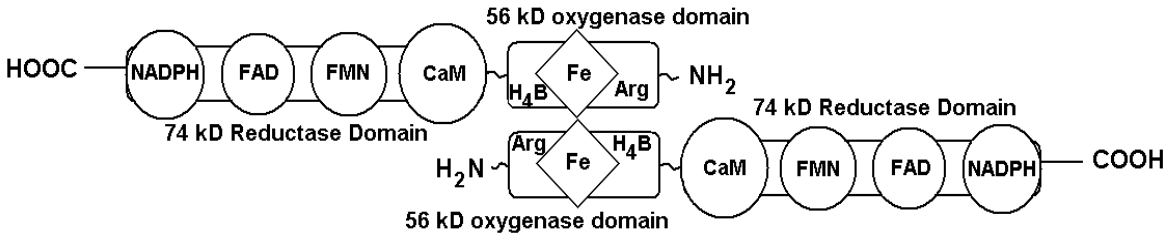

Figure 1.1: Dimeric form of iNOS with iron heme, arginine substrate, and tetrahydrobiopterin bound to the oxygenase domains. In the reductase domains, HOOC = carboxyl end of enzyme, NADPH = Nicotinamide adenine dinucleotide phosphate, FAD = Flavin Adenine Dinucleotide, FMN = Flavin Mononucleotide, and CaM = Calmodulin.

All three NOS isoforms are found in dimeric form with each monomer comprised of two separate domains with distinct functionality, the reductase (flavin) domain and the oxygenase (heme) domain. The two monomeric reductase domains, operating independently even when in dimeric form as shown in the schematic figure 1.2, are responsible for shuttling electrons to the dimeric oxygenase core, much in the same way that cytochrome P450 reductases act to shuttle electrons to other P450 oxygenase enzymes. This is accomplished through a balanced network of NADPH as the initial electron donor and bound flavin co-factors FAD and FMN, with calmodulin acting as a gate to facilitate rapid electron transfer to the oxygenase domains, allowing for the enzyme's catalytic function.

The electron shuttle begins with the oxidation of NADPH, which donates two electrons per NADPH molecule at a potential of approximately -0.320 V. The electron shuttle proceeds energetically downhill as FAD accepts the electrons from NADPH. The reduced FAD transfers electrons to FMN, which eventually reduces the heme iron in the oxygenase domain. The electron transfer from FAD ➔ FMN is markedly affected by enzyme cofactor calmodulin, and catalytic function of NOS would essentially deactivate at this point in the process due to slow electron transfer kinetics.

It is currently believed that calmodulin does not so much thermodynamically assist in the electron transfer to FMN, but that it vastly improves the kinetics of the reaction, acting as a switch to activate catalytic function in NOS isoforms by removing

the reaction's kinetic bottleneck[20]. With calmodulin present and bound to NOS reductase domain, electron transfer from FMN ➔ FAD proceeds rapidly enough to allow the enzyme to perform catalytically [20]. Figure 1.2 shows the electron shuttle within the reductase domain bound cofactor calmodulin-Ca^{+2}.

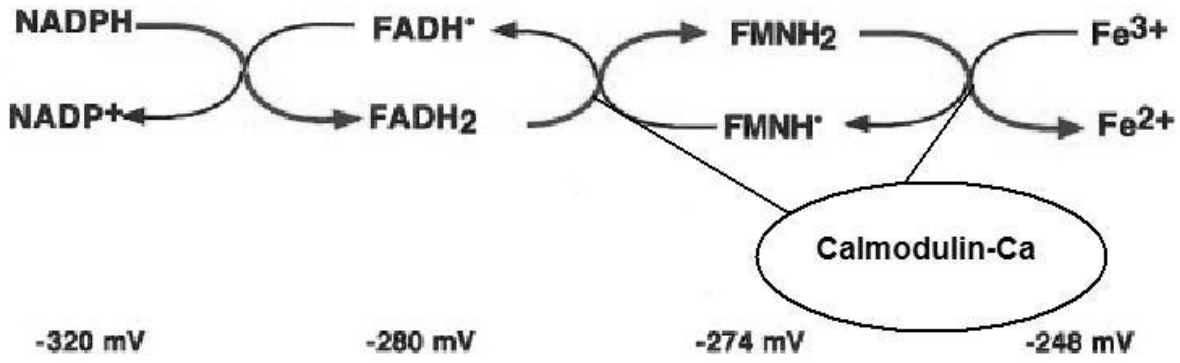

Figure 1.2: The electron transfer shuttle within the NOS reductase domain with approximate electron potentials assigned to each step. Modified from original scheme by W.K. Alderton, *et al,* 2001 Biochemical Society.

As complicated as is the activity in the reductase domain to shuttle electrons to the heme oxygenase domain, so is the activity within the oxygenase domain itself. The reaction that takes place is rather simple to describe as a two-step oxidation of L-arginine to produce citrulline and NO, but there are checks and balances that govern the catalytic process and make its fine balance an interesting study.

Two NOS oxygenase monomers, each having binding sites for heme, substrate L-arginine, and enzyme cofactor tetrahydrobiopterin, are bound together in dimeric form by a zinc tetrathiolate linkage in a head-to-head orientation[20, 35, 36]. The overall catalytic activity of NOS relies upon proper binding of these aforementioned cofactors, substrates, and linkages in order to stabilize each monomer and to ensure proper function in a thermodynamically favorable environment.

The heme iron of each oxygenase monomer is axially coordinated to the enzyme through four Fe-nitrogen linkages to the protoporphyrin IX. In the absence of the bound substrate and cofactor (L-arginine and tetrahydrobiopterin) the heme iron is normally in a six-coordinate low-spin state with one proximal Fe-S ligation to amino acid histidine and one distal ligation, usually to a water molecule found in the heme distal pocket, in addition to the four axial linkages.

This configuration requires more energy to transfer electrons from the reductase domain and renders the molecule catalytically inactive because of the high thermodynamic threshold. This non-catalytically active configuration of the ferric heme

can be converted to the more thermodynamically favorable five-coordinate low-spin state when in the presence of bound tetrahydrobiopterin and L-arginine, which slightly alter the geometry of the heme pocket[37]. This reconfiguration of the heme serves to break the sixth distal ligation[20] and lower the redox potential to within the energetic limits of the electron being transferred from the reducatase domain. Both six- and five-coordinate heme configurations are shown in figure 1.3.

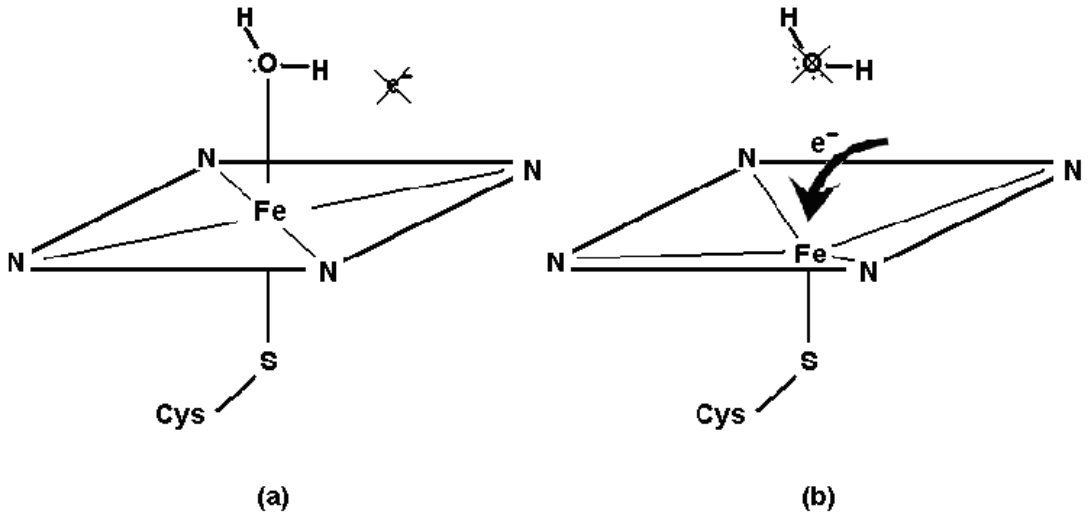

Figure 1.3: The heme pocket in (a) six-coordinate configuration with bound water prohibits electron transfer from the reductase domain, while the (b) five-coordinate breaks the sixth distal water ligation, allowing for electron transfer and subsequent binding of dioxygen to the heme iron.

In the first step of the oxidation of L-arginine to produce NO, addition of an electron (originating from NADPH) to the ferric heme forms the ferrous heme. With the substrate L-arginine bound directly above iron in the heme pocket, oxygen binds to the heme iron to form the ferrous-dioxy intermediate. The addition of two protons and a second electron from NADPH completes the first step with the formation of the intermediate compound N-hydroxy-L-arginine (NOHA).

A third electron is introduced from an additional 1/2 NADPH equivalent, along with another molecule of dioxygen to form the second ferrous-dioxy intermediate, this time an LHA-ferrous-dioxy compound. The addition of two more protons completes the reaction to form the final products citrulline and NO, with the heme iron returned to the ferric state ready to begin a new cycle with fresh substrates. The overall balanced equation is

L-arginine + 1.5 NADPH + 1.5 H^+ + $2O_2$ ➔ L-citrulline + 1.5 $NADP^+$ + $2H_2O$ + $^{\cdot}NO$

Figure 1.4 shows the two-step oxidation process of L-arginine to intermediate N-hydroxy-L-arginine to the final products L-citrulline and NO.

Figure 1.5 shows the overall scheme of the production of NO with electron donor NADPH, shuttling flavins, coenzymes calmodulin and tetrahydrobiopterin, and substrates dioxygen and L-arginine, along with zinc tetrathioltate[36, 38].

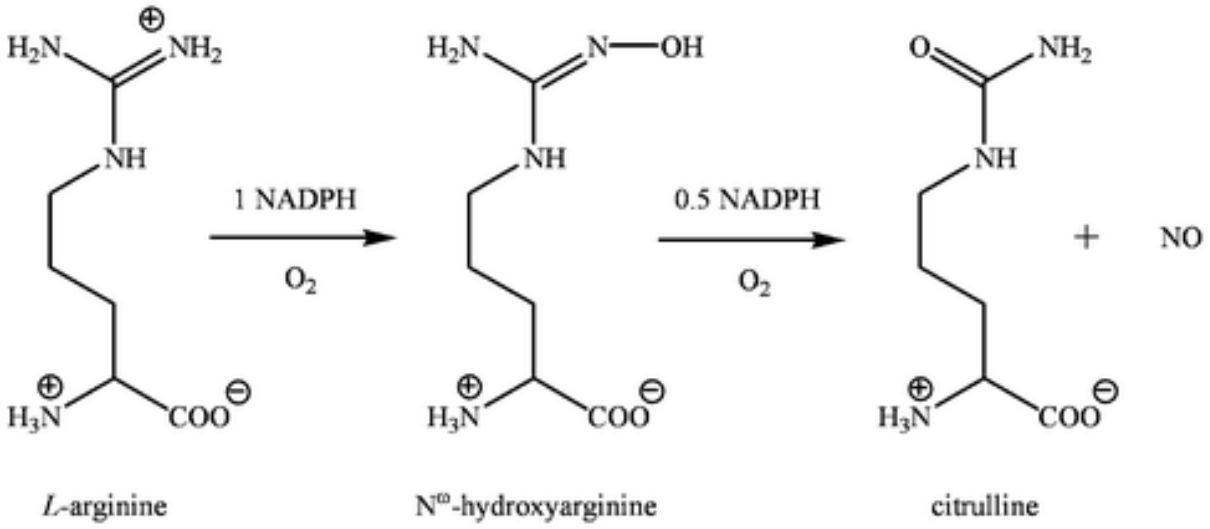

Figure 1.4: The two-step oxidation of L-arginine to produce nitric oxide and byproduct citrulline. This diagram does not stoichiometrically depict all reactants and byproducts. Reprinted from Royal Society of Chemistry.

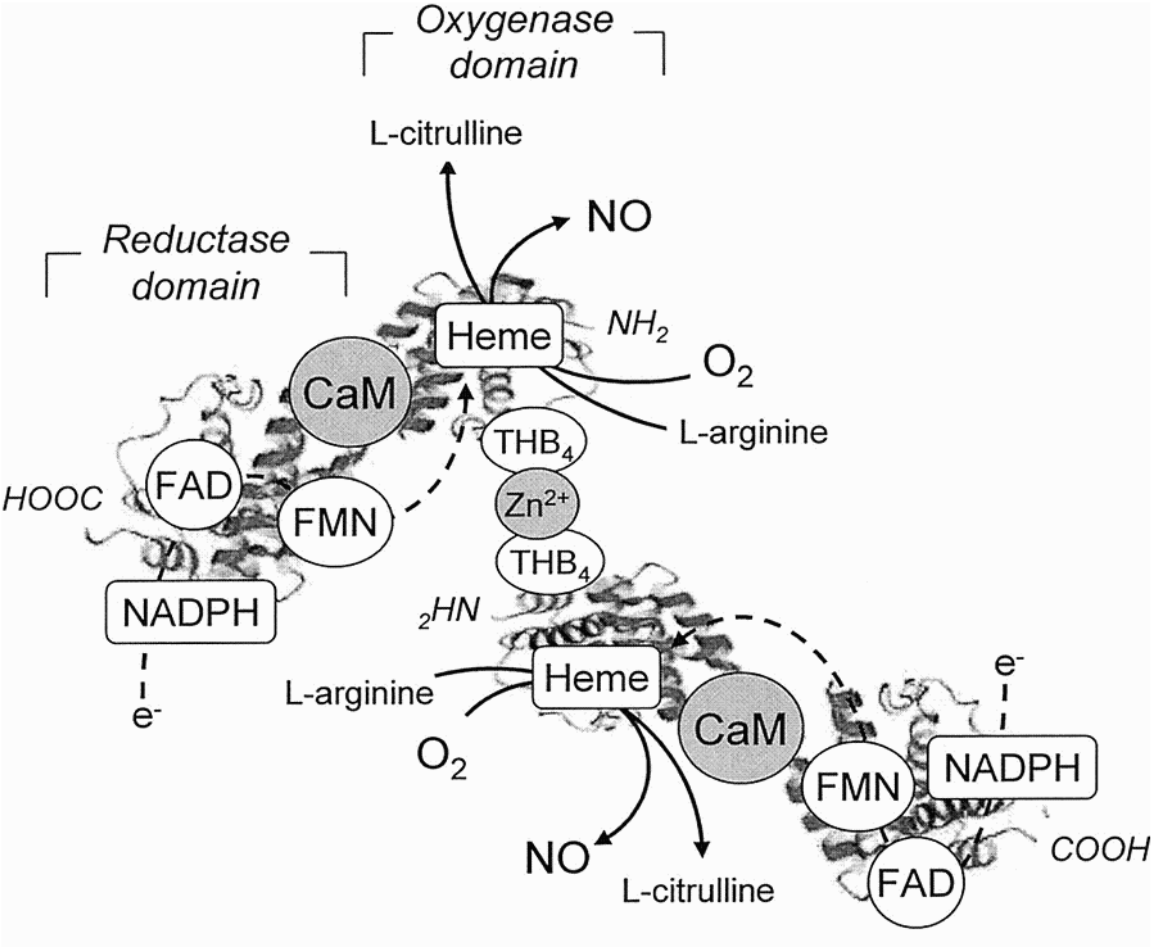

Figure 1.5: The production of NO from NOS in its dimeric form (not stoichiometrically balanced). Adapted from Mungrue (2002) via Fogli (2004).

There are many feedback inhibition mechanisms within the oxygenase domain that check this reaction, such that it can only occur under certain conditions. They are too many to cover within the scope of this text without losing focus, but examples of one that halts the catalytic process is the overproduction of NO[34].

NO, when present in larger quantities, can preferentially bind to the heme iron, alter the electronic configuration of the heme iron to low-spin hexacoordinate, and deactivate production by inhibiting the effective binding of dioxygen. Because of the inhibitory nature of NO, it may be of some interest to investigate catalytic functions in the presence of this small molecule. As such, we will briefly diverge from the main focus of exploring NOS and myoglobin catalytic activation of oxygen and also take a look at characteristics of NO catalysis. This will be addressed in section 3.2.

1.2.3 The Use of iNOS Oxygenase Domain in Electrochemically Driven Electron Transfer and Catalysis

The purpose of this study is not to examine the source and the means of electron transfer within the reductase domain, but to specifically look at quantifiable characteristics of electron transfer and catalytic activation of substrates within the NOS oxygenase domain. We measure the number of electron transfers, the energy associated with each of those electron transfers, and barriers within the oxygenase domain that affect

regular catalytic functioning, especially as it pertains to characteristic changes that may have an association with water/proton levels.

As previously described, the reductase domain of all three NOS isoforms biochemically provide electrons and drive electron transfer to the oxygenase domain to carry out NOS catalysis *in vivo*. In order to better quantify the kinetic and thermodynamic characteristics of electron transfer, we must have a means of producing and tracking electron transfers outside of the reductase domain, such that we can look at the very specific characteristics of electron transfers. Because we are able to electrochemically provide electrons in a controlled manner from an electrode, we can bypass the entire function of the reductase domain, directly drive redox and catalytic reactions within the oxygenase domain, and measure the associated thermodynamic and kinetic data.

We must therefore exclude the electron-donating reductase domain. Thus, it is essential to have a source of NOSoxy isoforms, without the presence of the reductase domains. We do this via protein expression and purification using standard molecular biology procedures as outlined in section 1.2.4. It is believed that the dimeric oxygenase domain will behave similarly to that in the native NOS enzyme due to the structural stabilization that occurs with the formation of the oxygenase dimer and with the additional allosteric effects of cofactor tetrahydrobiopterin and/or L-arginine in experiments where these are also present[39, 40].

1.2.4 Expression of iNOSoxy via Recombinant Plasmid DNA

We use an in-house protein expression and purification of the oxygenase domain via recombinant plasmid DNA based on known methods[41]. The pCWori vector, a generous gift from the laboratory of Dennis Stuehr at the Lerner Research Institute, is inserted into plasmid DNA and transformed into BL21 (DE3) ampicillin-resistant *e. Coli* as detailed by the Stuehr group[42]. This glycerol stock is then inoculated into 2 x 2 ml Luria Broth (LB) medium with 100 μg/ml added ampicillin and allowed to grow overnight at 37^{o}C.

Each aliquot of overnight culture is added to 500 ml autoclaved Terrific Broth (TB) medium and allowed to grow under light aeration and agitation at 37°C for about 3 hours or until 0.1 OD_{600} is reached. Temperature is dropped to 25°C until 0.3 – 0.8 OD_{600} is reached, at which time IPTG and δ-aminolevulinic acid are added to induce iNOSoxy protein production and to provide a heme precursor for the metalloprotein. The induced culture is again left overnight to produce maximum quantities of protein. Cells are harvested by centrifugation at 4,000 rpm at 4°C for 30 minutes, drained of supernate, and resuspended in a minimum of pH 7.6 lysis buffer containing base buffer, lysozyme, phenylmethanesulfonylfluoride (PMSF), Protease Inhibitor III (4-(2-Aminoethyl) benzenesulfonyl fluoride hydrochloride, aprotinin, leupetin, pepstatin A, bestatin, and L-3-trans-Carboxyoxiran-2-carbonyl)-L-leucyl-agmatin), DNase, and $MgCl_2$.

Cells are lysed by sonication at 15-second on, 45-second off intervals for a period of twenty minutes. The sonicated suspension is centrifuged at 12,000 g at 4°C for 30 minutes to precipitate cellular debris. The debris pellet is discarded and the crude supernatant lysate is collected. Protein precipitation is induced by gradual addition of 0.300 g/ml $(NH_4)_2SO_4$ over a period of 30 minutes followed by centrifugation at 10,000 rpm to collect the protein pellet. The pellet is again resuspended in a cocktail of base buffer, PMSF, and Protease Inhibitor III, and filtered through a 0.45 micron PES syringe filter.

A fresh, 4 ml dead volume Ni-NTA Agarose column is prepared for use by charging with 50 mM $NiSO_4$, followed by addition of a binding tris buffer before loading the filtered protein sample onto the column. The column is equilibrated with tris binding buffer and washed with a dilute (40 mM) imidazole wash buffer prior to elution with Ca. 200 mM imidazole elution buffer. One ml aliquots are collected and tested by UV-Vis for the presence of iNOSoxy.

The protein is collected off the column and dialyzed in 500 ml base buffer with 200 μl β-mercaptoethanol, changing dialysis solution twice during the overnight process. The dialyzed protein is further concentrated by centrifugation at 5000 rpm at 4°C using 30,000 MW cut-off Amicon® filters. Aliquots of the protein are flash-frozen with liquid nitrogen and stored at -80°C for future use.

After dialysis and concentration, SDS-PAGE confirms the presence of iNOSoxy and checks for the presence of contaminant proteins by marker comparison of molecular weights. Figure 1.6 shows the results of this test, indicating singular protein bands of the approximate molecular weight of iNOSoxy dimer. Additional conformation of the identity of the protein is provided by the iNOSoxy control lane, which matches perfectly with the two sample lanes.

Total protein concentration of 0.63 mg/ml is determined by Bradford Assay (Figure 1.7). UV-Vis analysis further confirms iNOSoxy concentration using a known extinction coefficient of the Soret band at 421 nm.

Griess Assay is performed to measure enzyme turnover, indirectly measuring NO by measuring NO_2^- concentration in solution. This is performed by introducing iNOSoxy enzyme in the presence of cofactor tetrahydrobiopterin and substrate intermediate L-hydroxyarginine with hydrogen peroxide as an initial electron donor to the process. Based on Griess Assay results, Typical iNOSoxy activity found was 1.67 mmol NO/(mmol iNOSoxy*min).

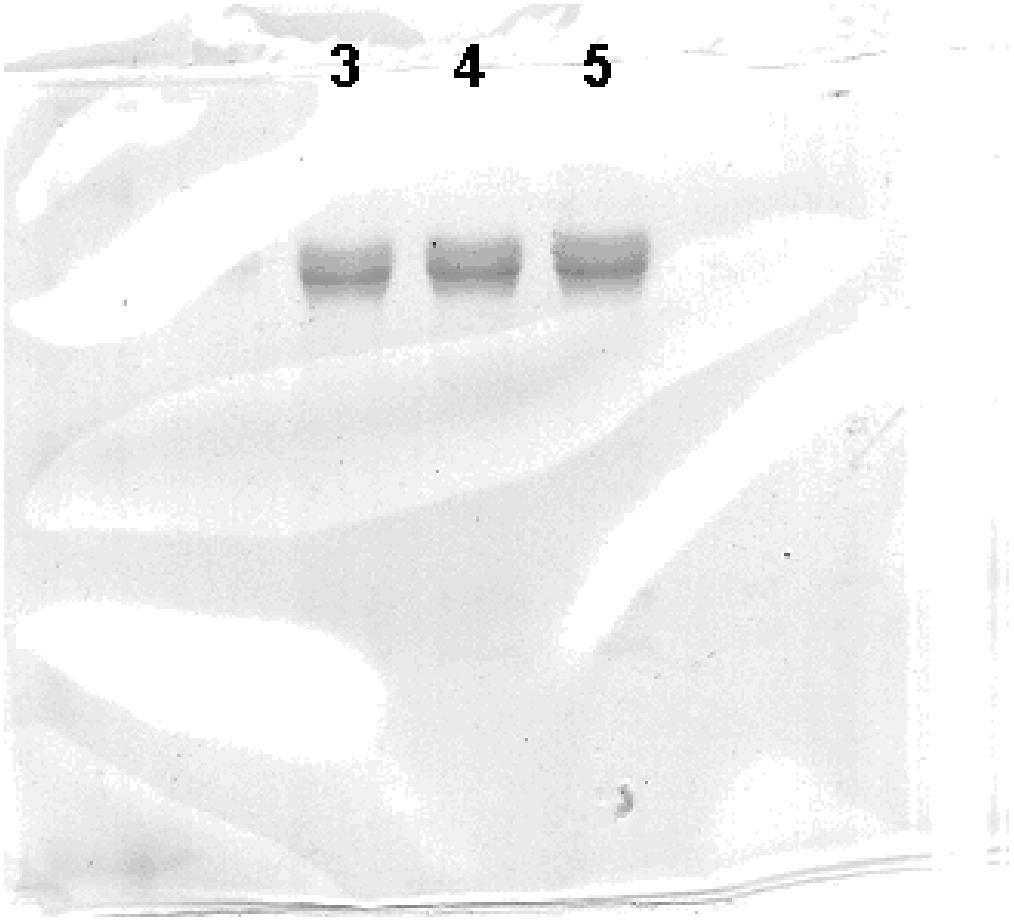

Figure 1.6: SDS-PAGE shows a single distinct band indicative of a pure protein compound with low concentration of contaminants. Expressed and purified iNOSoxy is found in lanes 3 and 4, with control iNOSoxy in lane 5.

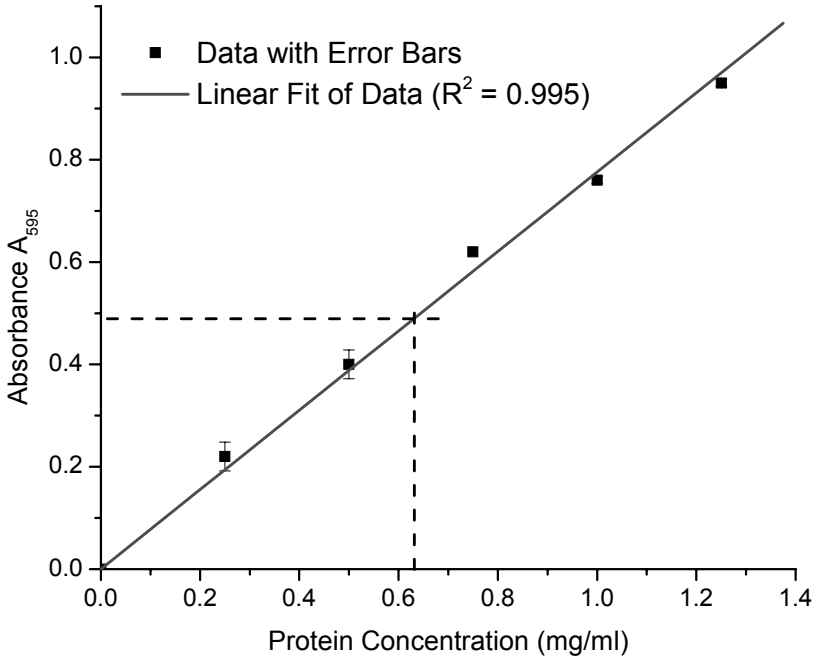

Figure 1.7: Bradford Assay shows that an average absorbance A = 0.49 corresponds to a total protein concentration of 0.63 mg/ml. Assuming the molecular weight of 112 kDa/mol, iNOSoxy concentration would be 0.28 μM.

1.2.5 The Structure and Function of Myoglobin

Myoglobin is a small, single-chain, globular heme-protein (17.8 kDa) that is found primarily in cardiac and skeletal muscle cells of mammals. Myoglobin consists of approximately 153 amino acids that are structurally arranged into eight α-helices that surround a hydrophobic, iron-containing porphyrin prosthetic group. Figure 1.8 shows the structure of myoglobin.

Because of its ability to quasi-reversibly transfer electrons in a very reproducible manner and because of its relatively simple structure, myoglobin is a good candidate for piloting a study that will eventually involve more complex metalloproteins[43] like nitric oxide synthase. *In vivo*, myoglobin is specifically designed to store oxygen and deliver it to the mitochondria as needed; myoglobin does this to the exclusion of all other possible functions, including electron transfer[44, 45]. However, in an oxygen-free environment, myoglobin's heme iron can be chemically or electrochemically reduced and re-oxidized. We can therefore measure the protein's electron transfer characteristics, and monitor how water/protons affect them.

Past experiments conducted in the absence of oxygen have established a baseline of myoglobin's electrochemical behavior in an aqueous environment, and have demonstrated quasi-reversible electron transfer to myoglobin both in solution and in thin films[46-49]. Several other studies have looked at myoglobin and other proteins in non-aqueous media[50-53], but these studies are complicated by changes that occur in the

protein's tertiary structures [52-55] in these organic solvents. Myoglobin has also been used to study the catalytic reduction of small molecules, which will be important to establishing baseline data relevant to that goal.

Figure 1.8: The structure of myoglobin showing α-helices and the heme center.

1.3 The Role of Water in Electron Transfer and Catalysis

Though water is essential to the biological function and structure of proteins[56], water's role in the process of electron transfer and catalytic functions is complex and not always very well understood. Water has been found to be involved in tunneling pathways in electron-transfer proteins and, in theoretical models, has been shown to accelerate electron transfer kinetics[57]. However, the quantity of available water and its proximity to the reaction site, in our case the heme pocket, determines the extent to which water plays a part in electron transfer tunneling. Other studies suggest that the hydrogen bonding network of water in proximity to the active electron transfer site raises the reorganization energy, and hence electron transfer activation energy needed for redox reactions and catalysis[45]. Thus, the dichotomous role that water plays in electron transfer to proteins makes it difficult to predict the exact effect that reduced water in the protein environment will have on catalysis and electron transfer kinetics and thermodynamics.

The role of water as a discrete entity in the heme vicinity and as a cooperative network on direct electron transfer to NOS oxygenase and other P450-type enzymes and proteins is also not clear. Not much information is currently available on the electron transfer characteristics of NOSoxy in hydrophobic environments, nor is much information available to describe the catalytic activation of molecular oxygen and/or full NOS turnover in a medium with limited supply of water or protons. In order to make progress toward understanding these aspects of NOS reaction, development of an

experimental system that can reproducibly drive direct electron transfer to NOS and monitor oxygen activation as well as measure NOS full catalysis in a non-aqueous environment is needed. It is also important that this system does not decrease protein functionality due to loss of structure[58].

Structural and hydrophobic differences may cause different proteins to respond differently to changes in water levels in their immediate environment. It is of particular interest to see how the electron transfer properties of proteins change in these proposed low-water conditions. Specifically, we wish to look for changes in electron transfer kinetics and activation energy to metalloproteins in extremely low-water conditions and as a function of increased water.

1.3.1 The Role of Protons in Catalytic Reduction of Oxygen

In previous work, it has been shown that two-electron, P450-catalyzed reduction of O_2 to H_2O_2 requires a source of protons for catalytic turnover[59], and that the availability of protons has an influence on the rate of proton transfer, and thus on the overall rate of catalysis. A lower concentration of protons also has, as noted in the previously cited research[60], a deleterious effect on electron transfer overpotential and thermodynamic characteristics of the catalytic reduction of oxygen. In the specific case of the catalytic reduction of oxygen, the absence of water must be examined for two very separate effects: how it affects the kinetics and thermodynamics of electron transfer due

to changes in tunneling and hydrogen bonding, and how it affects elementary steps of catalysis requiring proton transfers to proceed. In the specific case of NOS, measuring electron transfer to the NOS active site allows us to monitor each step of NO synthesis and to study the possible modulation of heme redox activity and its potential effect on NOS catalysis. Driving electrochemical reactions in a low-water/low-proton environment will also allow us to study how the presence of water, as a discrete molecule in the distal pocket and as a global network around the protein, affects NOS redox behavior, as well as early steps of oxygen activation in the catalytic NO biosynthesis.

1.4 Previous Work Involving Proton/Electron Transfer to Mb and NOS

Direct redox behavior of myoglobin and NOS enzymes can be measured using protein-*didodecyldimethyl ammonium bromide* (DDAB) thin films[61]. Redox properties of iNOSoxy in thin films have recently been characterized in aqueous solution. Some kinetic and thermodynamic aspects of oxygen activation as well as timing of proton transfers are key in the function of P450-NOS and the catalytic oxidation of L-arginine to produce NO; these are not fully understood, particularly in aqueous environment where proton supply cannot easily be controlled. In prior work by our group, square-wave voltammetry was used to measure the redox electrochemical properties of nNOSoxy/DDAB films on pyrolytic graphite electrode in pH 7 phosphate buffer[62]. Two reversible redox couples are observed that correspond to Fe^{III}/Fe^{II} and the Fe^{II}/Fe^{I} redox couples of nNOSoxy. Our group was able to take advantage of the nNOSoxy/lipid

microenvironment to enhance the enzyme electron transfer, making it possible to characterize electron transfer characteristics of NOS. The work further demonstrated that electron transfer to NOS has a pH dependence that indicates proton-coupled electron transfer, which is of particular significance to our current study, as we are directly examining the effects of low concentrations of protons on the thermodynamics and kinetics of electron transfer. Our group found a pH dependence in the formal reduction potential (E^0) of the Fe^{III}/Fe^{II} couple, and that E^0 has a linear relationship from pH 5 to 9 with a slope very close to the theoretical value of -58 mV/pH for reversible proton-coupled electron transfer, indicating that a single protonation occurs for every electron that is transferred to nNOSoxy.

As we aim to determine the role of water/protons in electron transfer to NOS, this key point leads us to the conclusion that kinetic and thermodynamic aspects of electron transfer are very closely related to the timing and availability of proton transfers. Thus, studying electron transfers with carefully modulated water and proton levels can provide valuable information regarding the function of NOS and the catalytic oxidation of L-arginine to produce NO. These proton levels will be controlled in a non-aqueous, ionic liquid environment.

1.5 The Use of Non-Aqueous Systems to Track the Role of Water

Aqueous electrochemical systems have been developed to study the redox and catalytic properties of NOS, myoglobin, and other proteins and enzymes[62] but they may not provide accurate data concerning enzymes that operate in relatively hydrophobic environments such as lipid bilayers, and may not put the role of water in electron transfer and catalysis under the spotlight. As a result, little information is currently available on the electron transfer characteristics of NOS in hydrophobic environments, nor is much information available to describe the catalytic activation of oxygen and/or full NOS turnover in a medium with limited supply of water or protons.

Studies that attempt to mimic the *in vivo* environment of a bilayer and/or to investigate the effect of water[50-54] have been complicated by the fact that the protein's structure-function is not always conserved. Past studies indicate that the redox and catalytic properties of metalloproteins can change in some non-aqueous, non-polar organic solvents[62], even though many of these organic solvents do not directly cause denaturation or significant changes in conformation of the protein structure[55, 62-65]. As the protein structure does not change significantly, the absence of water in electron transfer pathways and the reduction of hydrogen bonds around the protein molecule and in the immediate location of the heme pocket must be examined as a possible cause for the changes in electrochemical properties and protein function[45, 66]. A major drawback to this type of non-aqueous investigation is that further interrogation using low-

level additions of water in non-polar solvents is prohibited because of obvious water-solubility issues.

Using polar organic solvents to overcome the problem of water modulation creates additional problems, as these tend to cause allosteric changes and denaturation of protein structure[52-54], masking the role of water as it pertains to any observed changes in enzyme function. Thus the use of various organic solvents in an attempt to mimic these hydrophobic environments faces the drawback of inaccurate determinations of actual electron transfer characteristics that may govern true membrane-supported, redox-driven enzymatic processes.

1.6 Background on Ionic Liquids

In order to offer closer measurements of redox properties governing the function of NOS and other hemeproteins, it is essential to develop a system that provides tight control of water/proton supply, and yet does not decrease protein functionality due to loss of structure as is the case with many organic non-aqueous models. Ionic liquids are proposed as the electrolytic medium because they possess many characteristics that could allow for the study of how electrochemical processes occur in nearly anhydrous environments. Specifically, the ionic liquid *butyl methyl imidazolium tetrafluoroborate* (BMIM BF_4) has many properties that lend itself to this type of electrochemical investigation.

Ionic liquids are non-aqueous electrolytes that are non-volatile, making them of particular interest for future research in "Green" environmentally-friendly electrochemistry. Most ionic liquids have a broad electrochemical window, further suiting them to electrochemical applications. There are many different cationic/anionic combinations which gives broad possibilities when choosing which ionic liquid to use in a particular electrochemical experiment. Though ionic liquids have been studied extensively for the past two decades, their use in bioanalytical applications is still somewhat limited. Solubility of enzyme cofactors and substrates such as tetrahydrobiopterin and L-arginine for NOS may present a barrier to study their effect in insoluble *butyl methyl imidazolium tetrafluoroborate*. This limitation makes it difficult to drive NO catalysis in the same fashion as was done in previous studies[67], and the supply of substrate L-arginine in particular must be controlled in some other manner that will be discussed *vide infra*.

Ionic liquid butyl methyl imidazolium tetrafluoroborate (BMIM BF_4, Figure 1.9) was chosen as the electrolytic medium in the current study. It is a nearly anhydrous solvent that, unlike most organic solvents, is chemically close to and compatible with the "ionic-melts" in cell walls and cell compartments, and thus unlikely to denature globular proteins or affect their tertiary and secondary structure[68-70]. BMIM BF_4 is also water-miscible[71] so that the percentage of water present may be modulated from near zero levels (<0.01%) to greater than 50%, if desired. Water levels in the BMIM BF_4 are 0.40 – 0.50% as received, but the use of 3Å molecular sieves can bring the water level below 0.01%, as measured by thermogravimetric analysis.

Not all ionic liquids are capable of this type of water modulation, as some ionic liquids appear to be quite hydrophobic. An example of a common hydrophobic ionic liquid is the *butyl methyl imidazolium hexafluorophosphate* (BMIM PF_6). Though different only by the type of anion, this ionic liquid has hydrophobic properties because the hexavalent structure of PF_6^- distributes charge better than the BF_4^- anion, making it less likely to engage in hydrogen bonding[72]. BMIM PF_6 is a suitable electrolytic solvent for strictly hydrophobic studies, but not for our particular study where modulating the amount of available water is key to the project.

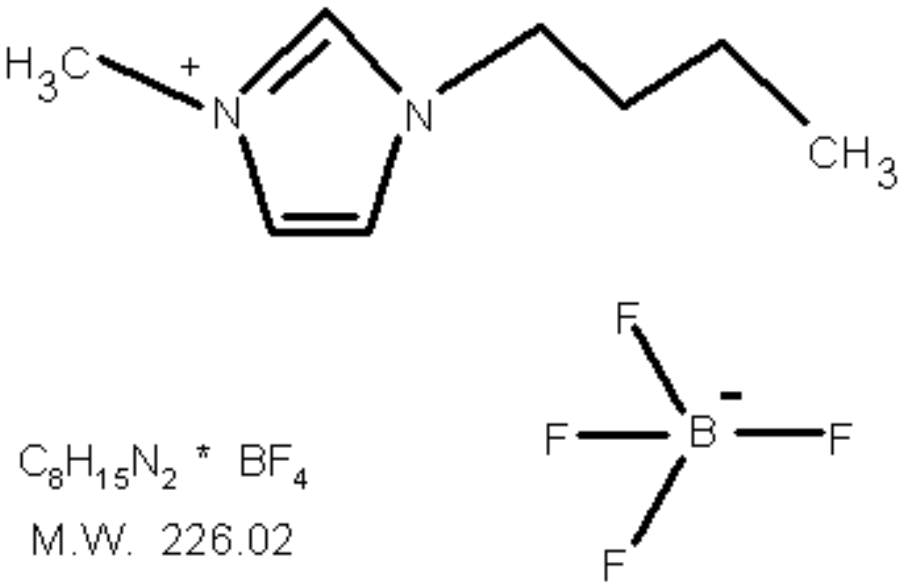

Figure 1.9: The structure of 1-butyl-3-methyl-3H-imidazol-1-ium tetrafluoroborate (BMIM BF_4).

Catalytic processes in ionic liquids have been previously reported. Ionic liquids have been used as catalysts and co-catalysts in a number of different processes[69, 73] and also as solvents of choice for certain catalytic reactions, though none specifically involving the catalytic reduction of oxygen by biomolecules. Our past studies involving myoglobin in BMIM BF_4 suggest that water-protein interactions may affect electron transfer to proteins; myoglobin in BMIM BF_4 had lower electron transfer activation energy and faster electron transfer rates as compared to aqueous buffers. We were also able to drive the catalytic reduction of oxygen in myoglobin, showing that BMIM BF_4 is a suitable electrolytic medium to use in our study of NOS function in hydrophobic environments.

Ionic liquid BMIM BF_4 can be either purchased or synthesized by a method modified from a previously published procedure[74].

- Stir 80 ml 1-methylimidazole and102 ml 1-chlorobutane at 65-75*C for 72 hours
- Add 100 ml water to reduce viscosity
- Add 158 ml aqueous tetrafluoroboric acid (50% w/w) dropwise to convert to $NaBF_4$
- Stir overnight, then extract ionic liquid with two 150 ml portions of dichloromethane
- Wash with water to pH 6, rotary evaporate to remove water and dichloromethane
- Makes about 200 g at 90% Yield, enough to run approximately 65 trials

In our batch of ionic liquid prepared in-house, water is reported at 0.40% by thermogravimetric analysis. Water is then removed from the ionic liquid by the use of 3Å molecular sieves to a level of 0.01%, which is consistent with the levels used in this study. IR analysis confirms the identity of the product as compared to a sample purchased from a commercial source, as seen in figure 1.10.

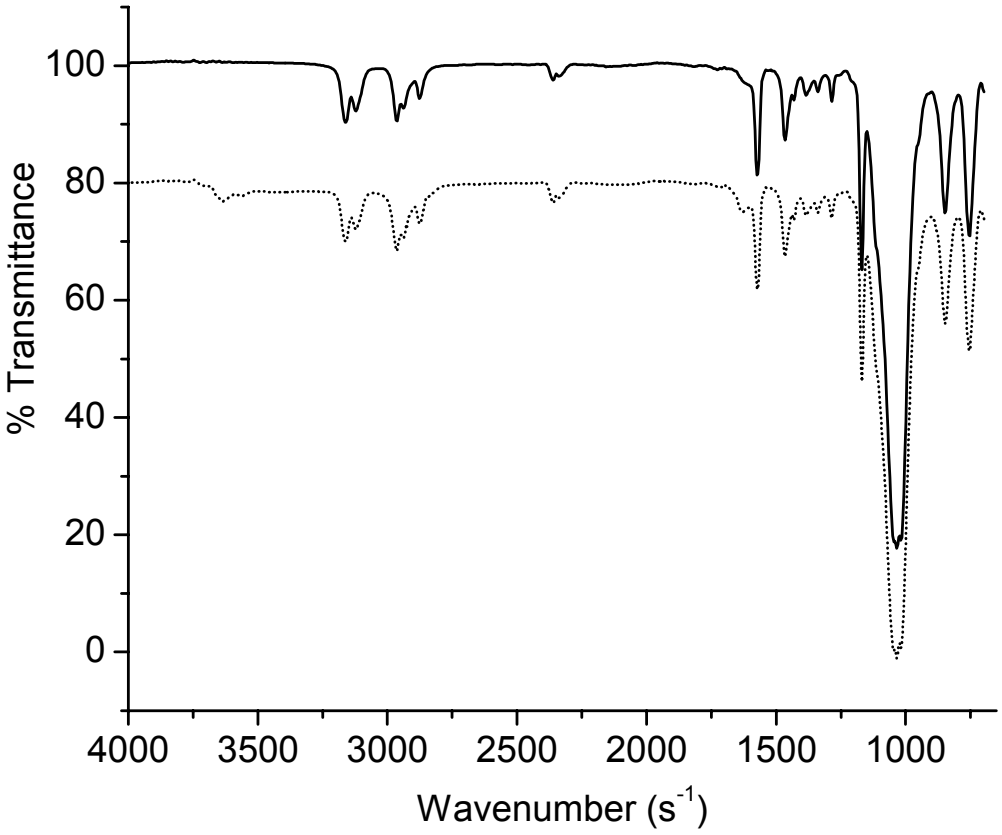

Figure 1.10: IR spectrum for(···) ionic liquid $BMIM_4$ synthesized in our laboratory vs. (—)spectrum for $BMIM_4$ purchased from Sigma-Aldrich.

1.7 Ionic Liquids in the Study of Protein Stability and Function

Many metalloproteins have been found to be stable in ionic liquids[68, 70, 75, 76] and are able to retain their basic functionality. It has been reported thatenzymes have tremendous stability and retain their activity better in ionic liquids than in water or other solvents[75]. It was also reported that biocatalytic reactions in ionic liquids demonstrate greater enantioselectivity, enzyme stability and faster rates as compared to aqueous systems[70, 75, 77]. The many different cationic/anionic combinations of ionic liquids also provide different physical and chemical characteristics depending upon the end use[78, 79].

Spectroscopic analysis confirms that the protein in films used in the current study maintains structural integrity in the ionic liquid. Ionic liquids such as BMIM BF_4 are also water-miscible so that the level of water or D_2O may be modulated from near zero levels to greater than 50%, if desired.

1.8 Electrochemical Techniques Used to Characterize Protein Function

Primarily, we use two techniques to measure the electrochemical characteristics of the hemeprotein used in our study. Cyclic voltammetry is used when both reduction and oxidation potentials are key to the analysis, while square wave voltammetry is used to more accurately measure formal reduction potential when it is essential to have a clear signal with less interference from background charging current.

1.8.1 Cyclic Voltammetry

Cyclic voltammetry (CV) is used extensively in the course of this study to make electrochemical measurements to characterize the charge transfer and catalytic functions of both myoglobin and NOS. In cyclic voltammetry, the electrode potential is ramped linearly as a function of time. When the electrode reaches a given potential, predetermined by each experimental trial, the potential ramp is reversed until the original starting potential is reached. This cyclic ramping can happen once or multiple times during a single experiment according to the needs of that particular experiment. Typical parameters that can be changed in CV to produce desired results are:

- Starting Potential
- Ending Potential
- Scan Rate
- Number of segments (two segments to complete a cycle)

Figure 1.11 shows potential vs. time for a typical experiment within our current study, where the starting potential is 0.2 volts, the ending potential is -0.6 volts, the scan rate is 0.200 V/sec, and the number of segments is four (two complete cycles).

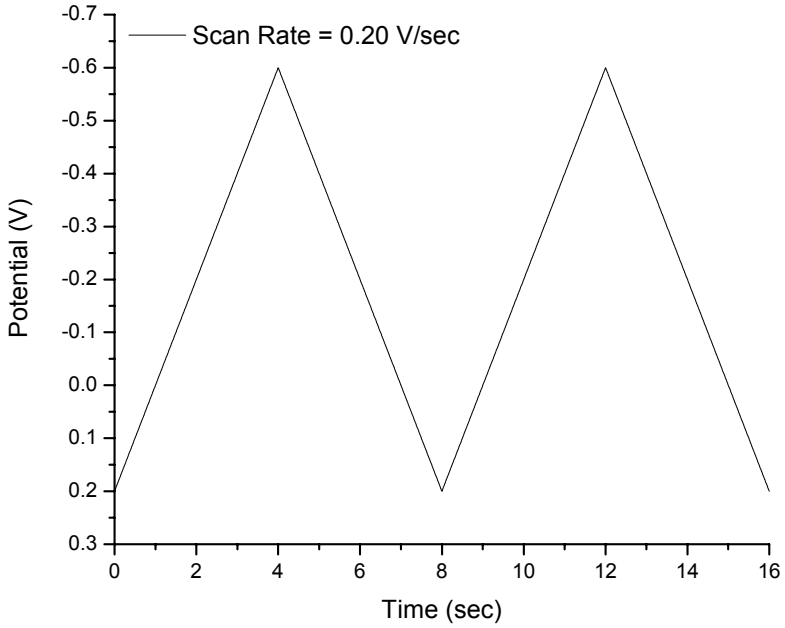

Figure 1.11: Potential vs. time for a typical cyclic voltammetry experiment within our current study, where the starting potential is 0.2 volts, the ending potential is -0.6 volts, the scan rate is 0.200 V/sec, and the number of segments is four (two complete cycles).

The current at the working electrode is plotted versus potential to produce a cyclic voltammogram. When the potential is ramped from high to low, as is typical in our study, the forward scan produces a current peak for the reduction of analytes through the range of the potential scanned. The current reaches a maximum and diminishes as the analyte concentration is depleted close to the electrode surface.

In the case of reversible redox couples, when the applied potential is ramped in the reverse direction (from low to high potential), it will reach the oxidation potential of the reduced analyte, producing an oxidation current that is opposite of that produced in the forward scan. Figure 1.12 shows a typical cyclic voltammogram of a quasi-reversible analyte, where key characteristics of electron transfer can be measured. ($E_R - E_O$) is used to determine the ΔE_P, which gives indications as to the reversibility of the redox couple and the electron transfer kinetics. $(E_R - E_O)/2 = E^0$, the formal reduction potential, can also provide information about the thermodynamics involved in the redox reaction.

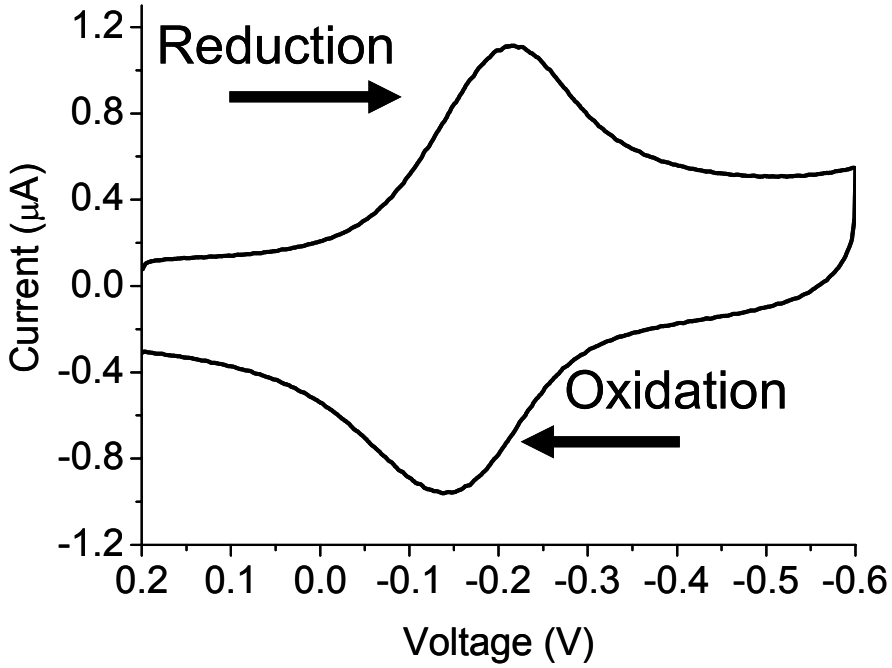

Figure 1.12: A typical one-cycle cyclic voltammogram where applied voltage induces reductions and oxidations. The resulting current from electron transfer is plotted vs. applied voltage.

1.8.2 Square Wave Voltammetry

Square Wave Voltammetry (SWV) is similar to a single segment of a CV scan, in that both systems ramp voltage linearly as a function of time, except SWV does not ramp smoothly like CV. In SWV, the potential ramp is accompanied by a superimposed square-waveform that changes the potential in a "two-steps-forward, one-step-back" fashion. The current is measured at the end of each half-cycle, so that capacitive charging current is minimized, increasing the signal-to-noise ratio and the sensitivity of the method. Because the current is sampled twice during each square wave cycle, the net current can be read as the forward current minus the reverse current. This results in some attributes typical of a CV to be lost, such as being able to monitor kinetics and reversibility of the redox couple, while other aspects of the data analysis are enhanced, such as the signal peak height and the true formal reduction potential of the species. Figure 1.13 shows the square-waveform as a function of time. Figure 1.14 shows a typical square-wave voltammogram.

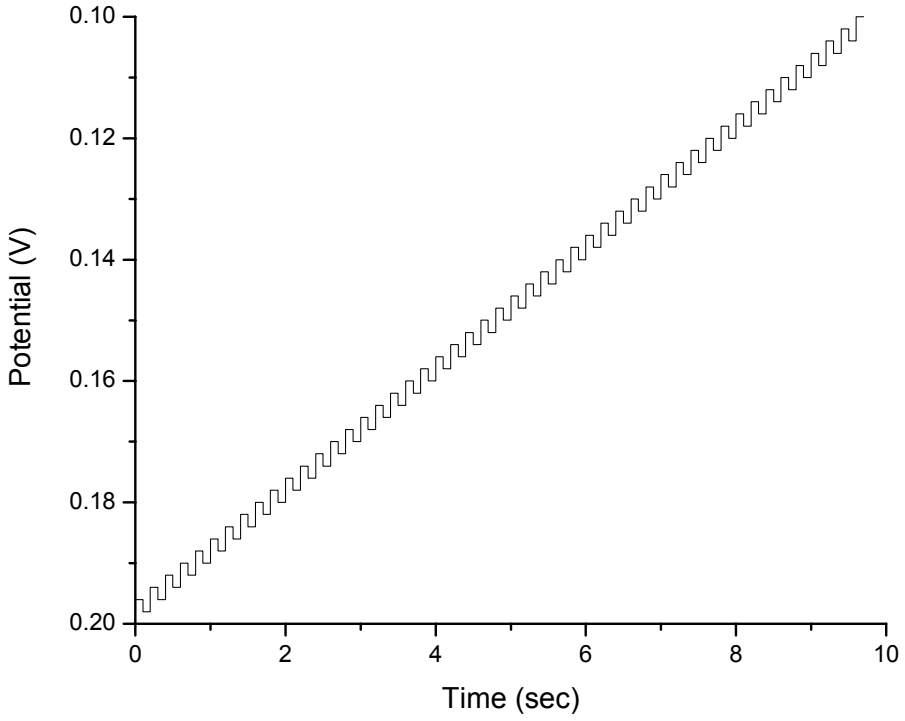

Figure 1.13: In Square Wave Voltammetry, potential ramp is accompanied by a superimposed square-waveform. This figure represents only a portion of the usual range of potential swept during an average experiment in this study.

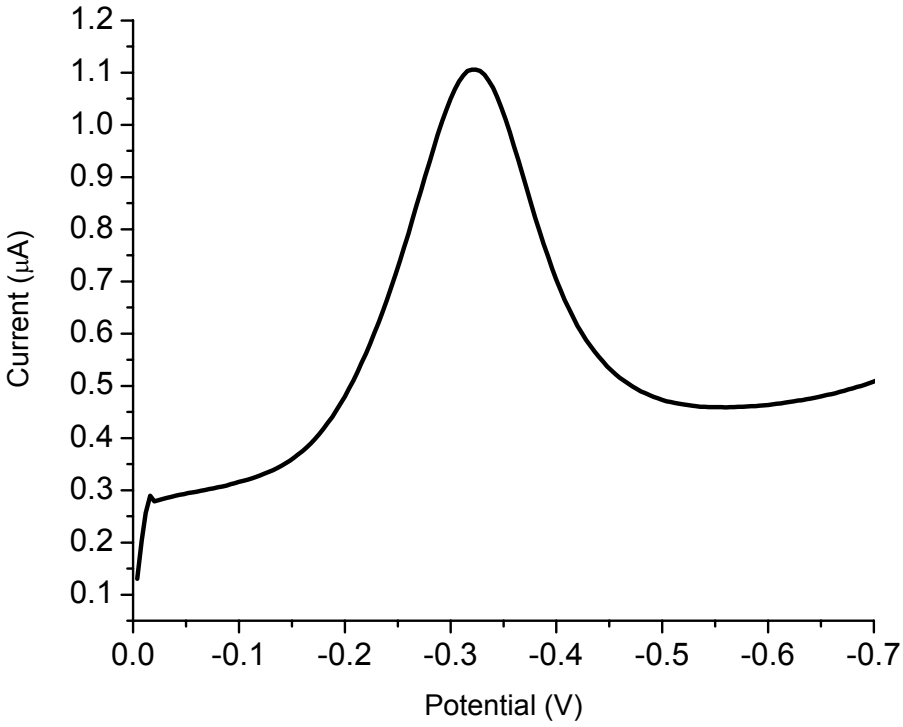

Figure 1.14: A typical Square Wave Voltammogram as seen in this study.

1.9 The Use of Protein Thin-Films to Characterize Protein Function

Our approach is to use Protein film voltammetry to measure key characteristics of electron transfer to protein/lipid thin films. Protein film voltammetry is a standard method for recording redox of molecules of interest. This technique is used in our labs to study direct electron transfer and catalytic properties of large proteins and enzymes such as myoglobin and iNOSoxy.

The premise of protein film voltammetry is to immobilize the electroactive protein molecule under investigation on the working electrode surface, such that the redox active site can participate in rapid interfacial charge transfer. With the protein immobilized in this fashion, it is possible to interrogate redox-active metalloproteins such as myoglobin and NOS because diffusion to and from the electrode is minimized [80, 81].

Protein-lipid bilayer films use small quantities of protein. These films have long been used to examine the redox and catalytic behavior of a wide variety of metalloproteins[47-49, 82, 83]. We measure the formal reduction potential and current response of Fe^{III}/Fe^{II} redox couples in myoglobin/DDAB surfactant films on pyrolytic graphite in ionic liquid BMIM BF_4. The results are compared to Mb/DDAB in aqueous buffer to note any differences in electron transfer activation energy and other key indicators mentioned earlier. We measure and compare ΔE_p of Mb/DDAB as a function

of scan rate in ionic liquid and in aqueous buffer to compare the kinetics of electron transfer to myoglobin in each system.

1.10 References

1. Butler, A.R. (1990). Nitric oxide - its role in the control of blood pressure. Chemistry in Britain *26*, 419-421.
2. Marín, J., and Sánchez-Ferrer, C.F. (1990). Role of endothelium-formed nitric oxide on vascular responses. General Pharmacology: The Vascular System *21*, 575-587.
3. Luescher, T.F. (1991). Endothelium-derived nitric oxide: the endogenous nitrovasodilator in the human cardiovascular system. European Heart Journal *12(Suppl. E)*, 2-11.
4. Marsh, N., and Marsh, A. (2000). A Short History of Nitroglycerine and Nitric Oxide in Pharmacology and Physiology. Clinical & Experimental Pharmacology & Physiology *27*, 313-319.
5. Guthrie, F. (1859). Contributions to the knowledge of the amyl group, I, Nitryl of amyl and its derivitives. J. CHEM. SOC. *11*, 245-252.
6. Brunton, T.L. (1867). On the use of nitrite of amyl in angina pectoris. Lancet *ii*, 97-98.
7. Murrell, W. (1879). Nitro-glycerine as a remedy for angina pectoris. Lancet *i*, 80-81.

8. Scwartz, A.M. (1946). The cause, relief, and prevention of headaches arising from contact with dynamite. New England Journal of Medicine *235*, 541-544.

9. Raab, W., and Lepeschkin, E. (1950). Antiadrenergic effects of nitroglycerin on the heart Circulation *1*, 733-740.

10. Eldridge, F.L., Hultgren, H.N., Stewart, P., and Proctor, D. (1955). Effect of nitroglycerin on the cardiovascular system Stanford Medical Bulletin *13*, 273-283.

11. Katsuki, S., Arnold, W., Mittal, C., and Murad, F. (1977). Stimulation of guanylate cyclase by sodium nitroprusside, nitroglycerin and nitric oxide in various tissue preparations and comparison to the effects of sodium azide and hydroxylamine. Journal of cyclic nucleotide research *3*, 23-35.

12. Martin, W., Furchgott, R.F., Villani, G.M., and Jothianandan, D. (1986). Phosphodiesterase inhibitors induce endothelium-dependent relaxation of rat and rabbit aorta by potentiating the effects of spontaneously released endothelium-derived relaxing factor. Journal of pharmacology and experimental therapeutics *237*, 539-547.

13. Martin, W., Furchgott, R.F., Villani, G.M., and Jothianandan, D. (1986). Depression of contractile responses in rat aorta by spontaneously released endothelium-derived relaxing factor. Journal of pharmacology and experimental therapeutics *237*, 529-538.

14. Ignarro, L.J., Byrns, R.E., Buga, G.M., and Wood, K.S. (1987). Endothelium-derived relaxing factor from pulmonary artery and vein possesses pharmacologic

and chemical properties identical to those of nitric oxide radical Circulation research *61*, 866-879.

15. Ignarro, L.J., Buga, G.M., Wood, K.S., Byrns, R.E., and Chaudhuri, G. (1987). Endothelium-derived relaxing factor produced and released from artery and vein is nitric oxide Proceedings of the National Academy of Sciences of the United States of America *84*, 9265-9269.

16. Palmer, R.M., Ferrige, A.G., and Moncada, S. (1987). Nitric oxide release accounts for the biological activity of endothelium-derived relaxing factor. Nature *327*, 524-526.

17. Knowles, R.G., Merrett, M., Salter, M., and Moncada, S. (1990). Differential induction of brain, lung and liver nitric oxide synthase by endotoxin in the rat. Biochemical journal *270*, 833-836.

18. Koshland Jr., D.E. (1992). The molecule of the year. Science *258*, 1861.

19. Snyder, S.H. (1992). Nitric oxide and neurons. Current Opinion in Neurobiology *2*, 323-327.

20. Alderton, W.K., Cooper, C.E., and Knowles, R.G. (2001). Nitric oxide synthases: Structure, function and inhibition. Biochemical Journal *357*, 593-615.

21. Palacios, M., Knowles, R.G., Palmer, R.M., and Moncada, S. (1989). Nitric oxide from L-arginine stimulates the soluble guanylate cyclase in adrenal glands. Biochemical and biophysical research communications *165*, 802-809.

22. Tayeh, M.A., and Marletta, M.A. (1989). Macrophage Oxidation of L-Arginine to Nitric Oxide, Nitrite, and Nitrate. Journal of Biological Chemistry *264*, 19654-19658.

23. Kwon, N.S., Nathan, C.F., and Stuehr, D.J. (1989). Reduced Biopterin as a Cofactor in the Generation of Nitrogen Oxides by Murine Macrophages. Journal of Biological Chemistry *264*, 20496-20501.

24. Schmidt, H.H.H.W., Smith, R.M., Nakane, M., and Murad, F. (1992). Ca2+/Calmodulin-Dependent NO Synthase Type I: A Biopteroflavoprotein with Ca2+/Calmodulin Independent Diaphorase and Reductase Activities. Biochemistry *31*, 3243-3249.

25. Culotta, E., and Koshland Jr., D.E. (1992). NO News is Good News. Science *258*, 1862-1865.

26. Tay, Y.M.S., Lim, K.S., Sheu, F.-S., Jenner, A., Whiteman, M., Wong, K.P., and Halliwell, B. (2004). Do Mitochondria make Nitric Oxide? No? Free Radical Research *38*, 591-599.

27. Wang, J., Stuehr, D.J., Ikedo-Saito, M., and Rousseau, D.L. (1993). Heme Coordination and Structure of the Catalytic Site in Nitric Oxide Synthase. Journal of Biological Chemistry *268*, 22255-22258.

28. Abu-Soud, H.M., Wang, J., Rousseau, D.L., Fukuto, J.M., Ignarro, L.J., and Stuehr, D.J. (1995). Neuronal Nitric Oxide Synthase Self-inactivates by Forming a Ferrous-Nitrosyl Complex during Aerobic Catalysis. Journal of Biological Chemistry *270*, 22997–23006.

29. Crane, B.R., Arvai, A.S., Ghosh, D.K., Wu, C., Getzoff, E.D., Stuehr, D.J., and Tainer, J.A. (1997). The structure of nitric oxide synthase oxygenase domain and inhibitor complexes. Science *278*, 425-431.

30. Stuehr, D.J. (1997). Structure-Function Aspects in the Nitric Oxide Synthases. Annual Review of Pharmacological Toxicology *37*, 339-359.

31. Fischmann, T.O., Hruza, A., Niu, X., Fossetta, J.D., Lunn, C.A., Dolphin, E., Prongay, A.J., Reichart, P., Lundell, D.J., Narula, S.K., and Weber, P.C. (1999). Structural characterization of nitric oxide synthase isoforms reveals striking active-site conservation. Nature Structural and Molecular Biology *6*, 233-242.

32. Abu-Soud, H.M., Feldman, P.L., Clark, P., and Stuehr, D.J. (1994). Electron Transfer in the Nitric-Oxide Synthases. Journal of Biological Chemistry *269*, 32318-32326.

33. Hurshman, A.R., and Marletta, M.A. (1995). Nitric Oxide Complexes of Inducible Nitric Oxide Synthase: Spectral Characterization and Effect on Catalytic Activity. Biochemistry *34*, 5627-5634.

34. Abu-Soud, H.M., Ichimori, K., Presta, A., and Stuehr, D.J. (2000). Electron Transfer, Oxygen Binding, and Nitric Oxide Feedback Inhibition in Endothelial Nitric-oxide Synthase. Journal of Biological Chemistry *275*, 17349-17357.

35. Handy, D.E., and Loscalzo, J. (2006). Nitric Oxide and Posttranslational Modification of the Vascular Proteome Arteriosclerosis, Thrombosis, and Vascular Biology *26*, 1207-1214.

36. Fogli, S., Nieri, P., and Breschi, M.C. (2004). The role of nitric oxide in anthracycline toxicity and prospects for pharmacologic prevention of cardiac damage. FASEB J. *18*, 664-675.

37. Crane, B.R., Arvai, A.S., Ghosh, D.K., Wu, C., Getzoff, E.D., Stuehr, D.J., and Tainer, J.A. (1998). Structure of nitric oxide synthase oxygenase dimer with pterin and substrate. Science (Washington, D. C.) *279*, 2121-2126.

38. Mungrue, I.N., Husain, M., and Stewart, D.J. (2002). The role of NOS in heart failure: lessons from murine genetic models. Heart Fail. Rev. *7*, 407–422.

39. Ghosh, D.K., and Stuehr, D.J. (1995). Macrophage NO synthase: characterization of isolated oxygenase and reductase domains reveals a head-to-head subunit interaction. Biochemistry *34*, 801-807.

40. Ghosh, D., Abu-Soud, H.M., and Stuehr, D.J. (1995). Reconstitution of the Second Step in NO Synthesis Using the Isolated Oxygenase and Reductase Domains of Macrophage NO Synthase. Biochemistry *34*, 11316-11320.

41. Abu-Soud, H.M., Gachhui, R., Raushel, F.M., and Stuehr, D.J. (1997). The Ferrous-dioxy Complex of Neuronal Nitric Oxide Synthase: Divergent Effects of L-Arginine and Tetrahydrobiopterin on its Stability. Journal of Biological Chemistry *272*, 17349 - 17353.

42. Ghosh, D.K., Wu, C., Pitters, E., Moloney, M., Werner, E.R., Mayer, B., and Stuehr, D.J. (1997). Characterization of the Inducible Nitric Oxide Synthase Oxygenase Domain Identifies a 49 Amino Acid Segment Required for Subunit Dimerization and Tetrahydrobiopterin Interaction. Biochemistry *36*, 10609-10619.

43. Ivanova, E.V., and Magner, E. (2005). Direct electron transfer of haemoglobin and myoglobin in methanol and ethanol at didodecyldimethylammonium bromide

modified pyrolytic graphite electrodes. Electrochemistry Communications *7*, 323-327.

44. King, B.C., Hawkridge, F.M., and Hoffman, B.M. (1992). Electrochemical studies of cyanometmyoglobin and metmyoglobin: implications for long-range electron transfer in proteins. Journal of the American Chemical Society *114*, 10603-10608.

45. Van Dyke, B.R., Saltman, P., and Armstrong, F.A. (1996). Control of Myoglobin Electron-Transfer Rates by the Distal (Nonbound) Histidine Residue. Journal of the American Chemical Society *118*, 3490-3492.

46. Stargardt, J.F.H., Fred M.; Landrum, H. Lynn (1978). Reversible heterogeneous reduction and oxidation of sperm whale myoglobin at a surface modified gold minigrid electrode. Analytical Chemistry *50*, 930-932.

47. Rusling, J.F.N., Alaa Eldin F. (1993). Enhanced electron transfer for myoglobin in surfactant films on electrodes. Journal of the American Chemical Society *115*, 11891-11897.

48. Nassar, A.E.F.W., William S.; Rusling, James F. (1995). Electron Transfer from Electrodes to Myoglobin: Facilitated in Surfactant Films and Blocked by Adsorbed Biomacromolecules. Analytical Chemistry *67*, 2386-2392.

49. Rusling, J.F.N., Alaa-Eldin F. (1994). Electron Transfer Rates in Electroactive Films from Normal Pulse Voltammetry. Myoglobin-Surfactant Films. Langmuir *10*, 2800-2806.

50. Mabrouk, P.A. (1995). The use of nonaqueous media To probe biochemically significant enzyme intermediates: The generation and stabilization of horseradish

peroxidase compound II in neat benzene solution at room temperature. Journal of the American Chemical Society *117*, 2141-2146.

51. Mabrouk, P.A. (1995). First direct interfacial electron transfer between a biomolecule and a solid electrode in non-aqueous media: direct electrochemistry of microperoxidase-11 at glassy carbon in dimethyl sulfoxide solution. Analytica Chimica Acta *307*, 245-251.

52. Sivakolundu, S.G., and Mabrouk, P.A. (2000). Cytochrome c Structure and Redox Function in Mixed Solvents Are Determined by the Dielectric Constant. Journal of the American Chemical Society *122*, 1513-1521.

53. Sivakolundu, S.G., and Mabrouk, P.A. (2003). Structure-function relationship of reduced cytochrome c probed by complete solution structure determination in 30% acetonitrile/water solution. JBIC Journal of Biological Inorganic Chemistry *8*, 527 - 539.

54. Li, Q., and Mabrouk, P. (2003). Spectroscopic and electrochemical studies of horse myoglobin in dimethyl sulfoxide. JBIC Journal of Biological Inorganic Chemistry *8*, 83 - 94.

55. Spiro, T.G., and Kozlowski, P.M. (1998). Discordant Results on FeCO Deformability in Heme Proteins Reconciled by Density Functional Theory. Journal of the American Chemical Society *120*, 4524-4525.

56. Zhang, C.T., Enver; Ramdas, A.K.; Weiner, A.M.; Durbin, Stephen M. (2004). Broadened Far-Infrared Absorption Spectra for Hydrated and Dehydrated Myoglobin. Journal of Physical Chemistry B *108*, 10077-10082.

57. Lin, J., Balabin, I.A., and Beratan, D.N. (2005). The Nature of Aqueous Tunneling Pathways Between Electron-Transfer Proteins 10.1126/science.1118316. Science *310*, 1311-1313.

58. Rariy, R.V., and Klibanov, A.M. (1997). Correct protein folding in glycerol. PNAS *94*, 13520 - 13523.

59. Su, Y.O. (1985). Electrochemistry of metalloporphyrins and their catalytic reduction of oxygen at carbon electrodes. 12722-12723.

60. Degrand, C. (1984). Influence of the pH on the catalytic reduction of oxygen to hydrogen peroxide at carbon electrodes modified by an absorbed anthraquinone polymer. Journal of Electroanalytical Chemistry and Interfacial Electrochemistry *169*, 259-268.

61. Rusling, J.F., and Nassar, A.E.F. (1993). Enhanced electron transfer for myoglobin in surfactant films on electrodes. Journal of the American Chemical Society *115*, 11891-11897.

62. Bayachou, M., and Boutros, J.A. (2004). Direct electron transfer to the oxygenase domain of neuronal nitric oxide synthase (NOS): Exploring unique redox properties of NOS enzymes. Journal of the American Chemical Society *126*, 12722-12723.

63. Yennawar, N.H., Yennawar, Hemant P., Farber, Gregory K. (1994). X-ray Crystal Structure of y-Chymotrypsin in Hexane. Biochemistry *33*, 7326-7336.

64. Ryu, K., Dordick, Jonathan S. (1992). How Do Organic Solvents Affect Peroxidase Structure and Function? Biochemistry *31*, 2588-2598.

65. Fitzpatrick, P.A., Steinmetz, Anke C. U., Ringe, Dagmar, Klibanov, Alexander M. (1993). Enzyme crystal structure in a neat organic solvent. Proc. Natl. Acad. Sci. USA Biochemustry *90*, 8653-8657.

66. Taniguchi, I., Sonoda, K., and MieJSPS research fellow., Y. (1999). Electroanalytical chemistry of myoglobin with modification of distal histidine by cyanated imidazole. Journal of Electroanalytical Chemistry *468*, 9 - 18.

67. Boutros, J. (2007). Molecular function of nitric oxide synthase (NOS): Direct electrochemical investigation (Cleveland, Ohio: Cleveland State University).

68. Summers, C.A., and Flowers, R.A. (2000). Protein renaturation by the liquid organic salt ethylammonium nitrate. Protein Science *9*, 2001-2008.

69. Welton, T. (1999). Room-Temperature Ionic Liquids. Solvents for Synthesis and Catalysis. Chem. Rev *99*, 2071-2083.

70. Baker, S.N., McCleskey, T.M., Pandey, S., and Baker, G.A. (2004). Fluorescence studies of protein thermostability in ionic liquids. Chemical Communications *2004*, 940-941.

71. Madeira Lau, R., Van Rantwijk, F., Seddon, K.R., and Sheldon, R.A. (2000). Lipase-Catalyzed Reactions in Ionic Liquids. Org. Lett. *2*, 4189-4191.

72. Dzyuba, S.V., and Bartsch, R.A. (2002). Expanding the polarity range of ionic liquids. Tetrahedron Letters *43*, 4657-4659.

73. Welton, T. (2004). Review: Ionic liquids in catalysis. Coordination Chemistry Reviews *248*, 2459-2477.

74. Xu, D.-Q., Liu, B.-Y., Luo, S.-P., Xu, Z.-Y., and Shen, Y.-C. (2003). A Novel and Eco-friendly Method for the Preparation of Ionic Liquids. Synthesis *17*, 2626-2628.

75. Erbeldinger, M., Mesiano, A.J., and Russell, A.J. (2000). Enzymatic Catalysis of Formation of Z-Aspartame in Ionic Liquid: An Alternative to Enzymatic Catalysis in Organic Solvents. Biotechnology Progress *16*, 1129-1131.

76. Ohno, H.S., Chiiko; Fukumoto, Kenta; Yoshizawa, Masahiro; Fujita, Kyoko (2003). Electron Transfer Process of Polyethylene oxide-Modified Cytochrome c in Imidazolium Type Ionic Liquid. Chemistry Letters *32*.

77. Park, S., and Kazlauskas, R.J. (2003). Biocatalysis in ionic liquids: advantages beyond green technology. Current Opinion in Biotechnology *14*, 432-437.

78. Branco, L.C.R., João N.; Moura Ramos, Joaquim J.; Afonso,Carlos A. M. (2002). Preparation and Characterization of New Room Temperature Ionic Liquids. Chemistry - A European Journal *8*, 3671-3677.

79. Olivier-Bourbigou, H., and Magna, L. (2002). Ionic liquids: perspectives for organic and catalytic reactions. Journal of Molecular Catalysis A: Chemical *182-183*, 419-437.

80. Armstrong, F.A. (1990). Probing metalloproteins by voltammetry. Structure and Bonding (Berlin, Germany) *72*, 137-221.

81. Armstrong, F.A.C., Raul; Heering, Hendrik A.; Hirst, Judy; Jeuken, Lars J. C.; Jones, Anne K.; Leger, Christophe; McEvoy, James P. (2000). Fast voltammetric studies of the kinetics and energetics of coupled electron-transfer reactions in proteins. Faraday Discussions *116*, 191-203.

82. Bayachou, M., Lin, R., Cho, W., and Farmer, P.J. (1998). Electrochemical Reduction of NO by Myoglobin in Surfactant Film: Characterization and Reactivity of the Nitroxyl (NO-) Adduct. Journal of the American Chemical Society *120*, 9888-9893.

83. Boutros, J., and Bayachou, M. (2004). Myoglobin as an Efficient Electrocatalyst for Nitromethane Reduction. Inorganic Chemistry *43*, 3847-3853.

CHAPTER II

REDOX PROPERTIES OF HEMEPROTEINS IN IONIC LIQUIDS

2.1 Characterization of Protein Thin Films in Ionic Liquid

As retention of protein structure is essential in the course of this study, it is important to ascertain that structure is conserved. This is done using infrared spectroscopy and UV-Vis spectroscopy[1, 2]. Infrared spectroscopy provides information about the secondary structures of proteins. The infrared amide I and II (carbonyl and C-N) bands are sensitive to conformation and can be altered by denaturation, which affects the local environment of the carbonyl and C-N bands of amide linkages.

UV-Vis can provide information regarding the hemeprotein's tertiary structure. A shift in a hemeprotein's Soret band [3, 4] can be indicative of a disruption in the ligation that normally occurs in the heme pocket. As water is important to our study, it is important to characterize the protein film with regard to the amount of water contained. Thermogravimetric Analysis (TGA) is used to characterize the amount of water in the film and may also provide a way to differentiate between water in the film and water bound to the protein[5].

2.1.1 Infrared Spectrophotometry

As myoglobin is being introduced into a new environment that might alter the protein's structure, it is prudent to check for possible damage to the secondary structure by examining whether the two amide bands are conserved. We use a Varian Scimitar FTS 2000 infrared spectrophotometer equipped with single-reflection diamond ATR to analyze for changes in secondary structure. As a positive control, myoglobin/DDAB film is cast onto the diamond ATR crystal and allowed to dry before IR analysis. The dried myoglobin/DDAB film is then submerged in ionic liquid BMIM BF_4 and scanned at five minute intervals for one hour to simulate the contact time that myoglobin has with ionic liquid throughout a normal experiment. Amide I and II bands of the Mb/DDAB film in ionic liquid are compared to dried Mb/DDAB. Figure 2.1 shows the two sets of absorption bands, where the amide I&II bands in dry myoglobin/DDAB film and myoglobin/DDAB film immersed in ionic liquid are nearly identical. The slight bulge on the amide II band (1539/cm) in figure 2.1(b) results from background interference caused by the BMIM BF_4. The conservation of shape and position of amide bands give no indication that myoglobin has been denatured in any way.

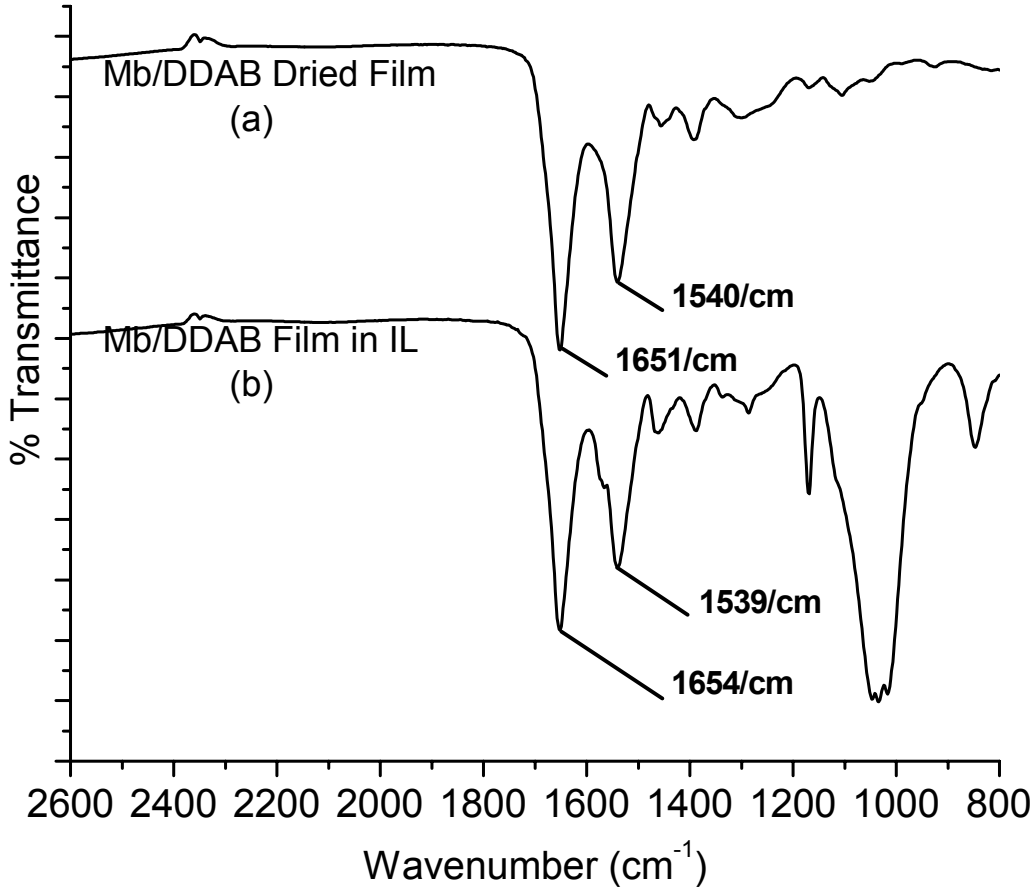

Figure 2.1: The infrared spectra of (a) myoglobin/DDAB dried film, and (b) myoglobin/DDAB film after one hour contact time with ionic liquid BMIM BF_4

It is also prudent to check for denaturation of iNOSoxy secondary structure, again by examining amide I & II bands to look for possible conformational changes. Figure 2.2 shows that the amide I & II bands in dry iNOSoxy/DDAB film and iNOSoxy/DDAB film immersed in ionic liquid are also nearly identical. Again, the slight bulge on the amide II band in figure 2.2b results from background interference caused by the BMIM BF_4. The spectrum for pure ionic liquid BMIM BF_4 is shown in figure 2.2c to confirm the source of the extraneous bulge on the amide II peak. The infrared analysis gives no indication that iNOSoxy has been denatured in any way.

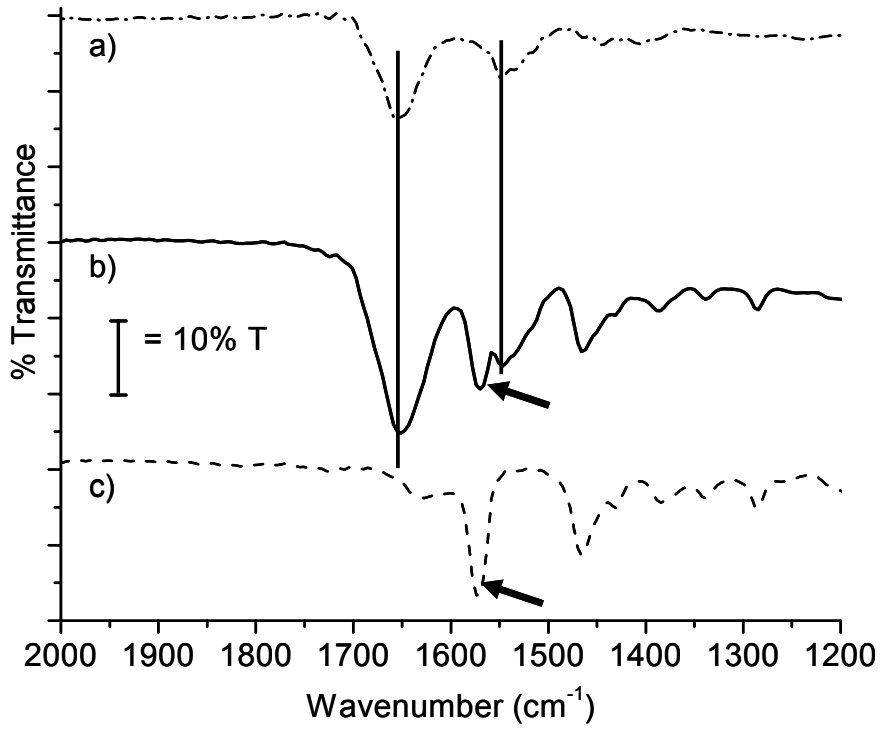

Figure 2.2: IR spectra of (a) iNOSoxy/DDAB dried film, (b) iNOSoxy/DDAB film after one hour contact time with BMIM BF_4, and (c) BMIM BF_4 background spectrum. Arrows point to the BMIM BF_4 peak and to the disruption in the iNOSoxy amide II band.

As a control, iNOSoxy is denatured by heating to 70°C in aqueous solution and cast with DDAB onto the diamond ATR crystal and allowed to dry. Figure 2.3 shows a close-up view of how the amide I & II bands are altered in this heat-denatured dry iNOSoxy/DDAB film.

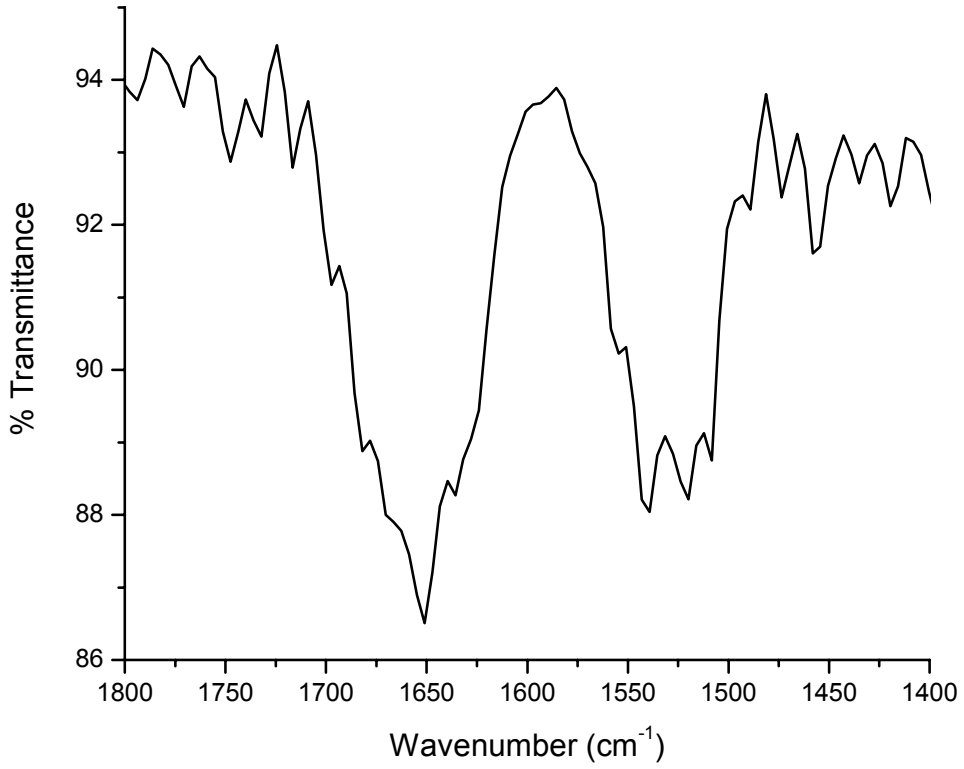

Figure 2.3: The infrared spectra of iNOSoxy/DDAB dried film, which had been denatured by heating in aqueous solution at 70°C.

2.1.2 UV-Vis Spectrophotometry

Mb/DDAB films (as outlined in section 2.2.1.1) are cast and allowed to dry overnight on quartz slides and submerged in deionized water and ionic liquid, respectively. UV/visible absorption spectra are recorded on an Agilent 8453 diode-array spectrophotometer. UV/Vis analysis of myoglobin's Soret band at 409 nm[3, 4] shows very little difference in the shape of the absorbance spectra between myoglobin/DDAB in ionic liquid vs. myoglobin/DDAB in water. Figure 2.4 shows a comparison of Mb/DDAB in water vs. BMIM BF_4, where there is no indication that the protein has denatured as a result of interactions with the ionic liquid.

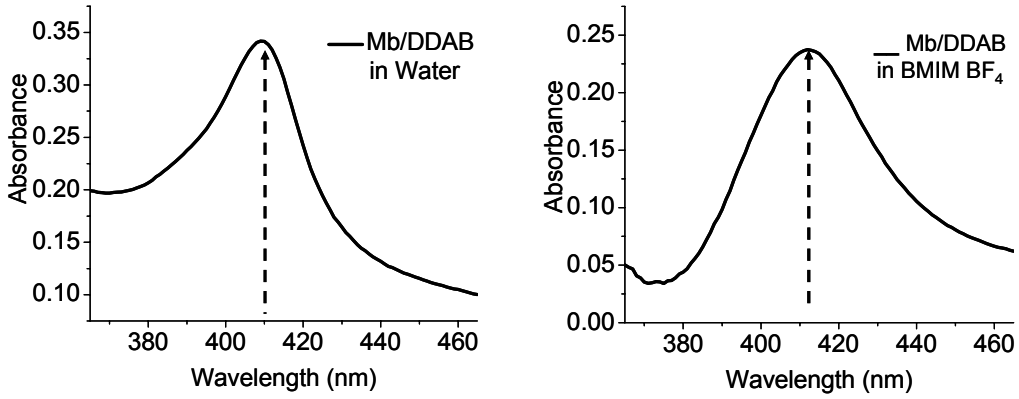

Figure 2.4: A comparison of the UV/Vis spectra of myoglobin's Soret band (a) in water and (b) in ionic liquid.

Similarly, iNOSoxy/DDAB films are also cast on quartz slides, allowed to dry overnight, and submerged in deionized water and ionic liquid, respectively. Figure 2.5 shows overlaid UV/Vis spectra for iNOSoxy/DDAB in water vs. BMIM BF_4. The spectra show very little difference in the shape or peak absorbance of the iNOSoxy Soret band [6, 7]. There is no indication that the protein has denatured as a result of interactions with the ionic liquid.

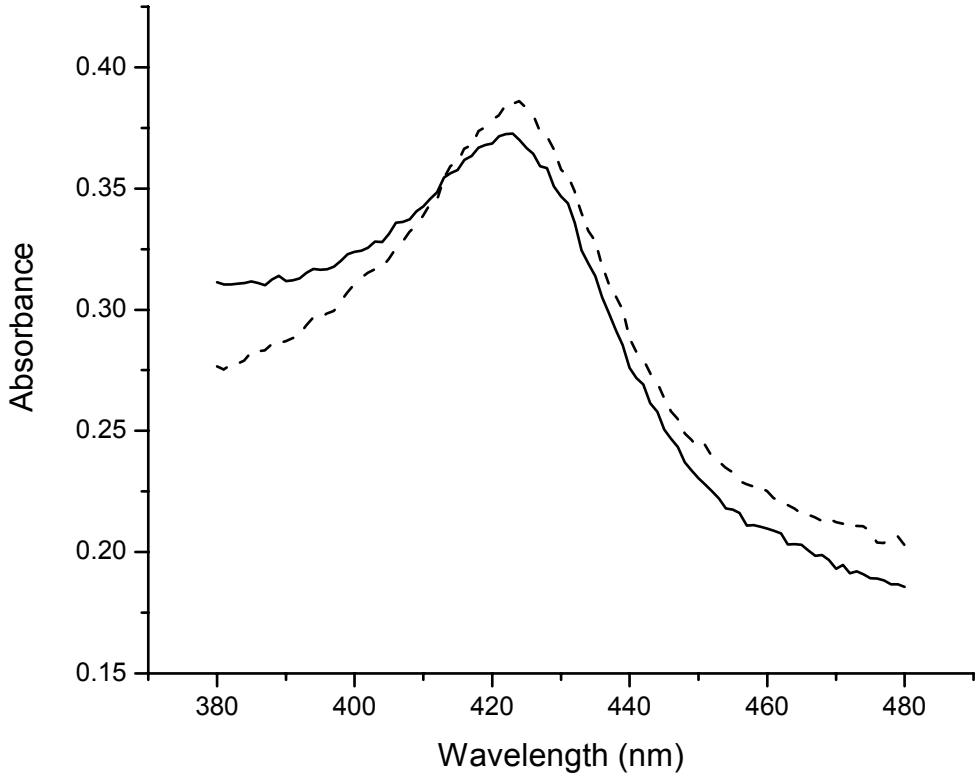

Figure 2.5: UV/Vis spectra of the iNOSoxy Soret band with iNOSoxy/DDAB film cast on quartz slide and submerged (—) in water and (---) in ionic liquid.

2.1.3 Thermogravimetric Analysis of Myoglobin

As water content is critical to the nature of these experimental trials, we use Thermogravimetric Analysis (TGA) to measure the amount of water contained in both the Mb/DDAB film and the ionic liquid solvent medium at various points in the experiment. Measurements are performed in triplicate and are reported to the nearest 0.01%. The data below represents typical results found for protein/DDAB films. Results for iNOSoxy films are omitted to avoid redundancy.

Methods to reduce water to a minimal level in the film and the solvent must be incorporated to study myoglobin's behavior at near-zero levels of available water. Recent studies of dehydrated myoglobin indicate that it is possible to dry the protein to 3.6% moisture in a desiccator that takes advantage of the equilibrium of relative humidities of various salts to achieve this end[4]. Because this process involves heating myoglobin to 100^{o}C, a temperature which could denature the protein, we instead use a < 1 ppm H_2O glove box under UHP (99.999%) nitrogen to dry Mb/DDAB films. Molecular sieves are added 3.0% (w/w) to BMIM BF_4 at least 24 hours prior to measurements to dry the ionic liquid. TGA shows that dehydration in the glove box reduces water in the protein film from 7.95% to 5.65%, whereas the molecular sieves were able to reduce water levels in the ionic liquid solvent to less than 0.01%.

The approximate weight of the dried Mb/DDAB film is 0.090 mg, with about 2/3 of the total weight coming from myoglobin. The typical amount of BMIM BF_4 used in

each experiment is 3000 mg. Table 2.1 shows the amount of water, by weight percent and by weight in milligrams, that can be found in the film and in the dry ionic liquid. The vast majority of available water comes from the ionic liquid, but it is also of considerable importance to minimize the amount of available water that can be bound to myoglobin in the protein/DDAB film.

	By Weight Percent	By Weight
H_2O in 0.090 mg Mb/DDAB Film	5.65%	0.005 mg
H_2O in 3000 mg Ionic Liquid	0.01%	0.300 mg

Table 2.1: Water in the myoglobin/DDAB film and in ionic liquids after treatment with 3Å molecular sieves. Mb/DDAB films have been dried in a glovebox with <1 ppm atmospheric H_2O present.

To illustrate the effect of changing the method of drying, we perform TGA on samples dried at 25% relative humidity and at < 1 ppm H_2O. Figure 2.6 shows the raw data from the TGA analysis of the Mb/DDAB film dried at 25% relative humidity. The myoglobin/DDAB film has two ranges where weight loss occurs that could be associated with water in the film. The first range is from 25 – 72^{o}C where 2.25% weight loss occurs with a peak loss at 33^{o}C, assigned to free water in the film. An additional 5.70% weight loss occurs in the second range from 72 – 150^{o}C with a peak loss at 115^{o}C, which is believed to represent water tightly bound to the amino acid residues.

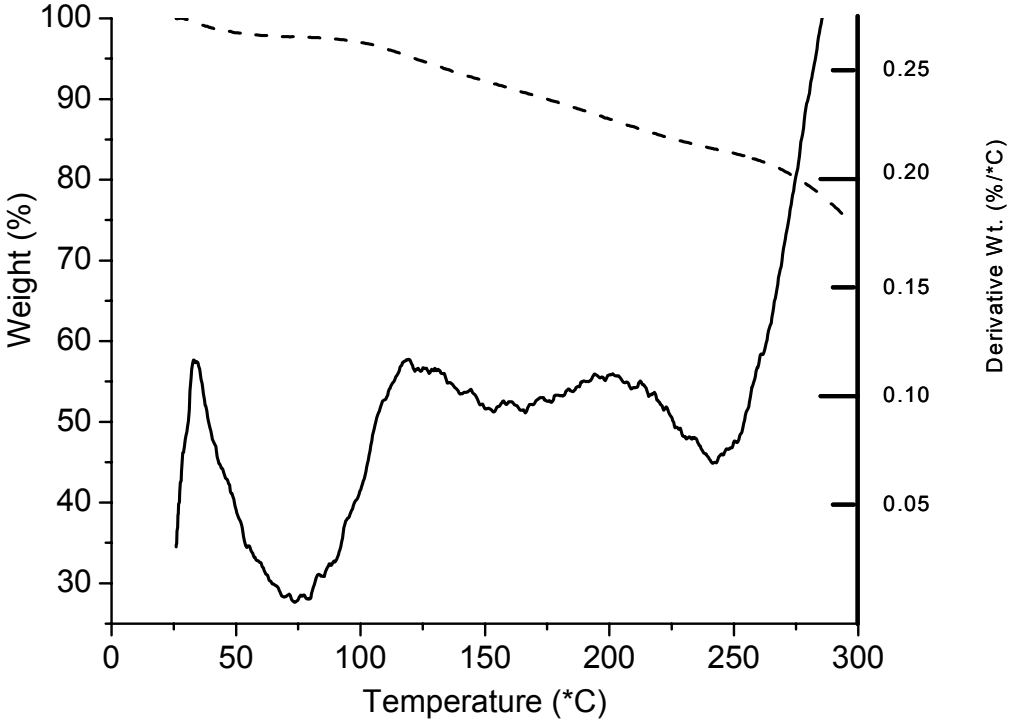

Figure 2.6: TGA of myoglobin/DDAB films dried at 25% relative humidity with total weight loss (---) and 1st derivative weight loss (—).

Figure 2.7 shows the raw data from the TGA analysis of the Mb/DDAB film dried in the < 1 ppm H_2O environmental chamber. The myoglobin/DDAB weight loss associated with free water in the film is at a much lower percentage of 1.05% with a range from 25 – 68°C and a peak loss at 30.1°C. The second range believed to represent the bound water shows a 4.60% weight loss in the temperature range of 68 – 152°C and a peak loss at 115°C. Drying the myoglobin/DDAB films by this method reduces the total available water in the film from 7.95% to 5.65%, which appears to be the maximum reduction of water using this method.

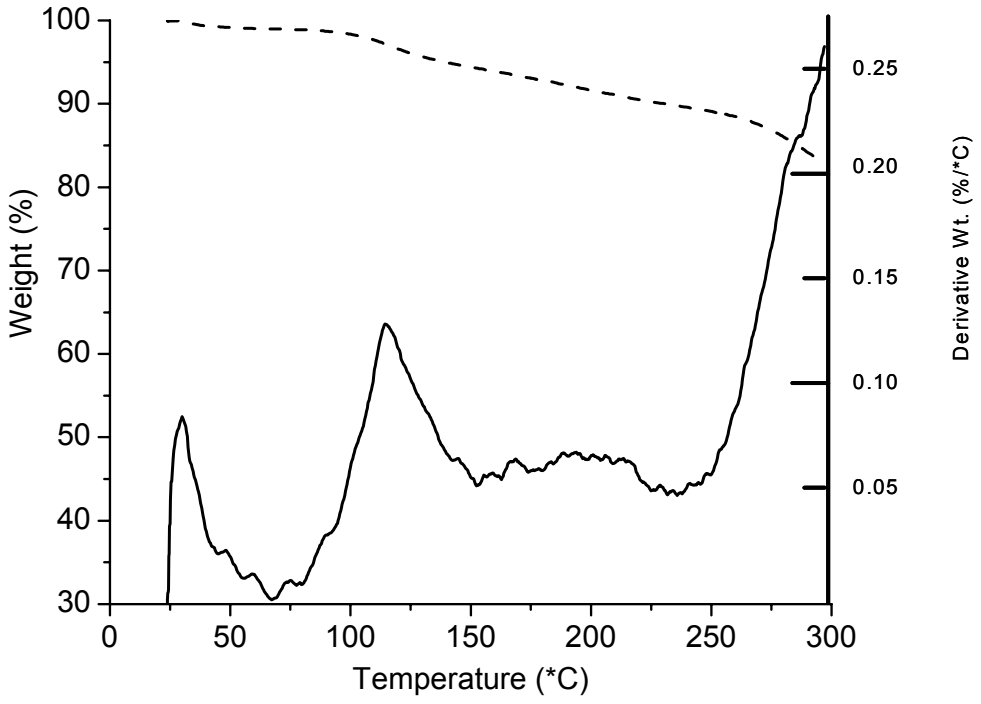

Figure 2.7: TGA of myoglobin/DDAB films dried in < 1 ppm atmospheric chamber with total weight loss (---) and 1st derivative weight loss (—).

2.1.4 Discussion

Changing the drying method lowers the total available water in the film from 7.95% to 5.65%. With the average myoglobin/DDAB film weighing 0.180 mg, this has effectively reduced the weight of water in the film from 0.007 mg to 0.005 mg, a reduction of about 29%. This pales in comparison with the amount of water available from ionic liquid BMIM BF_4 where the 0.01% water in the ionic liquid could provide as much as 0.30 mg water, or 60X more water in the bulk than is in the film. However, our goal is to minimize available water without disturbing the structure of the protein, so the procedure for modifying electrodes and storing them in the < 1 ppm H_2O environmental chamber will be part of the protocol of experimental design.

2.2 Characterization of Myoglobin Thin-Film Redox Properties in Ionic Liquid

Examining the electrochemical characteristics of both proteins as a function of time and of added water will provide some information about how each protein responds to the low-water environment and also to the bulk ionic liquid. Though our spectroscopic studies indicate that both proteins retain their structural integrity in ionic liquids, measuring the redox properties of these proteins after much time immersed in ionic liquid may provide additional insight as to the role of water. Starting our electrochemical studies with this premise will give a baseline of data from which to build our subsequent studies. We first examine how Mb films respond electrochemically as a function of time.

2.2.1 Myoglobin Redox Properties as a Function of Time

We use cyclic voltammetry to measure the formal reduction potential and current response of Fe^{III}/Fe^{II} redox couples in myoglobin/didodecyl dimethyl ammonium bromide surfactant films on pyrolytic graphite electrodes (Mb/DDAB/PG) in ionic liquid BMIM BF_4. This myoglobin/surfactant film methodology developed by Rusling, *et al*[2] is used to form a thin bilayer film on a pyrolytic graphite electrode. This method greatly increases the electrochemical response of myoglobin and reduces diffusion, as compared to measuring myoglobin redox and catalytic reactions in solution. Measurements are taken as a function of time and the results are compared to Mb/DDAB/PG in aqueous buffer to note any differences in electron transfer activation energy and other key indicators of electron transfer kinetics.

2.2.1.1 Experimental

Lyophilized myoglobin from horse skeletal muscle was obtained from Sigma-Aldrich and purified by passing through a 30,000 MW filter followed by concentration using a 3,000 MW filter[8]. Myoglobin solution is concentrated to ca. 0.75 mM as confirmed by absorbance measurement of the Soret band at 409 nm. Pyrolytic graphite (PG) was purchased from Union Carbide, cut into basal-plane oriented disks, and fabricated into homemade working electrodes[2]. Purum >97% BMIM BF_4 was obtained from Fluka Chemie GmbH (Sigma-Aldrich). Ionic liquid BMIM BF_4 is dried with 3Å

molecular sieves (Fisher Scientific) to a water level <0.01% as confirmed by thermogravimetric analysis. 3.0 ml ionic liquid is purged with 99.9% purity nitrogen gas for at least 30 min before the experiment and is kept oxygen-free during the course of the experiment. 100 mM pH 7.0 phosphate buffer is also deoxygenated for 30 minutes with nitrogen. 10 mM DDAB is prepared by dissolving DDAB powder (Acros Organics) in distilled water and sonicating for several hours until the solution turns clear. A Barnstead Nanopure Infinity system was used to purify distilled water to a specific resistance greater than 18 MΩ-cm.

Prior to coating, basal-plane pyrolytic graphite (PG) electrodes are polished consecutively using 0.3μm and 0.05μm alumina on Buehler microcloth. Electrodes are then sonicated in pure distilled water for 15 minutes and dried in air. The pyrolytic graphite electrode surface is modified with 5 μl of 10 mM DDAB[1] and 5 μl 0.75 mM myoglobin and allowed to slow-dry overnight**.** To measure and compare the effects at minimal water levels, electrodes are additionally dried by placing them in a <1 ppm H_2O glove box environment for 24 hours.

The three-electrode electrochemical cell consists of a silver wire (Ag) reference electrode, a Pt wire counter electrode, and a homemade pyrolytic graphite working electrode described above. The silver wire is used as a reference in lieu of a real half-cell[9, 10] in order to minimize the slight amount of water that may pass across a salt bridge and contaminate the dry BMIM BF_4. CH Instruments model CHI 440 electrochemical workstation is used to record cyclic voltammograms of the

myoglobin/DDAB film deposited on pyrolytic graphite electrode while in anhydrous ionic liquids. Cyclic voltammetry is performed in all solvents in a dry, oxygen-free nitrogen atmosphere. Water is added as indicated by the specific experimental procedure. Time intervals between scans are as indicated.

2.2.1.2 Results

Cyclic voltammetry is performed at a scan rate of 200 mV/sec and is repeated periodically over a period of five hours. Current response, formal reduction potential, and ΔE_P are measured and compared to aqueous systems. Faradaic response in ionic liquid is measured and compared to the response in pH 7.0 aqueous phosphate buffer. Reducing the available water in the film and in the bulk solvent drastically reduces the current output of the DDAB/Mb/PG electrode, as shown in Figure 2.8, which represents the cyclic voltammogram taken at the start of the experiment. Formal reduction potential is also shifted to lower energy in the ionic liquid system.

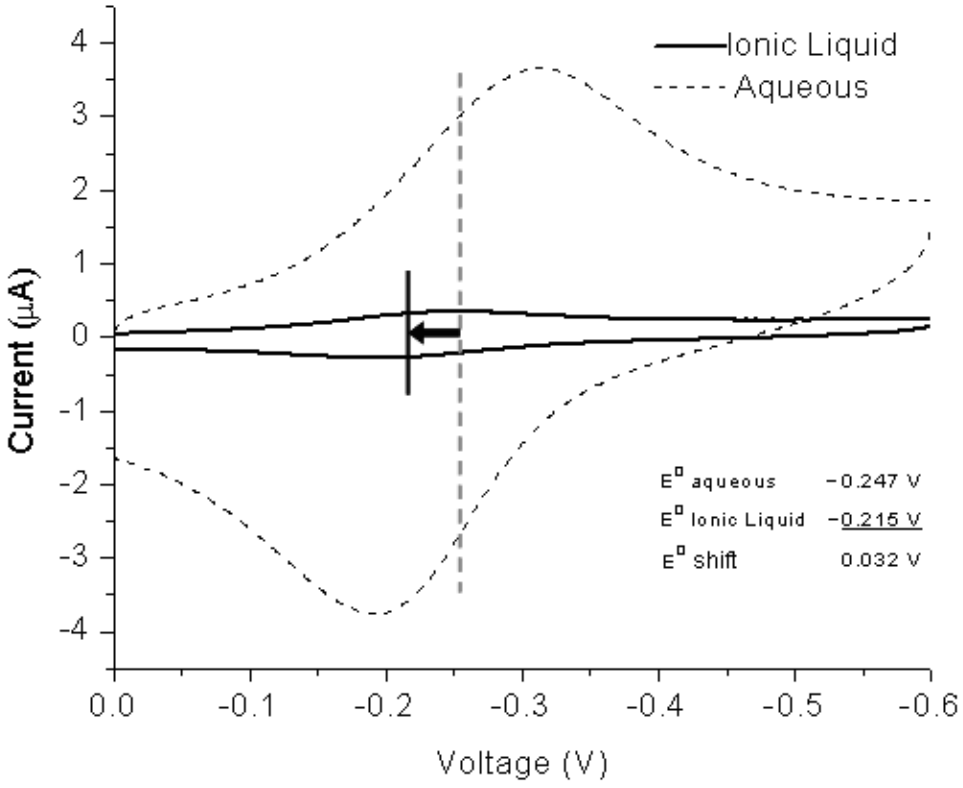

Figure 2.8: A comparison of myoglobin's current and formal reduction potential in dry (<0.01% water) ionic liquid and in aqueous pH 7 phosphate buffer.

As mentioned earlier, any changes in charge transfer characteristics can be used to provide insight into the function of myoglobin in this low-water environment. Figure 2.9 shows how cathodic and anodic current in BMIM BF_4 increases linearly as a function of time. This indicates that myoglobin is responding favorably to the ionic liquid environment. Before fully discussing and analyzing the data, we shift our focus to another parameter of interest: how does modulating the level of available water in the environment affect redox characteristics? Data will be discussed in greater detail in section 2.2.3.

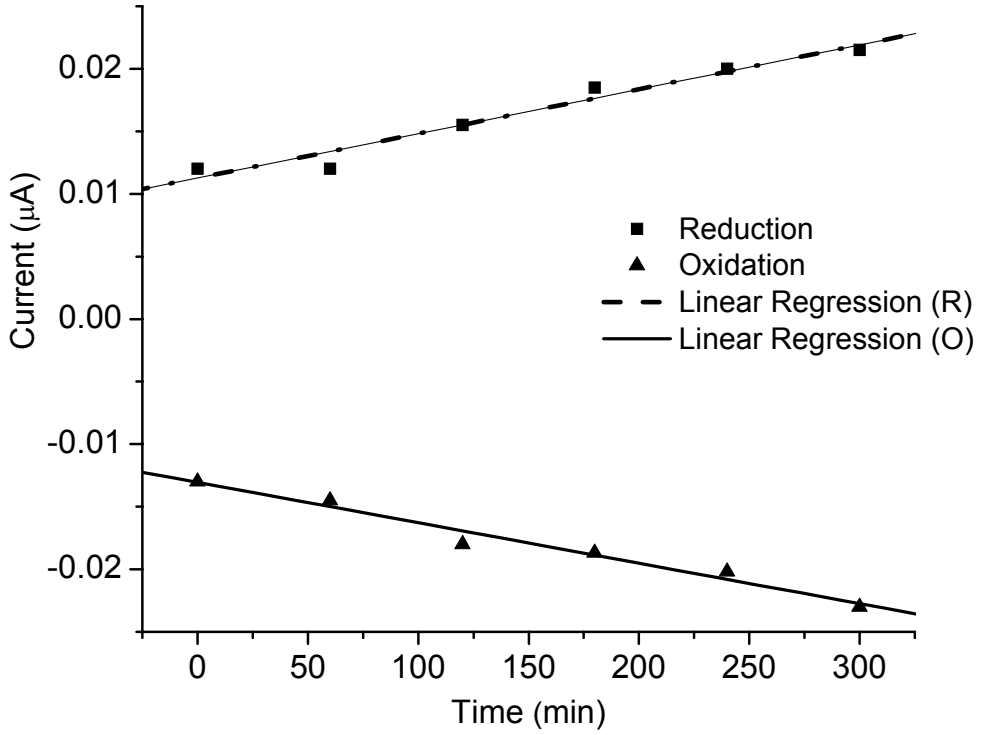

Figure 2.9: Changes in myoglobin's cathodic and anodic current in ionic liquids as a function of time, 0.01% water in the ionic liquid.

2.2.2 Myoglobin Redox Properties as a Function of Added Water

Once we established a baseline of data as a function of time, we looked into how myoglobin's redox characteristics change when controlled amounts of water are added to the system.

2.2.2.1 Experimental

The experimental set-up is identical to that outlined in section 2.2.1.1 with the exception of added deoxygenated water to the ionic liquid system. In this experiment, 0.45% water is added to the ionic liquid. Charge transfer characteristics already described are compared initially to aqueous, to the 0.01% ionic liquid, and are also measured as a function of time.

2.2.2.2 Results

The current response of Mb/DDAB film in 0.45% water-added ionic liquid increases compared to the 0.01% water system, but is still much lower than in aqueous buffer, as shown in figure 2.10. E^0 is shifted to higher potentials as compared to the 0.01% water system, and ΔE_p is lower, indicating faster electron transfer kinetics.

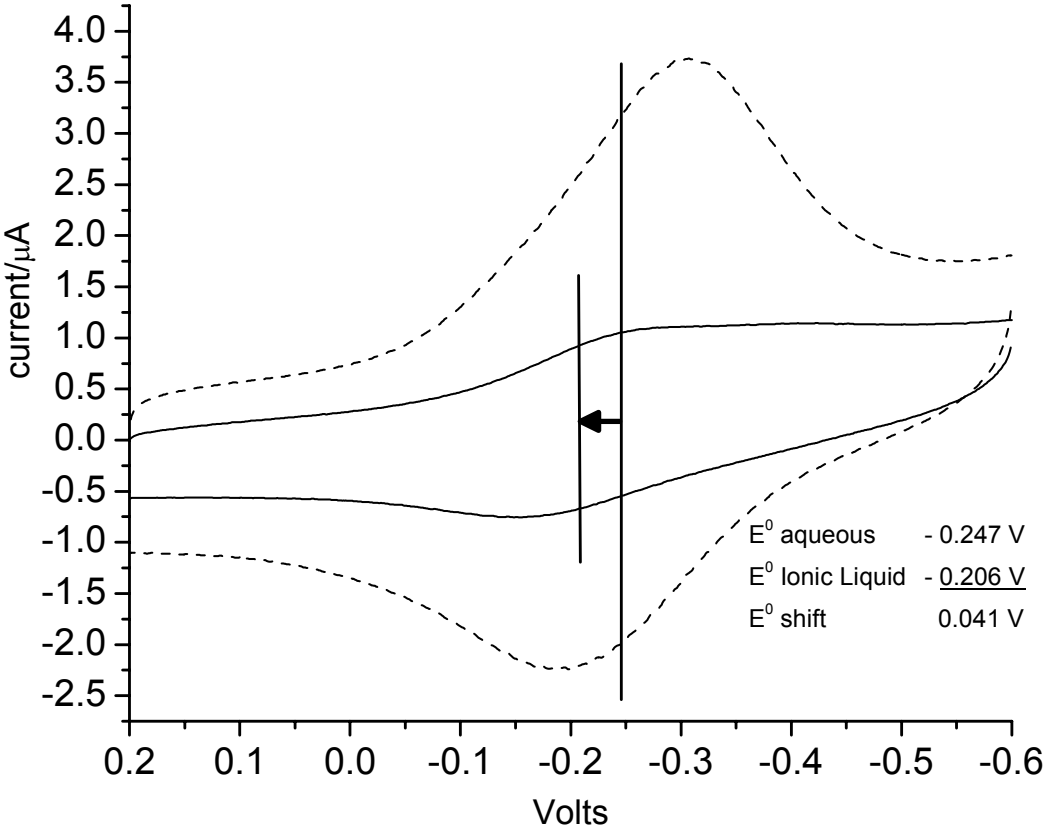

Figure 2.10: A comparison of myoglobin's formal reduction potential and current response with 0.45% water added to ionic liquid (—) and in aqueous pH 7 phosphate buffer (---).

We also monitored change in current as a function of time with the added 0.45% of water to see if there is a commensurate increase in current, as was seen in the dry (<0.01% water) ionic liquid. Figure 2.11 shows that though current values are higher in this experimental trial, there is still a linear increase of the current as a function of time. In addition to the observed linear increase in current as a function of time, ΔE_P values are comparably much larger with the added water. In aqueous buffer at a scan rate of 200 mV/sec, ΔE_P is 0.120 V, in ionic liquid with 0.45% water ΔE_P decreases to 0.107 V, and in the desiccated 0.01% water system ΔEp dramatically drops to approximately 0.060 V, indicating that the kinetics of electron transfer to myoglobin/DDAB film favors the low levels of water available and that the presence of even small amounts of water slows down this process. It should also be noted that despite the large increases in both current and ΔE_P, increasing the water from 0.01% to 0.45% did not cause an appreciable difference in the formal reduction potential. E^0 in both ionic liquid systems (with 0.01% and 0.45% water) stayed approximately 0.030-0.040 V lower than the aqueous system.

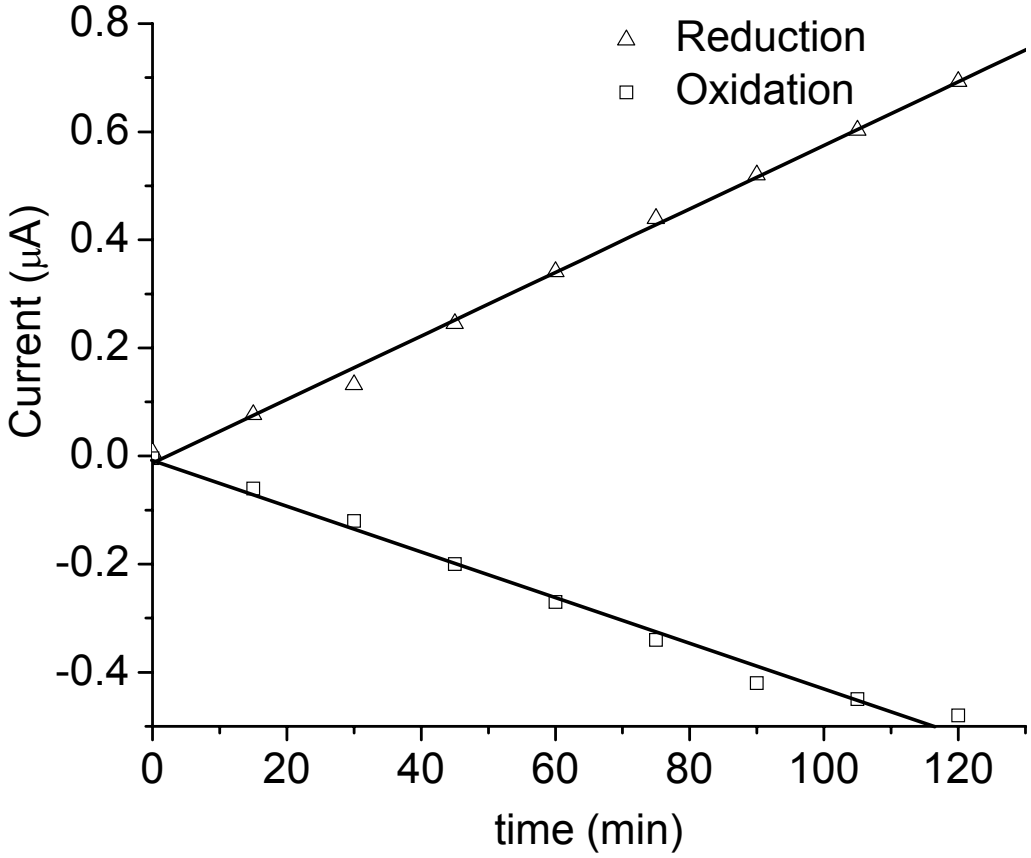

Figure 2.11: Myoglobin's changing current response as a function of time with 0.45% water added to ionic liquid.

2.2.3 Discussion: The Effect of Water and Time on Mb Redox Properties

Myoglobin's electrochemical response in the low water environment indicates that fewer electron transfers occur when water is taken away from the system. This is shown by the sharply reduced current response when water in the bulk is reduced to 0.45%, and is further demonstrated by the continued drop in current as more water is taken away from the system (0.01%).

However, formal reduction potential goes to more positive potential as water is removed from the system. The change in ΔE_P also indicates that electron transfer in the low water environment is faster, again indicating that water modulates the efficiency of charge transfers. Table 2.2 shows a comparison of some key characteristics of charge transfer in ionic liquid (both at 0.01% water and at 0.45% water) as compared to aqueous buffer, including ΔE_P and formal reduction potential E^0.

	E_C	E_A	$E^{0,}$	ΔE_P
Aqueous Buffer	-0.307	-0.187	-0.247	0.120
BMIM BF_4 (0.45% Water)	-0.260	-0.152	-0.206	0.108
BMIM BF_4 (<0.01% Water)	-0.246	-0.186	-0.216	0.060

Table 2.2: Redox characteristics as a function of water available to the myoglobin/DDAB film.

To closely investigate electron transfer kinetics in low-water, ionic liquid systems, ΔE_P is measured as a function of scan rate[11]. The ΔE_P of both aqueous and ionic liquid systems are nearly equal at the very low scan rates, but quickly diverge as the ΔE_P of the aqueous system continues to increase at a faster rate as a function of log (scan rate)$^{-1/2}$. Figure 2.12 indicates faster electron transfer rates for Mb/DDAB in nearly anhydrous ionic liquid.

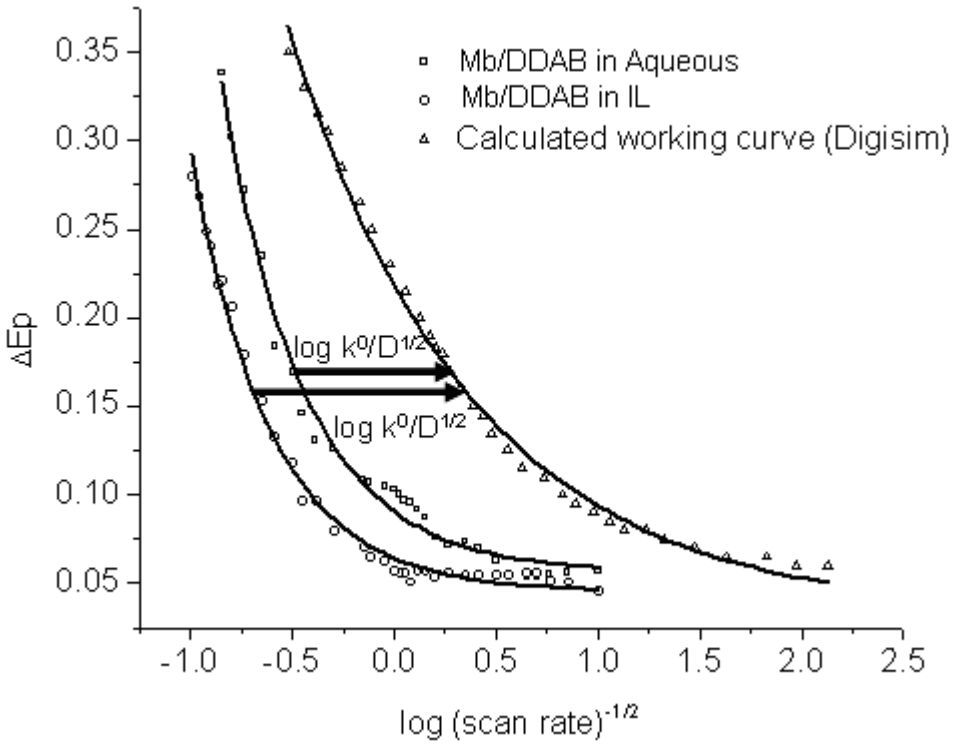

Figure 2.12: Changes in ΔE_P as a function of scan rate, comparing ionic liquid (<0.01% water) to aqueous, alongside a working curve calculated by Digisim® simulation package.

2.3 Characterization of Nitric Oxide Synthase Redox Properties in Ionic Liquid

We have already seen how myoglobin exhibits improved kinetics of electron transfer when water in the medium is reduced. Examining the electrochemical characteristics of NOS as a function of time and as a function of added water will provide much needed additional information about how each protein responds to the low-water environment and also to the bulk ionic liquid.

2.3.1 Nitric Oxide Synthase Redox Properties as a Function of Time

As in the case of myoglobin, we use cyclic voltammetry to measure the formal reduction potential, ΔE_P and current response of Fe^{III}/Fe^{II} redox couples in iNOSoxy/didodecyl dimethyl ammonium bromide surfactant films on pyrolytic graphite electrodes (iNOSoxy/DDAB/PG) in ionic liquid BMIM BF_4. The measurements are repeated as a function of time and the results are compared to iNOSoxy/DDAB/PG in aqueous buffer. Further, these results will be compared and contrasted against the myoglobin results in ionic liquid.

2.3.1.1 Experimental

The experimental set-up is much the same as that outlined in section 2.2.1.1, except that iNOSoxy is used in place of myoglobin on the electrode surface. iNOSoxy is prepared in-house through expression and purification as described in section 1.2.4, and is further purified through successive washings with distilled water followed by centrifugation with a 30,000 MW filter to bring the sample back to the original 30 μM concentration. This final step is done to remove most of the 10% glycerol that is present in iNOSoxy base buffer, which adds to the stability of the protein upon freezing. Without this final washing, the dried protein film on the electrode surface would contain primarily glycerol with very little protein as a weight-percent of the dried film.

The pyrolytic graphite electrode is prepared with 5 μl of 10 mM DDAB (aq) and 5 μl of 30 μM (aq) iNOSoxy and allowed to slow-dry overnight**.** To measure and compare the effects at minimal water levels electrodes are additionally dried by placing in a <1 ppm H_2O glove box environment for 24 hours. Ionic liquid BMIM BF_4 is dried with 3Å molecular sieves to a water level <0.01%. The ionic liquid is purged with 99.9% purity nitrogen gas for at least 30 min before the experiment and is kept oxygen-free during the course of the experiment. 100 mM pH 7.0 phosphate buffer is also deoxygenated for 30 minutes with nitrogen. The electrochemical cell set-up and experimental conditions are as outlined in section 2.2.1.1.

2.3.1.2 Results

Cyclic voltammetry is performed at a scan rate of 200 mV/sec and is repeated periodically over a period of one hour. Current response, formal reduction potential, and ΔE_P are measured and compared to aqueous systems. Faradaic response in ionic liquid is measured and compared to the response in pH 7.0 phosphate buffer. Reducing the available water in the film and in the bulk solvent drastically reduces the current output of the DDAB/iNOSoxy/PG electrode, as shown in Figure 2.13, which represents the cyclic voltammogram taken at the start of the experiment vs. aqueous pH 7.0 phosphate buffer.

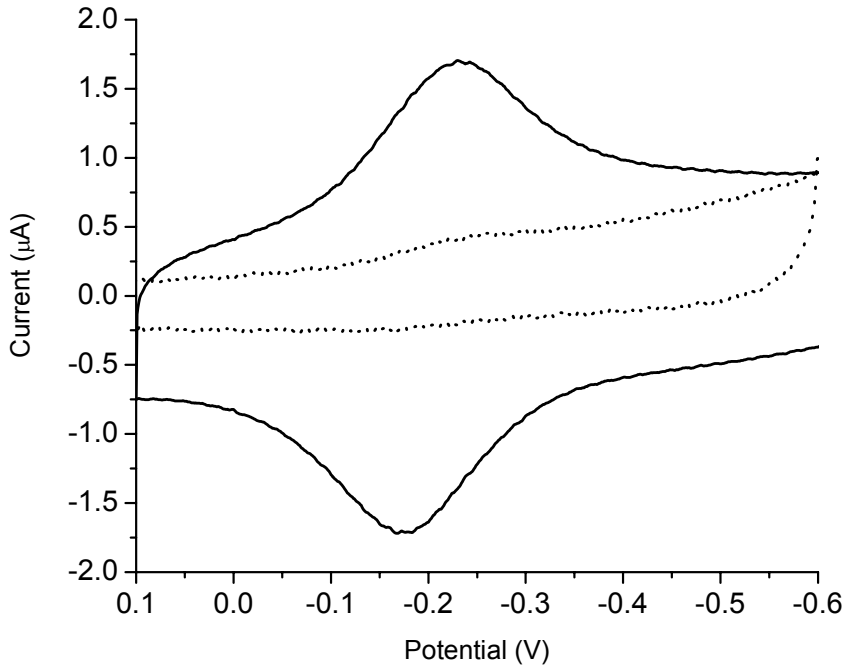

Figure 2.13: Comparing iNOSoxy films in aqueous pH 7.0 (—) and initially in dry ionic liquid (···).

Unlike the myoglobin experiments described earlier, in experiments performed with iNOSoxy/DDAB films in ionic liquid, current does not improve as a function of time. It is difficult to measure ΔE_P or formal reduction potential in the initial ionic liquid voltammogram. In addition, current drops to almost zero after one hour when water is further minimized in the bulk ionic liquid and in the film with the molecular sieves. Figure 2.14 shows how the already drastically reduced current seen in iNOSoxy after initial immersion in ionic liquid is reduced to almost background capacitive current. It is also difficult to measure changes in current as a function of time as was measured in figures 2.9 and 2.11, for the same reasons mentioned above.

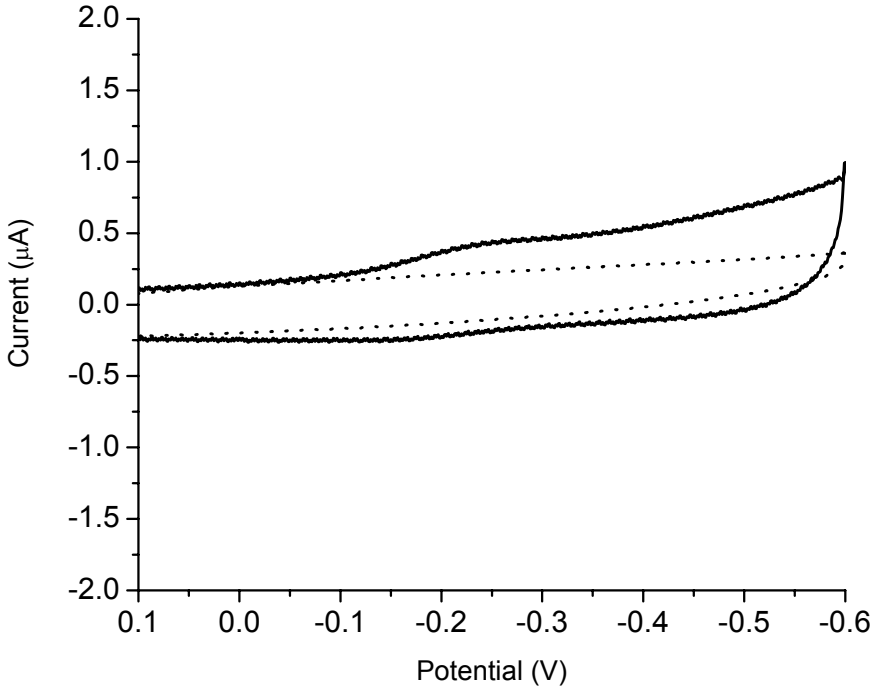

Figure 2.14: Comparing iNOSoxy films initially in 0.01% water ionic liquid (—) and after one hour immersion in the ionic liquid (···). Faradaic current is drastically reduced to almost zero.

2.3.2 Nitric Oxide Synthase Redox Properties as a Function of Added Water

2.3.2.1 Experimental

The experimental set-up is identical to that outlined in section 2.3.1.1 with the exception of added deoxygenated water to the ionic liquid system. In this experiment, water is added to the ionic liquid to a final level of 0.45%. Charge transfer characteristics already described are compared to aqueous, to the iNOSoxy in ionic liquid with 0.01% water, and are also measured as a function of time.

2.3.2.2 Results

The current response of iNOSoxy/DDAB film in 0.45% water-added ionic liquid increases compared to the 0.01% water system, but is still much lower than in aqueous buffer, as shown in figure 2.15. ΔE_P does not change much vs. the aqueous iNOSoxy/DDAB. E^0 is virtually unchanged from aqueous buffer but there are significant changes in current, similar to the behavior of myoglobin in ionic liquid.

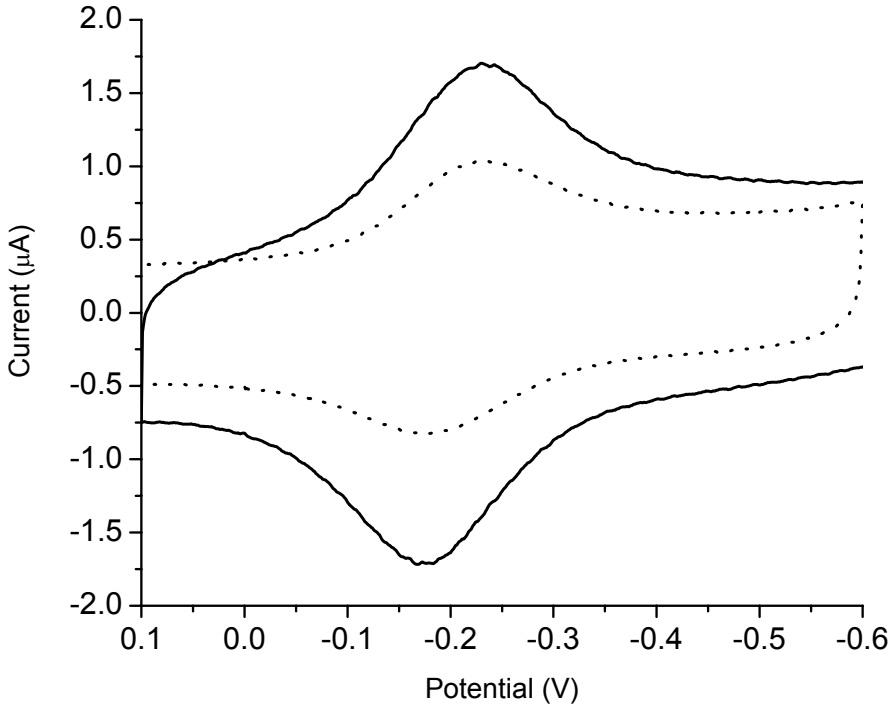

Figure 2.15: iNOSoxy films in aqueous pH 7.0 (—) and initially in ionic liquid with 0.45% water (···). Current is reduced with very little change in ΔE_P or formal reduction potential

2.3.2.3 Discussion

All observed experimental indicators, particularly a loss of faradaic current, show that water affects the reversibility of iNOSoxy's redox couple. The behavior of iNOSoxy is contrasted by myoglobin's redox characteristics, which show faster kinetics and improved current response as a function of time in the ionic liquid environment. Figure 2.16 shows overlaid cyclic voltammograms comparing iNOSoxy films initially immersed in ionic liquid with 0.45% added water and the same film after one hour.

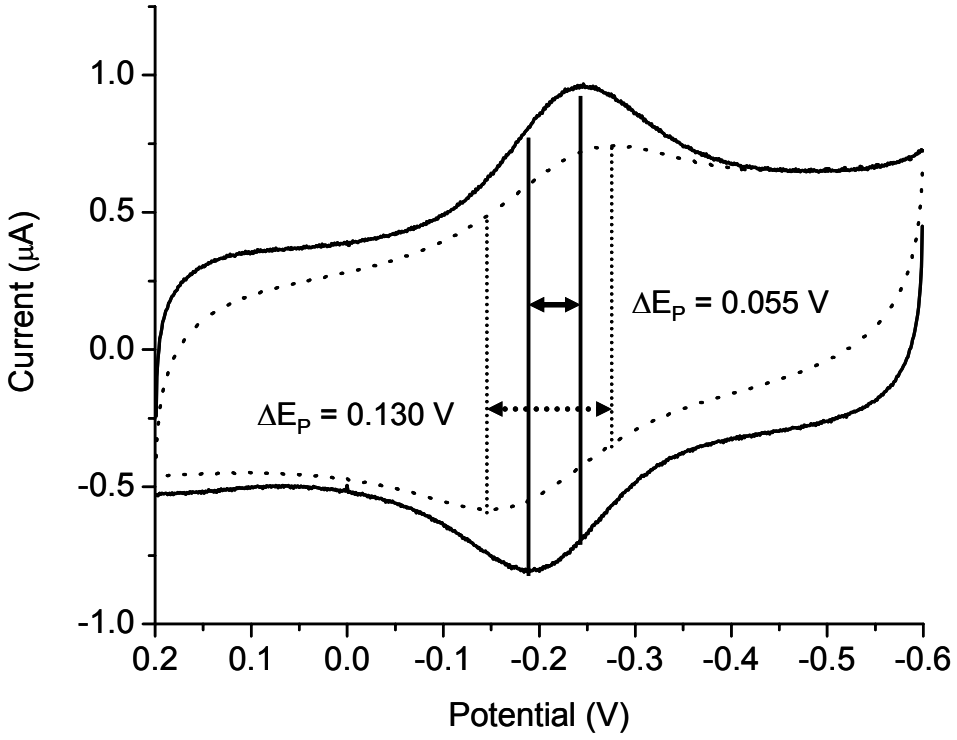

Figure 2.16: Changes in ΔE_P as a function of time, comparing iNOSoxy in ionic liquid (0.45% water) initially (—) and after one hour (····).

Figure 2.17 shows overlaid cyclic voltammograms comparing myoglobin films initially immersed in ionic liquid with 0.45% added water and the same film after one hour. The two figures describe the contrast that exists between iNOSoxy and myoglobin behaviors. While the current response and kinetics of electron transfer improve over time for myoglobin, the exact opposite is observed for iNOSoxy.

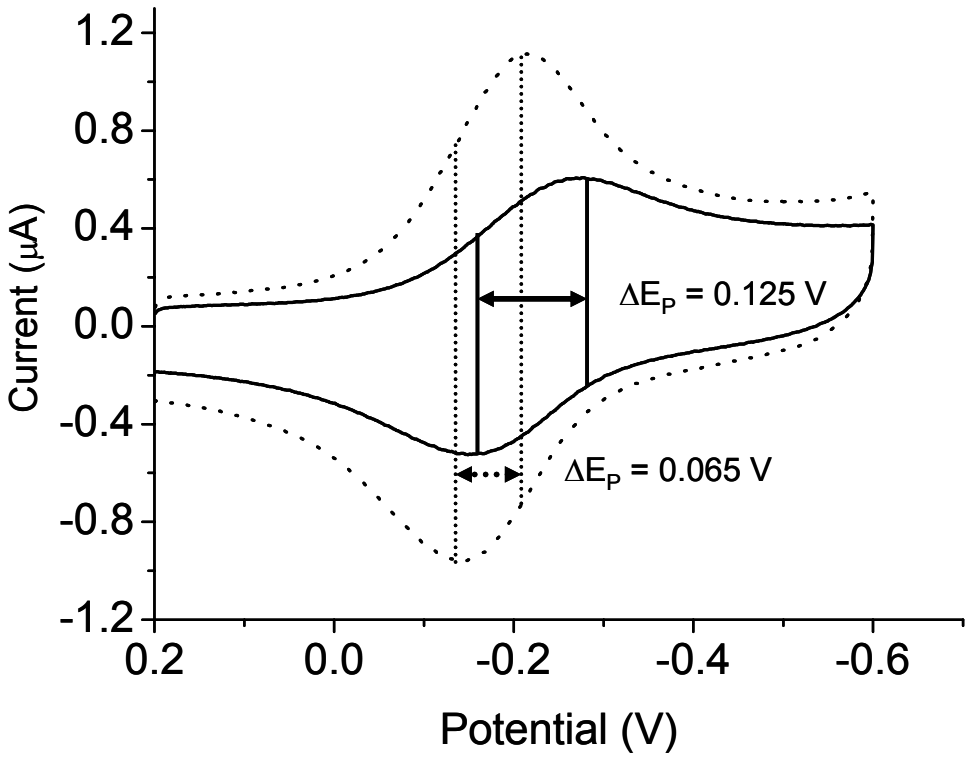

Figure 2.17: Changes in ΔE_P as a function of time, comparing myoglobin in ionic liquid (0.45% water) initially (—) and after one hour (····).

The combination of changes in proton availability due to the limited levels of water in this medium, changes of distal ligation of water, H-bonding in the distal pocket and in the global protein environment, and the presence of structured water and bulk water can all have an effect ET to metalloproteins like myoglobin and iNOSoxy. Further, the effect of each aforementioned factor may be different for each protein and can be difficult to predict. Beratan and coworkers use computational models to show the effects of water on electron transfer, and relate distance to the redox center and water availability as two key factors in determining water's role in electron transfer kinetics[12].

Computational models suggest that structured water close to amino acid residues (at a distance up to 3Å from the protein molecule) facilitate electron transfer by creating short tunneling pathways through either a single water molecule or through a network of constructively interfering water molecules close to the protein surface, which results in only a weak decay of electron coupling. Without this structured network, electronic coupling decays exponentially through this 3Å range, decreasing by as much as a factor of 1×10^3.

In addition to the normal electron coupling decay inherent to each molecule as a function of its size and average length of electron transfer pathway, the lack of structured water in our low-water study may further affect the electron transfer pathways to each molecule in ways not measureable in past aqueous studies. This may exacerbate the effects of electron coupling decay in protein molecules where structured water is not as tightly bound to the molecule, and may provide a rationale as to why myoglobin responds favorably to the low-water environment and iNOSoxy does not. In a random sampling of Protein Data Bank samples (crystal structures *1WLA, 1VXH, 1DWR, 1VXG, 1VXF*) myoglobin has an average 1.18 water molecules per amino acid, whereas iNOSoxy dimer (crystal structures *1N2N, 1DF1, 1M8D, 1MBE, 1M8H)* has only 0.34 water molecules per amino acid. This indicates that water may not be as tightly bound to the iNOSoxy molecule and that structured water may be less available as compared to the myoglobin molecule. If the crystal structures are an indication of each molecule's propensity to bind water near the surface, it would follow that iNOSoxy would tend to have an exponentially higher rate of electronic coupling decay and that this decay would increase

as a function of time due to additional diffusion of water into nearly anhydrous ionic liquid.

Additionally, it has been shown that the orientation of the molecule's redox center also has an effect on electronic coupling[13], and hemeproteins that can align the edge of the porphyrin with the wavefunction of a tunneling electron show improved electronic coupling. The smaller size (18.3 kDa vs. 112 kDa) of myoglobin as compared to iNOSoxy dimer may make it easier for myoglobin to reorient its redox center to improve reactivity and lower the activation energy of the redox reaction.

To analyze how electron transfer kinetics to iNOSoxy change in low-water systems, we measure ΔE_P at various scan rates. The ΔE_P of both aqueous and ionic liquid systems are nearly equal at the very low scan rates, but quickly diverge at faster rates. Figure 2.18 shows the changes of ΔE_P for iNOSoxy as a function of scan rate for the ionic liquid medium with 0.45% added water. This is compared with the behavior of the same protein in aqueous medium. The higher ΔE_P of iNOSoxy in ionic liquid with added water compared to the aqueous medium indicates slower kinetics of electron transfer when available bulk water is limited. As such, the availability of water and/or protons proves to be essential to the redox function of this protein.

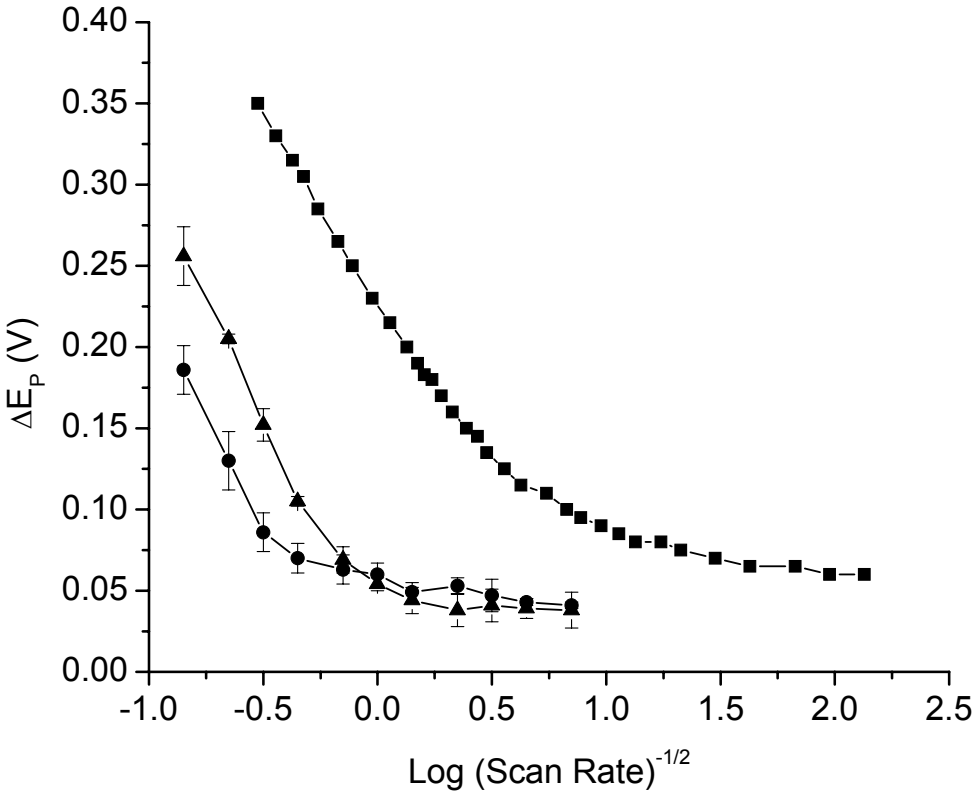

Figure 2.18: iNOSoxy in ionic liquid with 0.45% water ▲ has a larger ΔE_P as a function of scan rate as compared to iNOSoxy in aqueous ●. Digisim calculated working curve ■ is added for comparative purposes.

2.4 Characterization of Protein Thin Film Redox Properties in Ionic Liquid: Isotopic Effects Using D_2O

Our previous investigation indicates that reducing the amount of water available to metalloproteins can significantly impact electron transfer kinetics. In addition, our studies point to structural differences between hemeproteins as a contributing factor in these differences. Because of the myriad roles that water plays in elementary steps enzyme function[14], it is difficult to predict exactly how the electron transfer properties of proteins will change in the low-water environment. Classical isotopic exchange studies provide a means to interrogate the role of protons in elementary steps, such as electron transfer.

In this regard, D_2O has often been used as a water surrogate to study elementary steps where proton transfer is involved[15-18]. Deuterons should show a more pronounced effect on electron transfer steps where proton transfer is key. In this portion of the study, we substitute D_2O into the low water ionic liquid environment and we monitor the effect on electron transfer.

2.4.1 Experimental

Because of the need to reduce water to even lower levels and the need to replace most of the remaining water with deuterium oxide, it becomes necessary to introduce new

preparatory techniques, especially for myoglobin, DDAB, and iNOSoxy, which were previously cast onto pyrolytic graphite electrodes in aqueous solutions. Myoglobin and DDAB solutions are easily prepared with >99.0% deuterium oxide (Sigma-Aldrich) in place of H_2O, concentrated and/or purified to the desired concentrations, as described earlier. iNOSoxy is obtained as described earlier and is further purified by successive washings to replace H_2O with D_2O. 400 μl D_2O is added to 100 μl of aqueous iNOSoxy, the solution is allowed to equilibrate for 20 minutes and is then concentrated back to the original volume of 100 μl by centrifugation. This process is repeated 3X to drive the relative concentration of H_2O to approximately 0.16%. All other experimental conditions are as previously reported.

2.4.2 Results

Revisiting the data from figure 2.18, where ΔE_P of iNOSoxy/DDAB (H_2O) films in ionic liquid with 0.45% added H_2O are compared to ΔE_P of iNOSoxy/DDAB films in aqueous pH 7.0 buffer as a function of scan rate, it was shown that the electron transfer is slower in the ionic liquid system. In this current isotopic portion of our study, we overlay ΔE_P of iNOSoxy/DDAB films prepared in D_2O to compare the kinetics of both previously described systems against the D_2O system. In addition to the residual D_2O found in the film, 1.65% D_2O is added to the ionic liquid to provide for an environment where deuterons are in relatively abundant quantity. The ΔE_P of each system (aqueous, ionic liquid-H_2O, and ionic liquid-D_2O) is plotted as a function of log (scan rate)$^{-1/2}$.

Figure 2.19 shows the changes of ΔE_P as a function of scan rate for iNOSoxy in the ionic liquid/H_2O system and the ionic liquid/D_2O system. The higher ΔE_P of iNOSoxy in ionic liquid with added D_2O indicates slower kinetics of electron transfer when only deuterons are available. This indicates that deuterons do not facilitate rapid electron transfer as compared to protons, and points to proton involvement as a potential limiting factor in electron transfer and protein function.

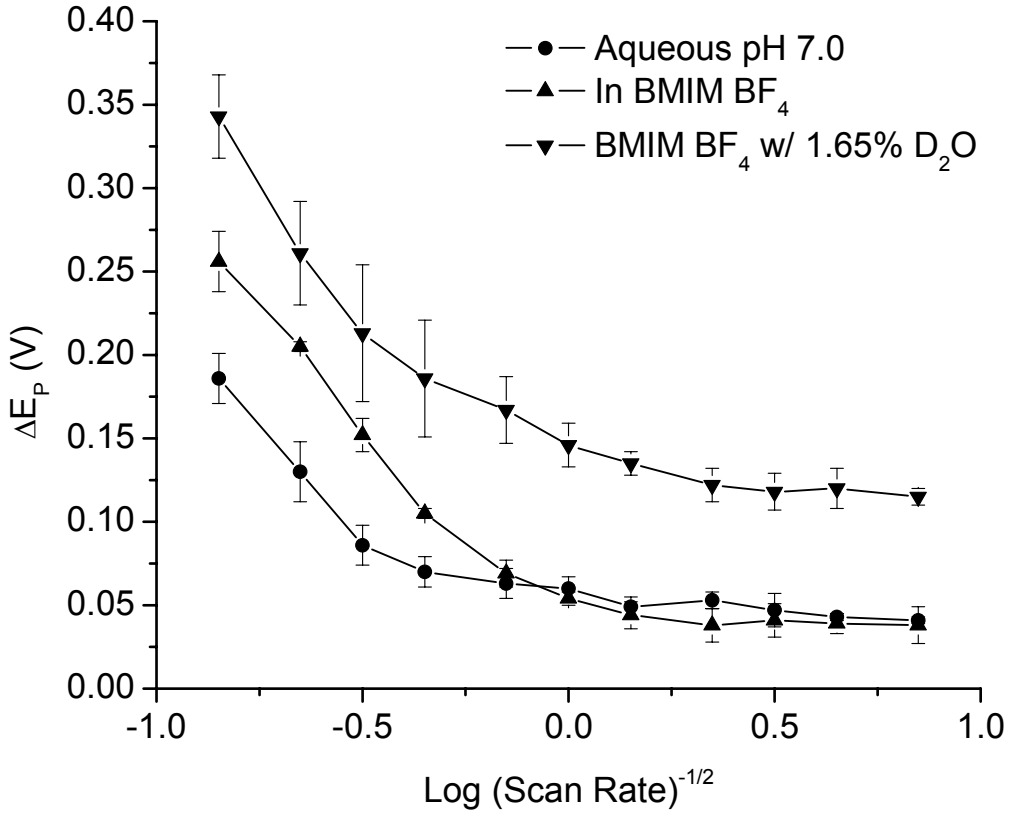

Figure 2.19: iNOSoxy (H_2O) in ionic liquid with 0.45% H_2O ▲ has higher ΔE_P as a function of scan rate as compared to iNOSoxy in aqueous ●. iNOSoxy (D_2O) in ionic liquid with 1.65% D_2O has slower electron transfer rates even at lower scan rates ▼.

Similarly, ΔE_P of myoglobin/DDAB films prepared in D_2O are compared to ΔE_P of myoglobin/DDAB films prepared in H_2O, where trace amounts of H_2O are still available in the film as a source of protons. The scan rates are again increased stepwise and the resulting ΔE_P is monitored. Since myoglobin showed faster kinetics with no added water unlike iNOSoxy, we also ran experiments with no added D_2O to the ionic liquid. Also, to compare to the iNOSoxy case, we additionally measured ΔE_P as a function of scan rate in the ionic liquid with added 1.65% D_2O. For the sake of clarity, the myoglobin aqueous data shown previously is excluded from this portion of the study.

Figure 2.20 shows that the kinetics of electron transfer to myoglobin in ionic liquid/H_2O are significantly faster than myoglobin prepared in D_2O. The addition of 1.65% D_2O shows sluggish electron transfer kinetics, slower than even the ionic liquid/H_2O system. This indicates that deuterons interfere with elementary steps of electron transfer and points to proton involvement as a potential limiting factor in electron transfer.

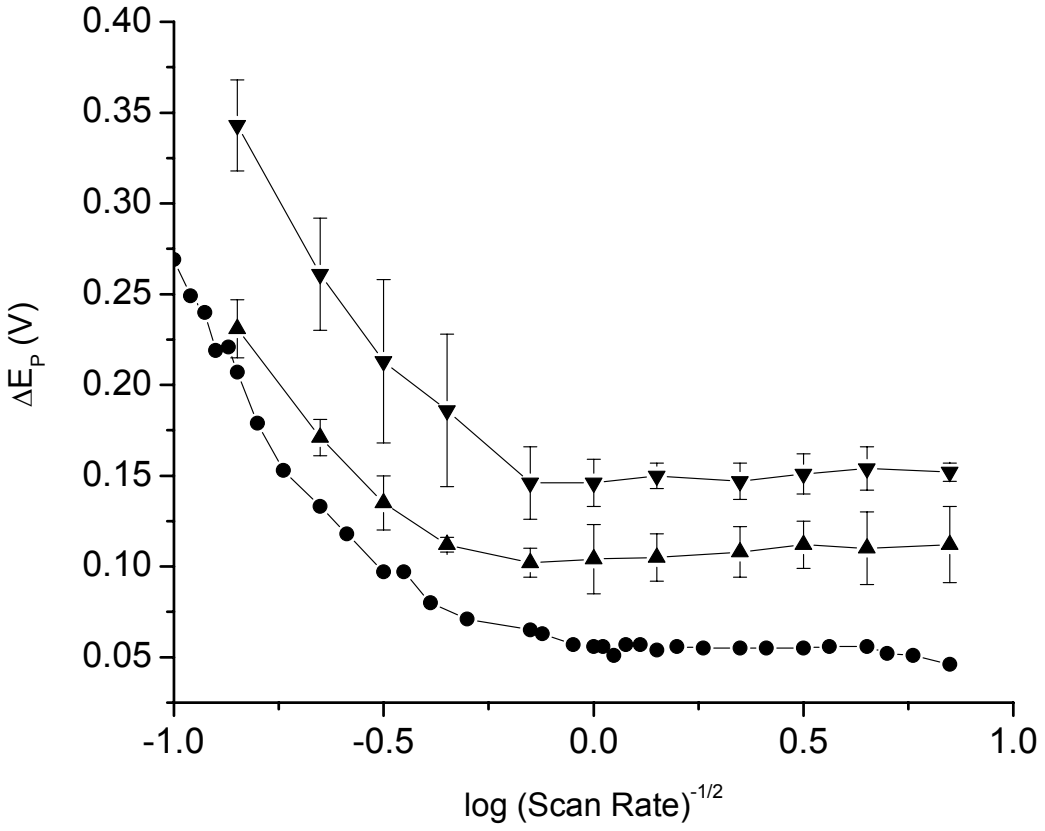

Figure 2.20: Myoglobin/D_2O in ionic liquid ▲ has a larger ΔE_P as a function of scan rate as compared to myoglobin/H_2O in ionic liquid ●. Myoglobin/D_2O in ionic liquid with 1.65% added D_2O has extremely challenged kinetics even at lower scan rates ▼.

2.4.3 Discussion

In section 2.3.2.3, we show that electron transfer to iNOSoxy is compromised when water/protons are removed, but it was not readily apparent if this effect is a result of water as a proton donor for gated electron transfer or if there are other considerations such as a loss of hydrogen bonding and/or tunneling pathways that cause the slower electron transfer. The data generated in the current section show that a replacement of

scarce protons with deuterons exacerbates the slowed kinetics of electron transfer, highlighting the role of protons as a factor to the observed slower electron transfer kinetics. Replacement of protons with deuterons has deleterious effects on electron transfer kinetics of myoglobin, as well. Myoglobin-D_2O, like iNOSoxy-D_2O, shows an overall increase in ΔE_P compared to films prepared with H_2O. Addition of the 1.65% D_2O further increases ΔE_P, an indication of deuteron-driven compromised kinetics of electron transfer. The behavior of both hemeproteins in the presence of D2O seems to point to elementary steps of proton transfer governing the overall kinetics of electron transfer.

2.5 Characterization of the Effect of Tetrahydrobiopterin-NOS Binding in Thin Film Bathed in Ionic Liquids

Earlier studies in aqueous systems established that substrate arginine and cofactor pterin binding to NOS enzymes causes the heme iron spin state to shift from low-spin to high-spin and helps facilitate electron transfer to the heme active site[19]. This process, which can be seen spectroscopically as a blue-shift in the Soret band, results in a more positive formal reduction potential of the Fe-III/Fe-II redox couple. Aqueous studies suggest that this shift can be as great as 0.100 V upon binding of the cofactor tetrahydrobiopterin[20]. The ionic liquid medium, as noted previously, limits the available amount of water and protons. As tetrahydrobiopterin binding at the docking site involves hydrogen bonding, we next examine if cofactor binding is affected by limited bulk water in dry ionic liquid.

2.5.1 Experimental

NOS is prepared and purified as mentioned in section 2.3.1.1. In this section, tetrahydrobiopterin (H_4B) is added to the aqueous NOS on a 10:1 mol/mole heme basis and allowed to equilibrate for four hours to allow proper time for the cofactor to bind. As a control, additional electrodes are prepared as above, but without the added cofactor. All other experimental factors are consistent with those previously reported.

To determine how cofactor binding affects the speed of electron transfer to iNOSoxy, we measure ΔE_P at various scan rates and compare to iNOSoxy without cofactor. We also use square wave voltammetry (SWV) to ascertain the formal potential of the redox couple, comparing the formal reduction potential of iNOSoxy without H_4B to NOS with the cofactor present.

2.5.2 Results and Discussion

As was discovered earlier in sections 2.3 and 2.4, electron transfer to iNOSoxy is very sluggish in low-water (<0.01%) conditions. This is also the case with the cofactor H_4B present, as well, prompting the addition of water as in previous experiments. Figure 2.21 shows ΔE_P as a function of log (scan rate)$^{-1/2}$ for the two systems (with and without cofactor) after addition of 1.65% water, where differences in ΔE_P between the NOS-only

and NOS-H_4B electrodes became measureable. In this experimental trial, ΔE_P is approximately 0.012 V lower in the presence of the enzyme cofactor over the entire range of scan rates.

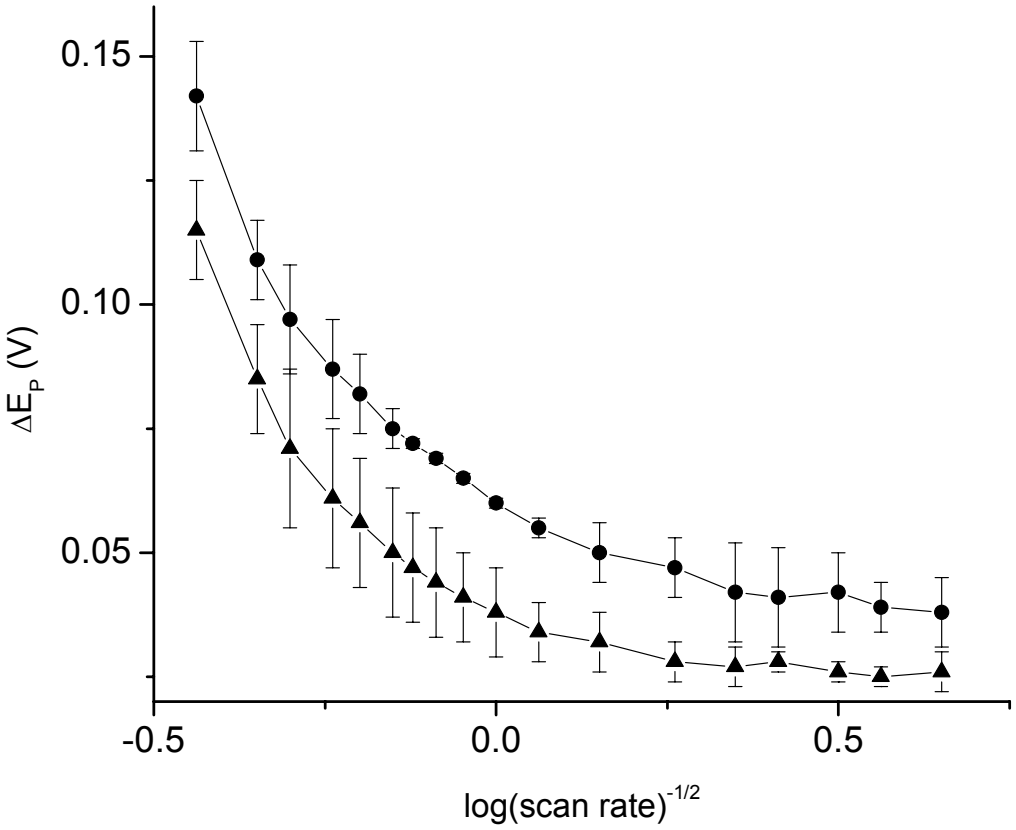

Figure 2.21: ΔE_P of iNOSoxy/DDAB with pterin cofactor in ionic liquid with 1.65% water added ▲ as compared to iNOSoxy/DDAB without pterin cofactor ●.

The kinetic data indicates that electron transfer is facilitated by the presence of H_4B. We also examined the square wave voltammetry of iNOSoxy protein with and without pterin cofactor to determine if the presence of H_4B affects the formal reduction potential of the heme iron. Figure 2.22 shows overlaid square wave voltammograms for the protein with and without the cofactor present. Though not as sharp a contrast to one another as was found in the aqueous studies cited earlier[20], the formal reduction potential of iNOSoxy with bound pterin is shifted about 30 mV toward positive potential as compared to iNOSoxy without bound cofactor.

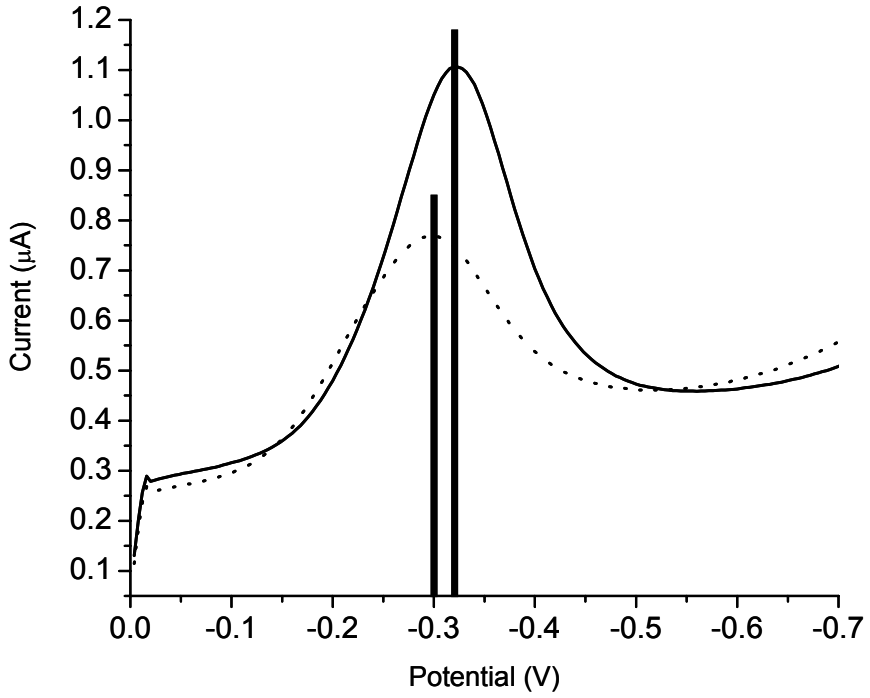

Figure 2.22: SWV of iNOSoxy/DDAB with cofactor in ionic liquid with 1.65% water added (···) has a lower formal reduction potential as compared to iNOSoxy/DDAB without cofactor tetrahydrobiopterin (—).

Tetrahydrobiopterin clearly plays a role in facilitating electron transfer to the NOS oxygenase active site even in low-water conditions, though the effect is less pronounced than in aqueous systems. There is a marked difference in kinetics that translates into lower activation energy for the Fe III/Fe II redox couple.

2.6 Chapter II Summary and Conclusions: A Comparison of Differential Behaviors of Myoglobin vs. NOS

In section 2.1, we see how characterization of NOS and myoglobin films confirms protein stability in the ionic liquid system, as had been reported in previous examples in the literature[21-24]. In section 2.2, we see how electron transfer to myoglobin actually improves in the low-water ionic liquid medium, while in the case of iNOSoxy, it is shown in section 2.3 that a lack of available water hinders electron transfer. It is speculated that structural differences between NOS and myoglobin, the relative size of the molecules, and the availability of structured water at the protein surface may cause the NOS to be sluggish while myoglobin actually has improved electron transfer kinetics.

In the study involving D_2O, we find that electron transfer to both proteins is slower when the few available water molecules in the film are replaced with deuterium oxide by exchange from the bulk. This leads to the conclusion that another contributing factor to the sluggish electron transfer to NOS is not necessarily a lack of available water as a molecular entity, but the lack of protons that the water provides. When protons are

available in limited supply, electron transfer to myoglobin is faster than in aqueous systems, though a near-absence of protons slows electron transfer to myoglobin, as was seen in the experiment involving D_2O.

iNOSoxy, in contrast to myoglobin, does not allow for rapid electron transfer with limited protons, which again is likely related to structure and the mobility of the limited water in and around the protein's active site. It follows that iNOSoxy, another molecule with proton-mediated electron transfer, would also not function well in the D_2O system, as is found in section 2.4. So, with myoglobin, we have a structure that allows protein function when protons are limited, while NOS has limited function, though both proteins do not function well when deuterons are substituted for protons.

In the presence of bound tetrahydrobiopterin, the cofactor clearly plays a role in facilitating electron transfer to the NOS oxygenase active site even in low-water solutions. There is a pronounced enhancement of kinetics of electron transfer to the Fe III active site. A major flaw with this portion of the study is that we cannot truly examine cofactor binding to NOS in the low-water environment, as the cofactor binding in this study occurs when the NOS is in aqueous solution.

2.7 References

1. Bayachou, M., Lin, R., Cho, W., and Farmer, P.J. (1998). Electrochemical Reduction of NO by Myoglobin in Surfactant Film: Characterization and Reactivity of the Nitroxyl (NO-) Adduct. Journal of the American Chemical Society *120*, 9888-9893.
2. Rusling, J.F., Nassar, Alaa Eldin F. (1993). Enhanced electron transfer for myoglobin in surfactant films on electrodes. Journal of the American Chemical Society *115*, 11891-11897.
3. Sivakolundu, S.G., and Mabrouk, P.A. (2000). Cytochrome c Structure and Redox Function in Mixed Solvents Are Determined by the Dielectric Constant. Journal of the American Chemical Society *122*, 1513-1521.
4. Zhang, C., Tarhan, E.; Ramdas, A.K.; Weiner, A.M.; Durbin, Stephen M. (2004). Broadened Far-Infrared Absorption Spectra for Hydrated and Dehydrated Myoglobin. Journal of Physical Chemistry B *108*, 10077-10082.
5. Presswala, L., Matthews, M.E., Atkinson, I., Najjar, O., Gerhardstein, N., Moran, J., Wei, R., and Riga, A.T. (2008). Discovery of bound and unbound waters in crystalline amino acids revealed by thermal analysis. Journal of Thermal Analysis and Calorimetry *93*, 295-300.
6. Ghosh, D., Abu-Soud, H.M., and Stuehr, D.J. (1995). Reconstitution of the Second Step in NO Synthesis Using the Isolated Oxygenase and Reductase Domains of Macrophage NO Synthase. Biochemistry *34*, 11316-11320.

7. Wang, J., Stuehr, D.J., Ikedo-Saito, M., and Rousseau, D.L. (1993). Heme Coordination and Structure of the Catalytic Site in Nitric Oxide Synthase. Journal of Biological Chemistry *268*, 22255-22258.

8. Nassar, A.E.F., Willis, W. S.; Rusling, James F. (1995). Electron Transfer from Electrodes to Myoglobin: Facilitated in Surfactant Films and Blocked by Adsorbed Biomacromolecules. Analytical Chemistry *67*, 2386-2392.

9. Lewandowski, A., Osinska, M., Swiderska-Mocek, A., and Galinski, M. (2008). A cryptate reference electrode for ionic liquids Electroanalysis *20*, 1903-1908.

10. Evans, R.G., Klymenko, O.V., Hardacre, C., Seddon, K.R., and Compton, R.G. (2003). Oxidation of N,N,N',N'-tetraalkyl-para-phenylenediamines in a series of room temperature ionic liquids incorporating the bis(trifluoromethylsulfonyl)imide anion. Journal of Electroanalytical Chemistry *556*, 179-188.

11. Bard, A.J., and Faulkner, L.R. (2000). Electrochemical Methods: Fundamentals and Applications, 2nd Edition (Wiley & Co.).

12. Lin, J., Balabin, I.A., and Beratan, D.N. (2005). The Nature of Aqueous Tunneling Pathways Between Electron-Transfer Proteins 10.1126/science.1118316. Science *310*, 1311-1313.

13. Moser, C.C., Chobot, S.E., Page, C.C., and Dutton, P.L. (2008). Distance metrics for heme protein electron tunneling. Biochimica et Biophysica Acta, Bioenergetics *1777*, 1032-1037.

14. Zhang, Z., Komives, E.A., Sugio, S., Blacklow, S.C., Narayana, N., Xuong, N.H., Stock, A.M., Petsko, G.A., and Ringe, D. (1999). The Role of Water in the Catalytic Efficiency of Triosephosphate Isomerase. Biochemistry *38*, 4389-4397.

15. Tu, C.K., Rowlett, R.S., Tripp, B.C., Ferry, J.G., and Silverman, D.N. (2002). Chemical Rescue of Proton Transfer in Catalysis by Carbonic Anhydrases in the ß- and C-Class. Biochemistry *41*, 15429-15435.

16. O'Donoghue, A.C., Amyes, T.L., and Richard, J.P. (2008). Slow proton transfer from the hydrogen-labelled carboxylic acid side chain (Glu-165) of triosephosphate isomerase to imidazole buffer in D2O. Organic & Biomolecular Chemistry *6*, 391-396.

17. Mie, Y., Yamada, C., Uno, T., Neya, S., Mizutani, F., Nishiyama, K., and Taniguchi, I. (2005). Notable deuterium effect on the electron transfer rate of myoglobin. Chemical communications *2*, 250-252.

18. Kang, S.A., Hoke, K.R., and Crane, B.R. (2006). Solvent isotope effects on interfacial protein electron transfer in crystals and electrode films. Journal of the American Chemical Society *128*, 2346-2355.

19. Werner, E.R.G., Antonius C. F.; Heller, Regine; Werner-felmayer, Gabriele; Mayer, Bernd. (2003). Tetrahydrobiopterin and nitric oxide: Mechanistic and pharmacological aspects. Experimental Biology and Medicine *228*, 1291-1302.

20. Boutros, J. (2007). Molecular function of nitric oxide synthase (NOS): Direct electrochemical investigation (Cleveland, Ohio: Cleveland State University).

21. Baker, S.N., McCleskey, T.M., Pandey, S., and Baker, G.A. (2004). Fluorescence studies of protein thermostability in ionic liquids. Chemical Communications *2004*, 940-941.

22. Olivier-Bourbigou, H., and Magna, L. (2002). Ionic liquids: perspectives for organic and catalytic reactions. Journal of Molecular Catalysis A: Chemical *182-183*, 419-437.

23. Park, S., and Kazlauskas, R.J. (2003). Biocatalysis in ionic liquids: advantages beyond green technology. Current Opinion in Biotechnology *14*, 432-437.

24. Welton, T. (2004). Review: Ionic liquids in catalysis. Coordination Chemistry Reviews *248*, 2459-2477.

CHAPTER III

CATALYTIC REDUCTIONS BY HEMEPROTEINS IN IONIC LIQUIDS

3.1 Metalloprotein-Mediated Reduction of Oxygen in Ionic Liquid as a Function of Added Water

In this study, we limit water levels and residual protons intrinsic to the ionic liquid BMIM BF_4 to examine the role that water in the film and bound to the protein has in catalytic reduction. We electrochemically drive metalloprotein-mediated catalytic reduction of oxygen in the non-aqueous ionic liquid environment and quantitatively study the changes in catalytic efficiency as a function of added water in order to gain an understanding of how proton supply helps regulate catalytic performance of the hemeproteins in question.

3.1.1 Experimental

Lyophilized horse skeletal muscle myoglobin (Sigma) is solubilized in distilled water, as previously detailed in section 2.2.1.1 and concentrated to approximately 0.75 mM. iNOSoxy preparation has also been outlined in detail (section 2.3.1.1) and is concentrated to c. 30 μM. Distilled water, 10 mM DDAB, and ionic liquid BMIM BF_4 are all prepared as previously described. Dissolved oxygen is removed by purging as previously described, and is reintroduced before catalysis by bubbling dry air. Linde Gas, <68 ppm H_2O, 19.5-23.5% O_2 (w/w) is used as a source of oxygen for the catalytic measurements. Basal-plane oriented pyrolytic graphite (PG) working electrodes are fabricated, prepared, and cast with protein/DDAB films as previously described. All other aspects of experimental set-up are as previously described. For baseline redox data, cyclic voltammetry (CV) is performed in oxygen-free BMIM BF_4 at varied scan rates as indicated for each experiment. For catalytic measurements, redox baseline current is compared to data collected after the addition of substrate oxygen. The quotient of the currents before and after the introduction of O_2 is reported as catalytic efficiency for each scan rate.

3.1.2 Results

The ratio of the reductive current at a saturated level of oxygen to baseline redox current at scan rates between 0.020 V/sec and 5.0 V/sec is reported as catalytic

efficiency. This is repeated with low levels of added water to note changes in the catalytic efficiency of myoglobin. The catalytic efficiency is plotted vs. log scan rate. Myoglobin-mediated catalytic reduction of oxygen is first measured in the unmodified dry (<0.01% water) ionic liquid. Water is subsequently added in 1.65% (v/v) aliquots to note resulting changes. Figure 3.1 shows that, though significantly lower than in aqueous systems, the catalytic reduction is substantial in the <0.01% water environment. Addition of water incrementally increases the catalytic efficiency, though not quite to parity with the aqueous system, as shown in Figure 3.2.

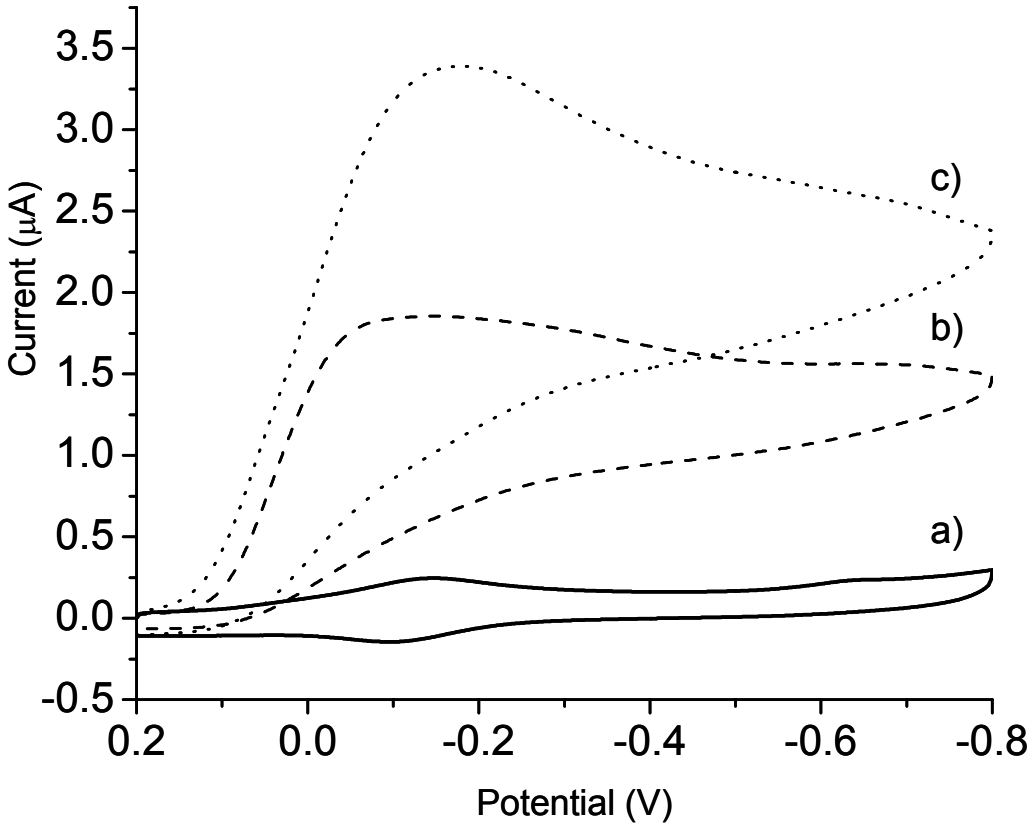

Figure 3.1: Myoglobin-mediated reduction of oxygen in ionic liquid BMIM BF_4. (a) baseline redox current, b) with saturated level of oxygen and no added water, c) with oxygen after addition of 1.65% water. Scan rate = 0.020 V/sec.

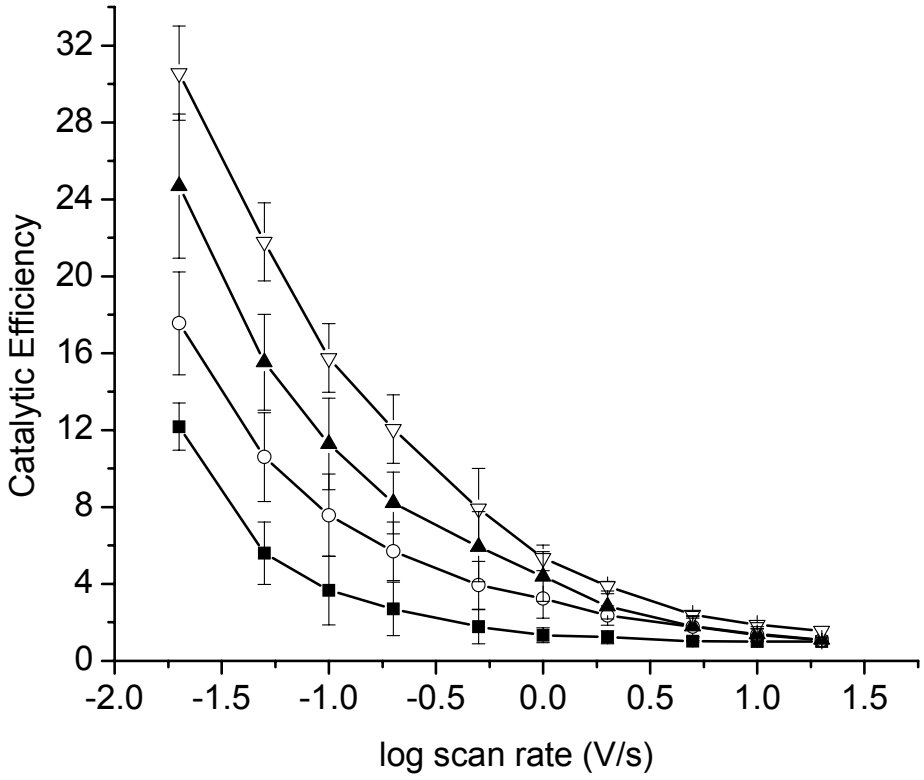

Figure 3.2: The increase in myoglobin catalytic efficiency as a function of added water in ionic liquid plotted vs. log scan rate, ■ with no added water, ○ 1.65% added water, ▲ 3.30% added water, and ▽ aqueous buffer.

Similar studies in iNOSoxy films show that catalysis is almost prohibited in the low water environment (figure 3.3a) indicating that the protein film does not adequately support catalytic activity under these conditions. However, after similar additions of water, in this case only after 1.65% was added, the catalytic efficiency was increased dramatically, as shown in Figure 3.3b. This increase in efficiency with only 1.65% added water is almost to parity with the aqueous system, as shown in Figure 3.4.

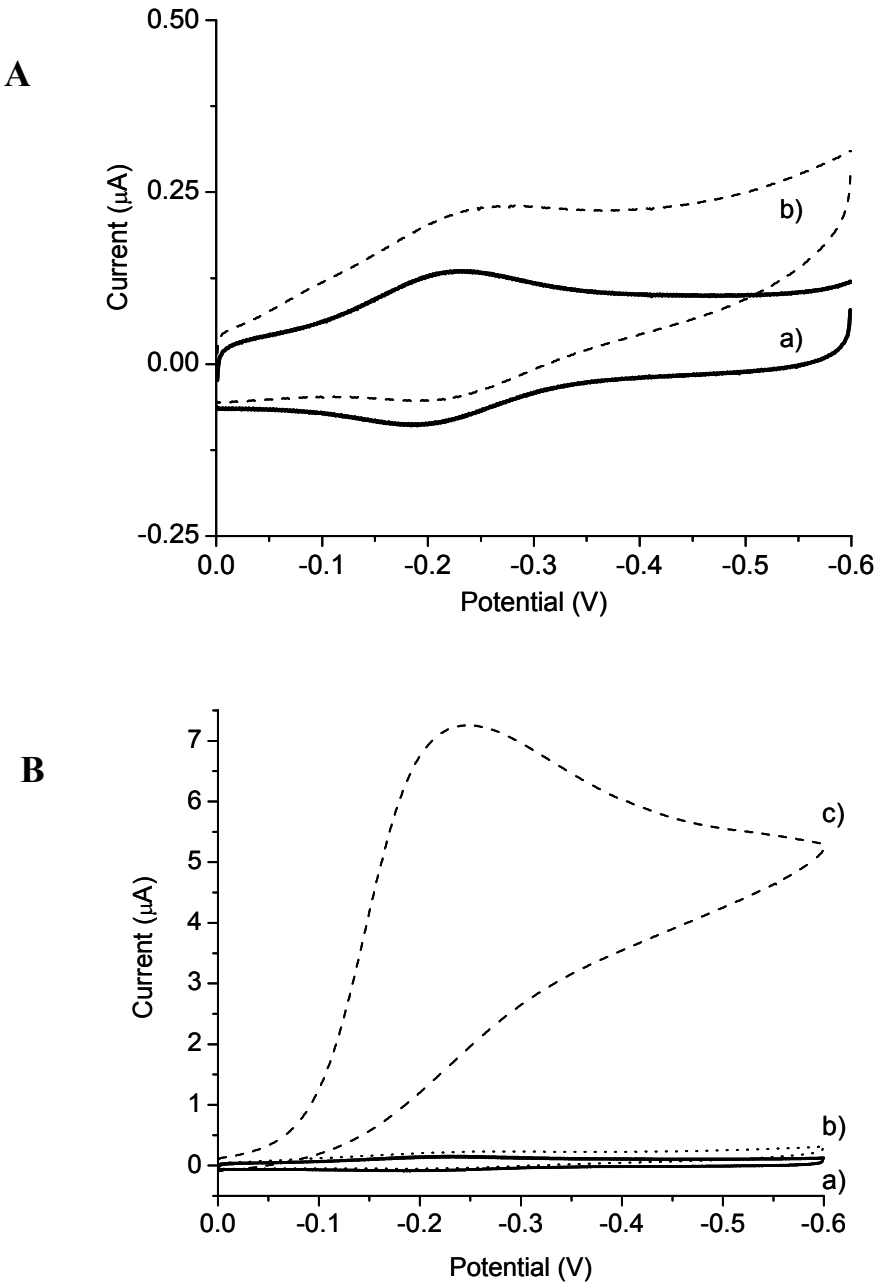

Figure 3.3: **A** (top figure) shows (a) just the baseline redox current and (b) the current after oxygen is added to the system. **B** (bottom figure) shows the same two currents with increased y-axis scale along with (c) 1.65% water. Scan rate = 0.020 V/sec.

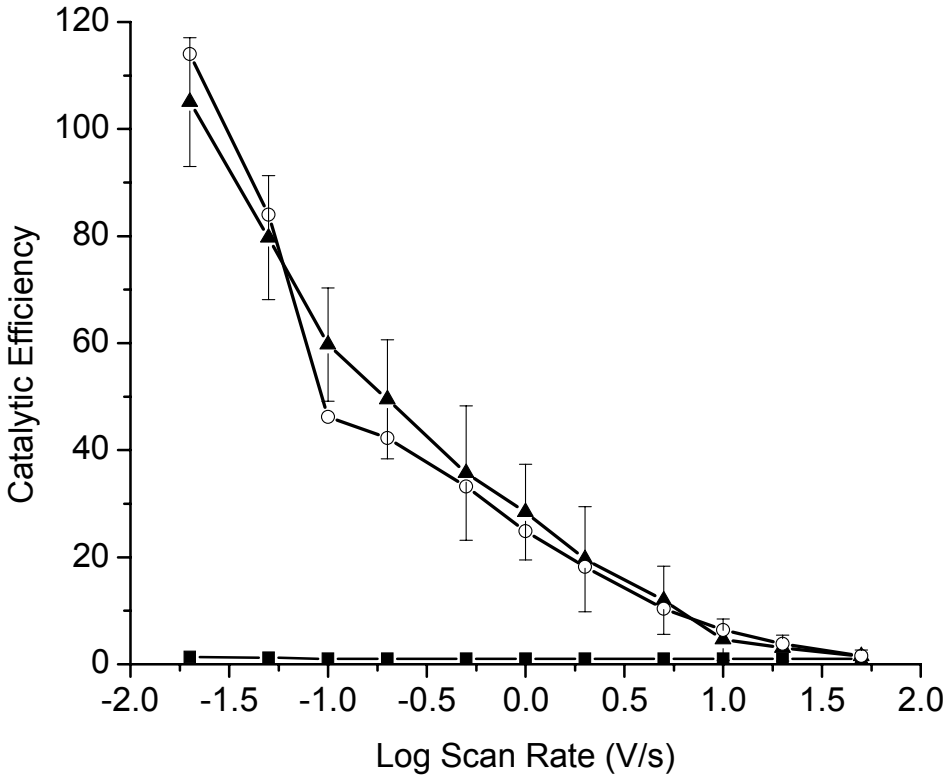

Figure 3.4: The increase in iNOSoxy-mediated catalytic efficiency as a function of added water plotted vs. log scan rate, ■ with no added water, ○ 1.65% added water, vs. ▲ aqueous buffer.

3.1.3 Discussion

The multifaceted role that water plays in electron transfer to proteins and in reductive catalysis makes it difficult to predict the exact effect that limited water in the global environment will have on catalysis and electron transfer kinetics and thermodynamics. Structural and hydrophobic differences may cause different proteins to respond uniquely to changes in water levels in their immediate environment.

We find that electron transfer characteristics to myoglobin in the nearly anhydrous ionic liquid environment actually improve as a result of limited water/proton levels, while in the case of iNOSoxy, redox properties become more sluggish in the near-total absence of water, a sign that iNOSoxy does not exchange efficient electron transfer when water and/or protons are extremely limited.

Heme-mediated catalytic reduction of oxygen has been shown to yield mainly H_2O_2. The two-electron catalytic reduction of O_2 to H_2O_2[1], where protons are necessary not only for proton-gated electron transfer[2], but are also consumed during the catalytic cycle[3-5], is more likely to be affected by the limited levels of protons/water[4]. The absence of water now needs to be examined for two separate effects: how it affects the kinetics and thermodynamics of electron transfers[6-9] that are essential to the catalytic cycle, and how the lack of protons can also possibly act as a limiting co-substrate in that cycle. Thus, even with more favorable electron transfer kinetics (as shown with myoglobin), proton availability may still confound the catalytic process.

The catalytic efficiency of myoglobin in the dry ionic liquid is only about half of that in water, indicating that though the electron transfer kinetics are favorable for catalysis, it is the lack of availability of protons as a feedstock that causes the reductive catalytic process to be less efficient than in aqueous systems. In accordance with this view, it is shown that the addition of small amounts (1.65% and 3.30%) of water to the nearly-aprotic global environment incrementally increases the catalytic efficiency of myoglobin to nearly the same level as the aqueous system. Again, this lowered catalytic

efficiency of myoglobin in the dry ionic liquid environment points to an increased demand on a limited quantity of protons, which only clearly appears during catalysis and is not as limiting in one-electron redox reactions in the absence of oxygen.

iNOSoxy exhibits a different scenario. The limited ability of iNOSoxy to transfer electrons in dry ionic liquid would seem to automatically translate to an inefficient catalytic reduction of oxygen, where multiple electron transfers must occur, coupled with a relative lack of protons that are essential to the catalytic process.

In the case of iNOSoxy, catalysis is severely limited and almost non-existent in the dry ionic liquid. Providing further evidence that there is a minimum amount of water needed for iNOSoxy to mediate oxygen reduction, there is tremendous improvement in catalytic response when even small aliquots (1.65%) of water are added to the bulk ionic liquid. iNOSoxy, which, unlike myoglobin, naturally carries oxygen catalytic processes as part of its function, only seems to require a small amount of water and protons to bring catalytic efficiency up to the level of the aqueous system. This could give another view to explain how the different NOS isoforms in different cellular environments exhibit varying catalytic activities. The difference in catalytic response between the two proteins also highlights the importance of water levels in relation to catalytic efficiency and, more importantly, shows that each protein has a different intrinsic response when placed under almost identical conditions.

Both proteins have similar amounts of available water in their protein/DDAB films. The protein-lipid bilayer films, used because of their increased efficiency while using very small quantities of protein in the film, [10-14] typically carry water levels between 5-6%, as protein-bound water cannot be easily removed by our current methods. Therefore, the observed changes in protein catalytic function must come back to structural differences.

Both proteins are performing the same catalytic function with approximately the same percentage of water in the film under dry conditions, yet they show vast differences in their ability to catalyze the reduction of oxygen in this environment. As was discussed previously (section 2.3.2.3), iNOSoxy has a larger, more complex structure as compared to myoglobin, and may not be able to reorient itself in the film as efficiently as myoglobin, making the redox center less accessible to the electron waveform[15]. Also previously discussed is the likely lack of structured water close to the protein molecule[16] (based on Protein Data Bank samples previously referenced), and size disparity between the two proteins which could lead to exponential electronic coupling decay[17] in iNOSoxy but not in myoglobin. The ability of bulk water to diffuse into the heme pocket may also be limited, which could also be deleterious to the process, where catalytic reduction only occurs to an appreciable degree after the addition of water. Also, iNOSoxy-mediated catalytic reduction is designed to only occur *in vivo* with bound tetrahydrobiopterin and L-arginine, which serve to change the electron configuration of the heme iron to a penta-coordinate high-spin state, allowing for efficient electron transfer. The lack of stabilizing pterin cofactor and substrate L-arginine could also be

pointed to as factors that reduce the catalytic efficiency of iNOSoxy. These factors are not essential to proper myoglobin function, which could also account for the improved electron transfer and catalytic behavior at the most-challenged 0.01% water level.

3.2 Metalloprotein-Mediated Reduction of Nitric Oxide in Ionic Liquid as a Function of Added Water

As we mentioned in section 1.2.2, because of the inhibitory nature of nitric oxide to NOS function, it may be of interest to investigate catalytic functions in the presence of nitric oxide.

3.2.1 Experimental

The experimental section is identical to that outlined in section 3.1.1, with the exception that NO is added in place of O_2. NO is bubbled into a small aliquot of dry ionic liquid for a period of 30 minutes until saturation is reached. Griess Assay is used to determine NO concentration. An average of four analyses of the saturated solution indicates that NO is soluble in BMIM BF_4 at a concentration of 7.1 mM +/- 0.7 mM. To measure the catalytic reduction of NO, needed aliquots of the 7.1 mM NO solution are added to produce desired levels of NO, as will be indicated in individual experiments.

3.2.2 Results and Discussion

We first examine the myoglobin-mediated catalytic reduction of NO in aqueous systems as a basis for comparison. As shown in figure 3.5, catalytic reduction appears to be at a saturated level at the 0.07 mM NO level, as there is not much difference between peaks at 0.07 mM, 0.14 mM, and 0.21 mM. To ensure that NO concentration does not become a limiting factor in catalysis we use the 0.21 mM level in the next part of this study.

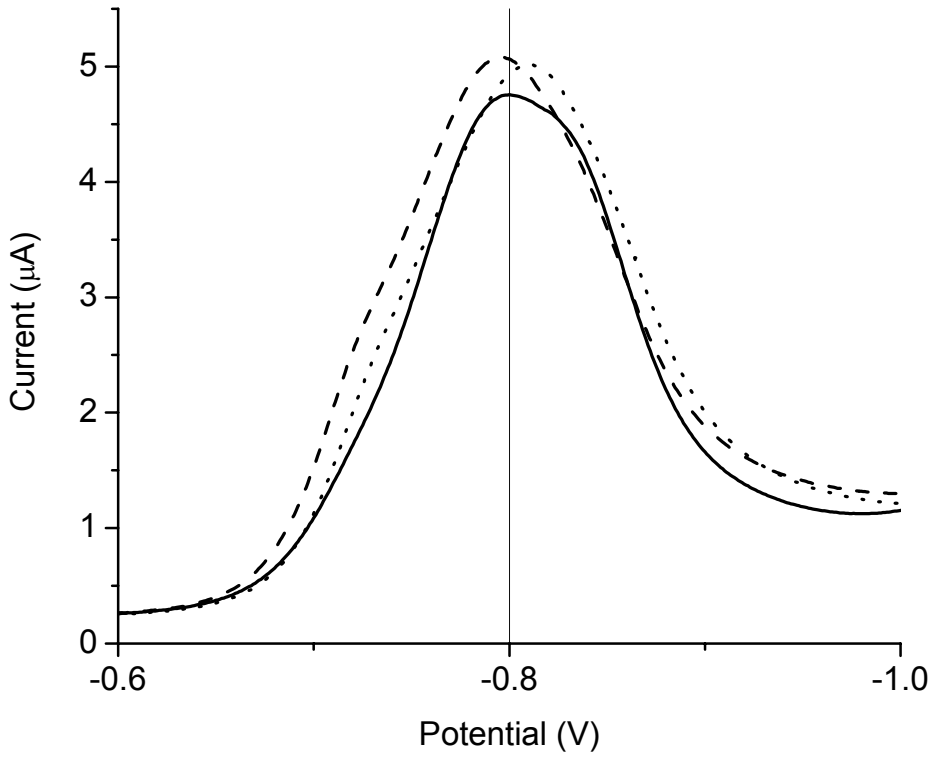

Figure 3.5: Myoglobin-mediated catalytic reduction of NO in aqueous pH 7.0 buffer with 0.07 mM NO (—), 0.14 mM NO (---) and 0.21 mM NO (···). For clarity, only the -0.6 V to – 1.0 V portion of the voltammogram is shown here.

Next we run parallel studies in the dry ionic liquid and add water as indicated. Figure 3.6a shows how myoglobin-mediated catalytic reduction of NO is sluggish, even at the highest level of NO, 0.21 mM. Figure 3.6b shows that catalytic reduction of NO improves with the addition of water. We also observe that after the addition of 6.6% water to the system the potential of the catalytic peak shifts to more positive potentials, approaching the -0.80 V threshold of the aqueous samples. Catalytic efficiency at this level of water is comparable to aqueous, based on non-catalytic current measured under the same conditions in the absence of NO.

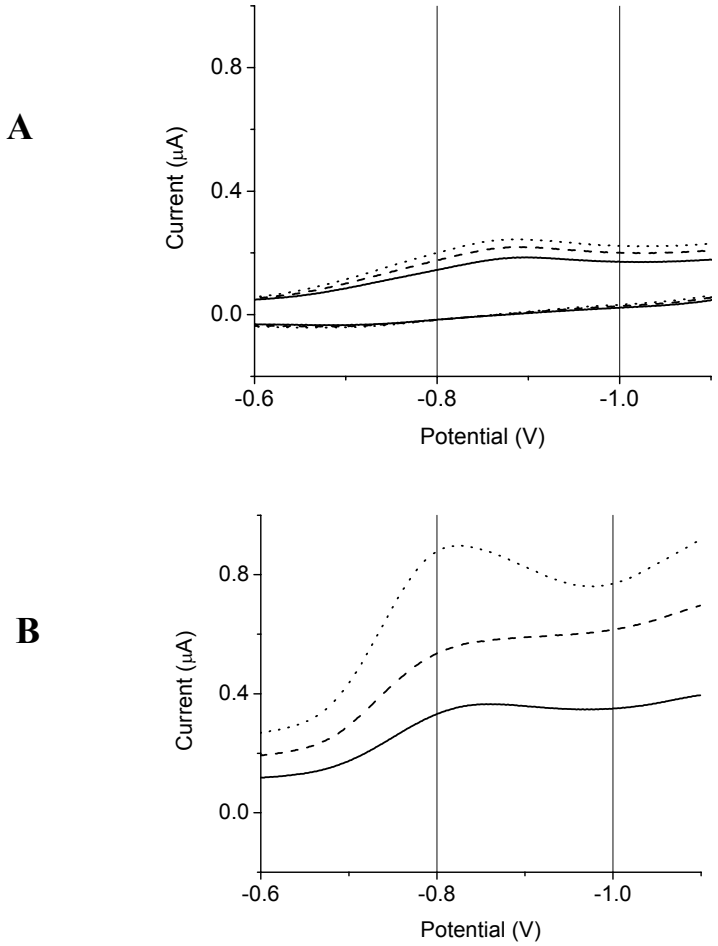

Figure 3.6 **A** (Top figure): Myoglobin-mediated catalysis in ionic liquid with 0.07 mM NO (—), 0.14 mM NO (---) and 0.21 mM NO (···). **B** (Bottom figure): After addition of 1.65% H_2O (—), 3.30% H_2O (---) and 6.60% H_2O (···). [NO] = 0.21 mM. For clarity, only the -0.6 V to – 1.1 V portion of each voltammogram is shown here.

We next examine the iNOSoxy-mediated catalytic reduction of 0.21 mM NO in aqueous systems. The iNOSoxy-mediated reduction of NO in aqueous buffer is shown in figure 3.7a, with a peak potential of -0.722 V and a catalytic efficiency of approximately 4.0 according to the ratio of catalytic peak to redox baseline. As in the myoglobin studies, catalytic reduction appears to be at a saturated level at the 0.07 mM NO level, as there is not much difference between peaks at 0.07 mM, 0.14 mM, and 0.21 mM, not shown here. To avoid complicating factors, 0.21 mM NO is used in the continuation of this study.

The experiment is then repeated with iNOSoxy films in the dry ionic liquid with water added as indicated. Figure 3.7b shows how iNOSoxy-mediated catalysis is even more sluggish than the myoglobin electrodes using NO at 0.21 mM. Figure 3.8 shows that iNOSoxy-mediated catalytic reduction of NO improves with the addition of water, but not nearly as much as the myoglobin case. Peak potential shifts to positive potentials (-0.736 V and -0.730 V) after the addition of 5.0 and 10.0% water, which approaches the -0.722 V threshold of the aqueous system. Catalytic efficiency after the addition of 10.0% water is almost equal to aqueous at approximately 4.1, based on non-catalytic (redox) current measured under the same conditions in the absence of NO.

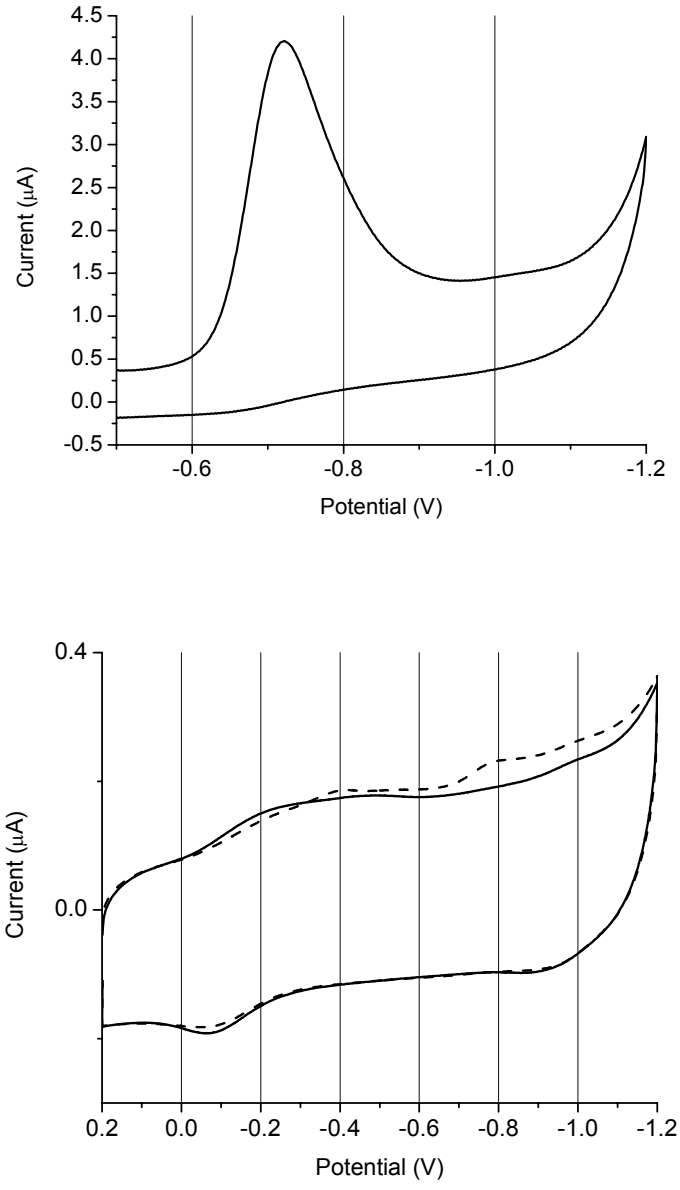

Figure 3.7: **A** (top figure) iNOSoxy-mediated catalysis in aqueous pH 7.0 buffer with 0.21 mM NO. **B** (bottom figure) iNOSoxy-mediated catalysis in BMIM BF_4 at 0.01% water with 0.21 mM NO (---) and in the absence of NO (—).

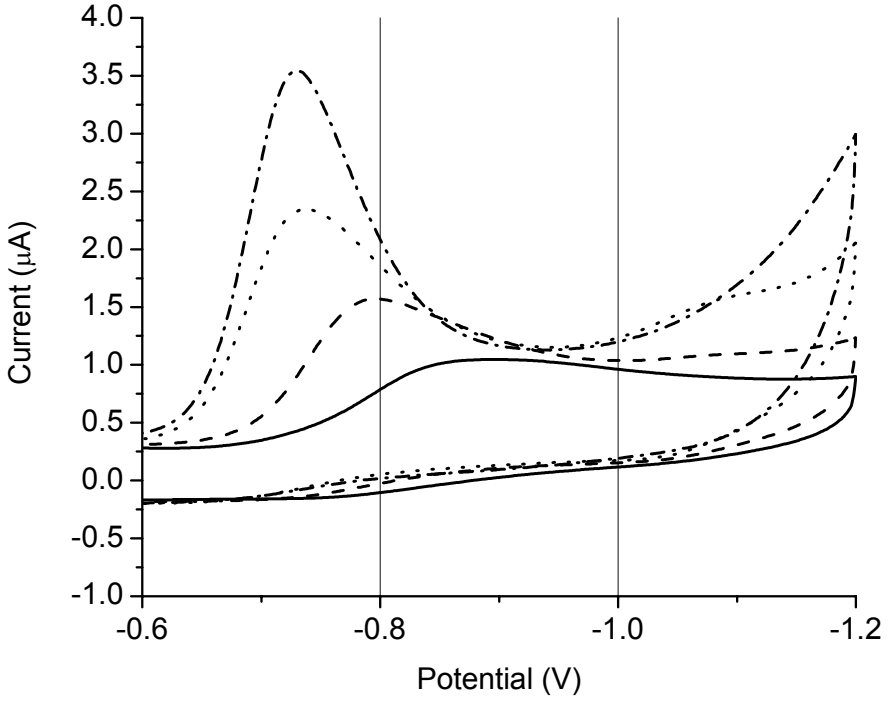

Figure 3.8: iNOSoxy-mediated catalysis in BMIM BF_4 with 0.21 mM NO at various levels of added water, 1.65% (——), 3.30% (----), 5.0% (···), and 10.0% (–·–·–·).

The metalloprotein-mediated reduction of NO occurs at much higher energies than the catalytic reduction of O_2. Catalysis in the dry ionic liquid system for both hemeproteins yields very little catalytic response, and peaks are shifted to lower potentials. The addition of water appears to aid in metalloprotein catalytic reduction. The addition of 6.60% water brings the myoglobin-mediated reduction potential to potentials seen in aqueous systems. It requires somewhat higher levels of added water (5.0-10.0 %) to bring the response of iNOSoxy system to that seen in the aqueous medium.

3.3 Metalloprotein-Mediated Reduction of O_2 in Ionic Liquid: Isotopic Effects Using D_2O

In section 2.4, we described how the substitution of D_2O for H_2O makes the kinetics of electron transfer slower as a result of proton-gated electron transfer. In the present study, we further interrogate the role of protons by adding D_2O to the BMIM BF_4 dry medium to note effects on the rate of catalysis with either myoglobin or iNOSoxy as hemeprotein catalysts.

Because the catalytic reduction of oxygen is known to involve protons, replacing protons with deuterons should have an effect on catalysis if proton transfer is a key rate determining step. By noting changes in current peak height and peak potential in the D_2O-containing environment, we will gain insights into the role of protons as a rate-determining step in catalysis. Additionally, we use D_2O/H_2O blends to further rationalize the observed changes in protein catalytic response.

3.3.1 Experimental

As noted in the redox studies involving deuterium, section 2.4.1, because of the need to replace most of the remaining water with deuterium oxide, it becomes necessary to introduce new preparatory techniques for myoglobin, DDAB, and iNOSoxy.

Lyophilized horse skeletal muscle myoglobin (Sigma) is solubilized in >99.0% deuterium oxide (Sigma-Aldrich) and purified[12] by filtering through a 30,000 MW exclusion filter membrane. The filtrate is then concentrated using a 3,000 MW filter membrane to approximately 0.75 mM. DDAB powder (Acros Organics) is solubilized in >99.0% deuterium oxide to a concentration of 10 mM and sonicated for a minimum of 4 hours until the resultant solution is clear. iNOSoxy is obtained as described before, through routine in-house expression in *E. coli* and purification of the His-tagged protein on a Ni-NTA Agarose column. iNOSoxy is further washed with D_2O to replace H_2O with D_2O. Typically, 400 μl D_2O is added to 100 μl of aqueous iNOSoxy to reduce the percentage of H_2O to 20%. The solution is allowed to equilibrate for 20 minutes and is then concentrated back to the original volume of 100 μl by centrifugation in Amicon centricon® tubes. This process is repeated 3X to drive down the relative concentration of H_2O to approximately 0.16%. This process also removes the glycerol from the iNOSoxy preparation, as described previously, while concentration is maintained at Ca. 30 μM.

Pyrolytic graphite electrodes are prepared as noted earlier (section 2.4.1), [13] and allowed to dry overnight in a dry glove box environment for 24 hours. All other experimental conditions are as previously described.

For non-catalytic redox data, cyclic voltammetry (CV) is performed in oxygen-free BMIM BF_4 at varied scan rates as indicated for each experiment. For catalytic measurements, non-catalytic redox currents are compared to currents collected after the addition of oxygen. The quotient of the two currents is reported as catalytic efficiency.

3.3.2 Results

In figure 3.9, the reductive current at a saturated level of oxygen is measured and compared to DDAB-only electrodes to observe the iNOSoxy-mediated catalytic reduction of oxygen in the relative absence of protons. There is very little difference in current and potential when comparing the two currents. The iNOSoxy-modified electrode shows slightly higher current with a small, if any, shift to positive potentials, indicating only minor protein-mediated reduction of oxygen.

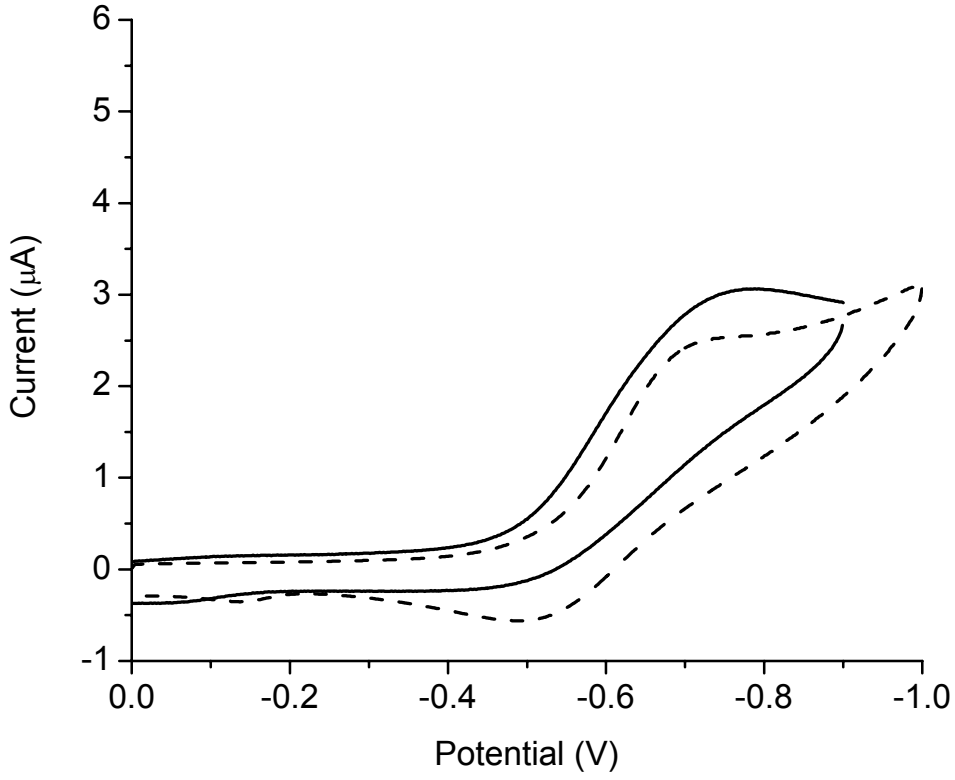

Figure 3.9: Cyclic voltammetry of iNOSoxy/DDAB in ionic liquid saturated with oxygen (──) as compared to DDAB-only electrode (-----). Scan rate = 75 mV/sec.

We repeat the scan with low levels of added D_2O (3.3%) to note any additional effects on the catalytic efficiency of the protein and compare the data to the analogous system where iNOSoxy-H_2O cast electrodes are run in ionic liquid with 3.3% added H_2O. Figure 3.10 shows the effect of the added 3.3% D_2O using iNOSoxy electrode as compared to a similar iNOSoxy electrode with added 3.3% H_2O. The reduction peak generated by the iNOSoxy with 3.3% H_2O has significantly higher peak current at very positive potentials as compared to the 3.3% D_2O system, confirming that the presence of H_2O is vital and greatly affects the outcome of enzyme-mediated reduction of oxygen.

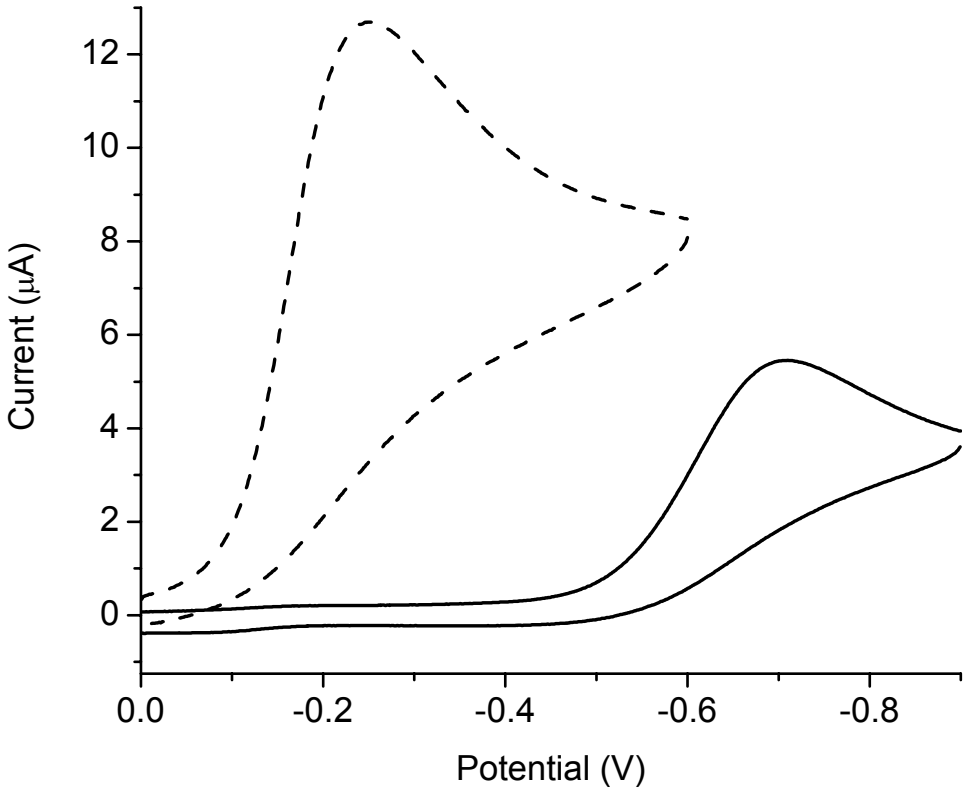

Figure 3.10: Cyclic voltammetry of iNOSoxy/DDAB in ionic liquid saturated with oxygen with 3.3% added D_2O (──) as compared to iNOSoxy/DDAB electrode in ionic liquid saturated with oxygen with 3.3% added H_2O (-----). Scan rate = 0.075 V/sec.

In analogous experiments, myoglobin-mediated catalysis is measured in the ionic liquid-D_2O system. In figure 3.11, the level of D_2O (and H_2O in the comparative CV) is less than that used in the iNOSoxy studies, 1.65% as compared to 3.30%, and scan rates are slower, with the scan rate of 0.020 V/sec used in the case of myoglobin, as compared to 0.075 V/sec for the NOS trials. Despite the minor differences in experimental set-up as compared to the NOS studies, the results show that myoglobin catalysis in the presence of controlled amounts of deuterium oxide is similar to the behavior NOS, in that the catalytic peak has been shifted to significantly higher energy with reduced current as compared to myoglobin-H_2O films run in ionic liquid with 1.65% H_2O.

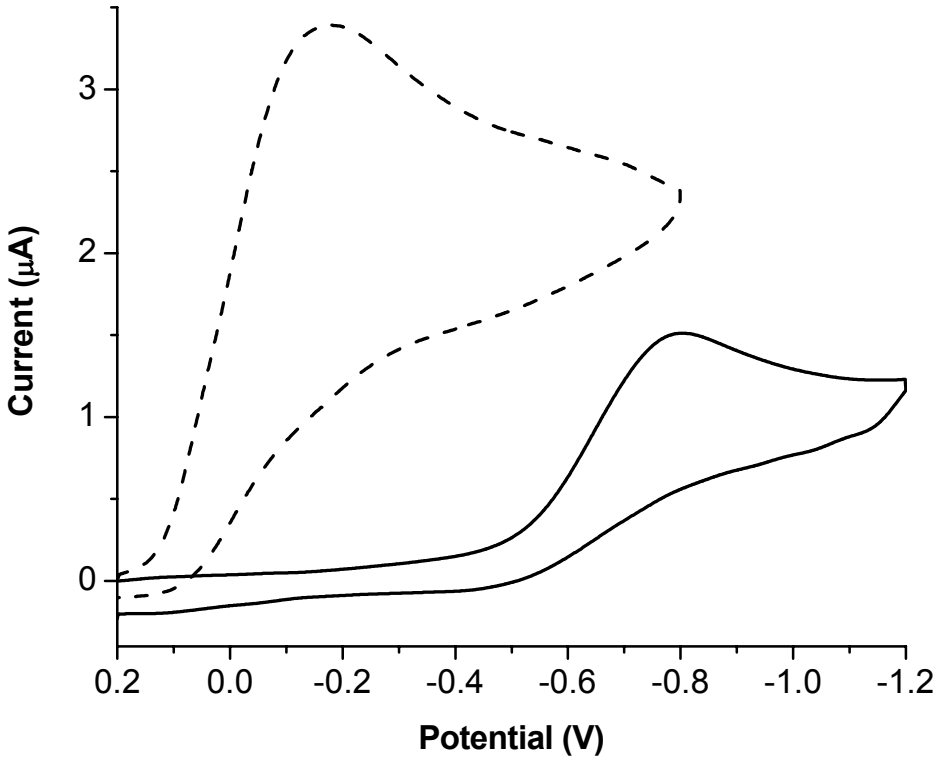

Figure 3.11: Myoglobin-D_2O/DDAB electrode in ionic liquid BMIM BF_4 saturated with oxygen after addition of 1.65% D_2O (—) as compared to myoglobin-H_2O/DDAB electrode in ionic liquid saturated with oxygen with 1.65% H_2O (-----). All scan rates are 0.020 V/sec.

3.3.3 Discussion

There is a clear difference in the catalytic response of both proteins when H_2O is replaced with D_2O, with catalytic efficiency decreasing significantly and peak current shifted to lower potentials, pointing to proton transfer and proton availability as rate-determining and limiting factors in the catalytic cycle. In section 3.1 we found that reducing the concentration of protons reduces the catalytic efficiency of both proteins, though in discreetly different ways.

In the current section 3.3 we see that replacing the limiting quantity of protons with deuterons not only limits the catalytic efficiency, it also greatly shifts catalytic peaks to relatively more negative potentials. In figure 3.9, where DDAB-only electrode is used as a control to show the non-mediated reduction of oxygen in the presence of deuterons compared to iNOSoxy electrode, we found there was a major difference: the DDAB electrode showed a relatively reversible voltammogram close to the formal potential of oxygen reduction, while the iNOSoxy electrode exhibited an irreversible voltammogram with slightly increased reduction current and a peak shifted to positive potentials. This change in behavior, though small in magnitude, is a clear indication of iNOSoxy-mediated catalytic reduction under these conditions.

In subsequent trials where D_2O is added to the medium in controlled quantities, we observe an increase in the reductive peak, though no significant change in peak potential. Figure 3.12 shows the difference between iNOSoxy electrodes in dry ionic liquid and after addition of 3.30% D_2O.

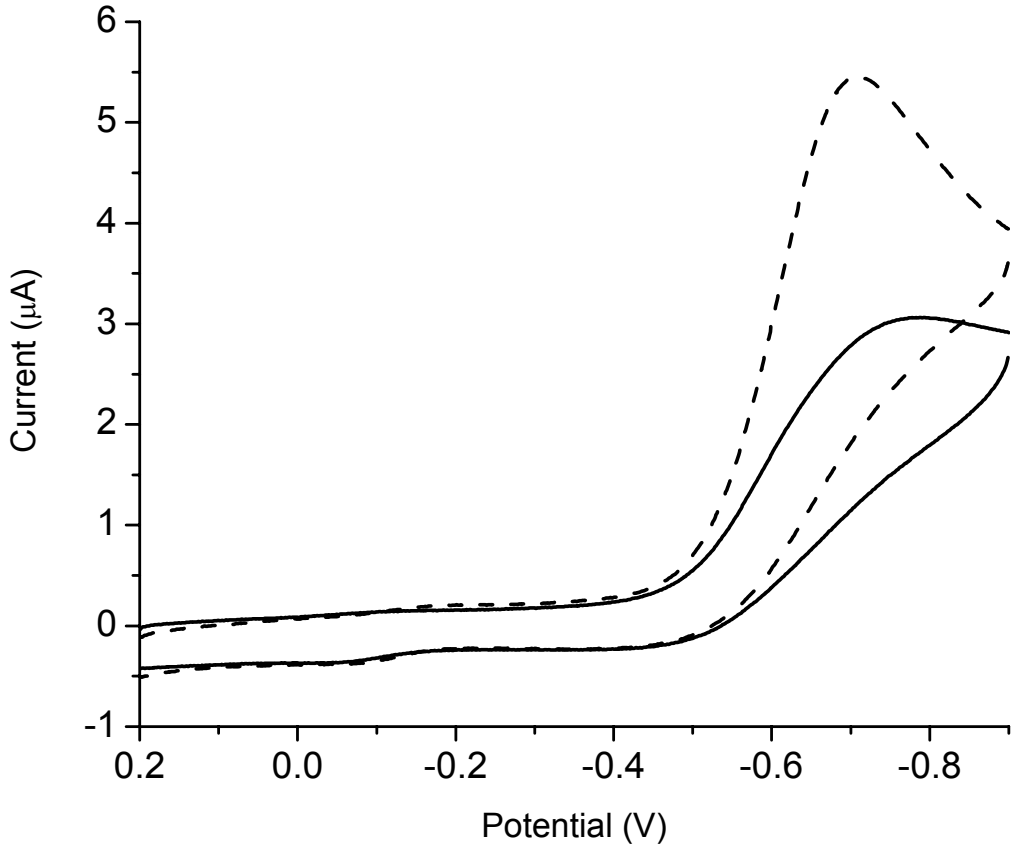

Figure 3.12: Cyclic voltammetry of iNOSoxy/DDAB in dry ionic liquid saturated with oxygen (──) as compared to iNOSoxy/DDAB electrode in ionic liquid saturated with oxygen with 3.3% added D_2O (-----). Scan rate = 0.075 V/sec.

Figure 3.13 shows that the further addition of H_2O to the ionic liquid system with D_2O not only increases catalytic peak current to a greater extent, but it also causes a shift towards positive potentials. This departure from the response seen with D_2O additions clearly highlights the role of protons in key elemental steps of iNOSoxy-mediated catalytic reduction of oxygen. The addition of 3.30% H_2O shifts the peak potential to more positive values.

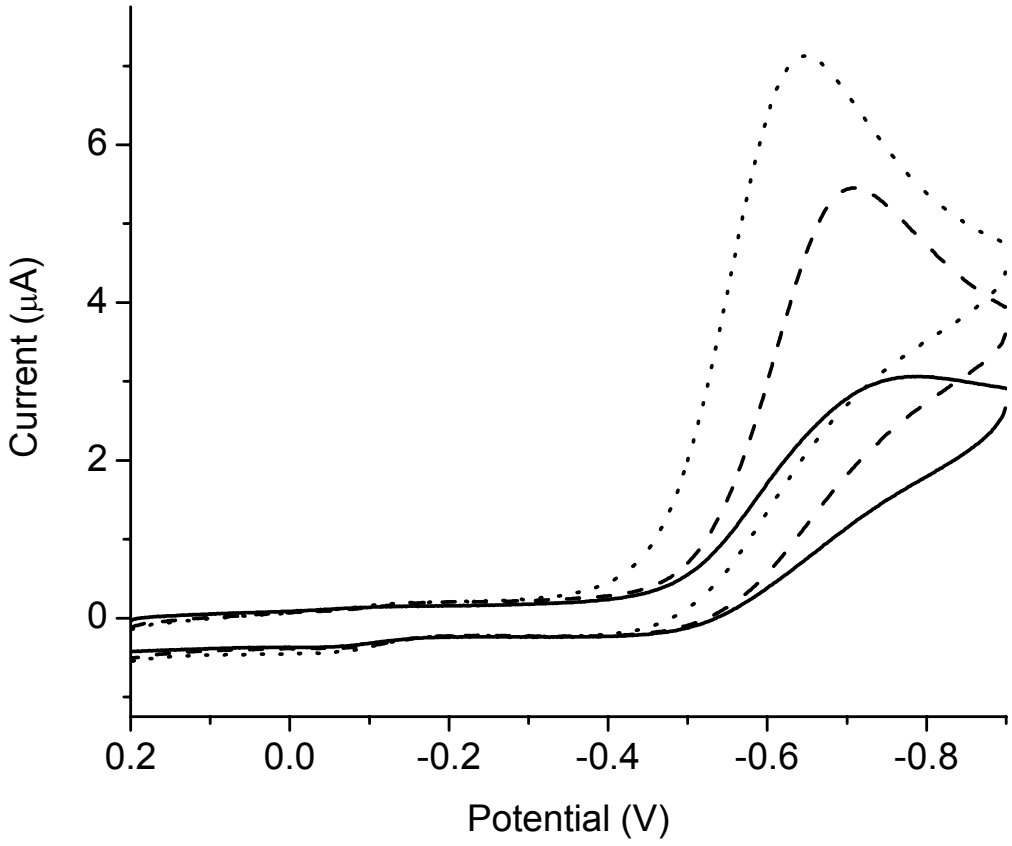

Figure 3.13: Cyclic voltammetry of iNOSoxy/DDAB in dry ionic liquid saturated with oxygen (──) as compared to iNOSoxy/DDAB electrode in ionic liquid saturated with oxygen with 3.3% added D_2O (-----) and after addition of 3.30% H_2O (····).
Scan rate = 0.075 V/sec.

Subsequent additions of water continue to shift the potential, as is shown in figure 3.14. This "hybrid" system, where both deuterons and protons are present, does not return to the peak potential of iNOSoxy-mediated reduction in ionic liquid/H_2O-only systems or aqueous buffers, but shows a definite shift toward that potential.

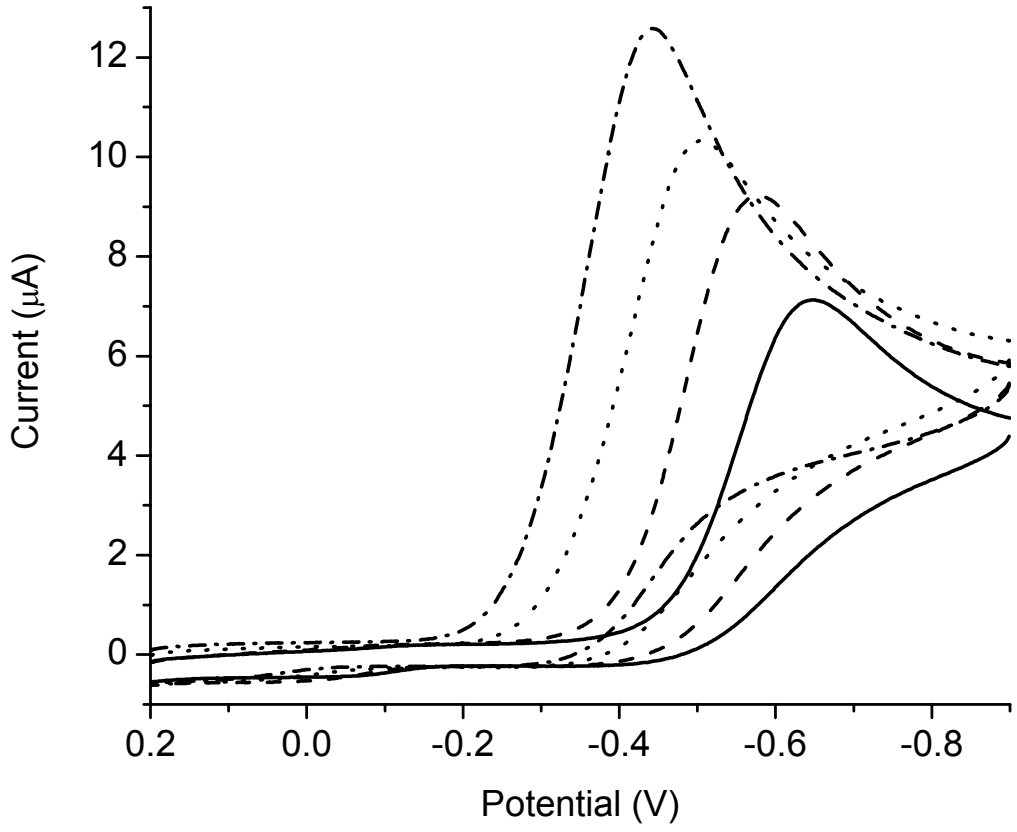

Figure 3.14: Cyclic voltammetry of iNOSoxy/DDAB in ionic liquid saturated with oxygen with 3.30% added D_2O and 3.30% H_2O (── **),** 10% H_2O (**-----**), 15% H_2O (···). and 20% (·–·–·). Scan rate = 0.075 V/sec.

Various combinations of water and deuterium oxide were used in the study of changing catalytic efficiency as a function of added H_2O and D_2O with similar results. When D_2O is added to the system, little change in peak potential occurs, which is sometimes accompanied by a slight increase in peak height, whereas the addition of H_2O almost always causes a change in peak potential and peak current. Figure 3.15 shows a voltammogram with a zoom at the peak region of this "hybrid" system that has 3.3% added D_2O and 20% added H_2O. Addition of another 10% D_2O to the medium results in little effect; however, addition of another 10% H_2O shows a continued increase in peak current accompanied by a slight shift in peak potential towards more positive potentials.

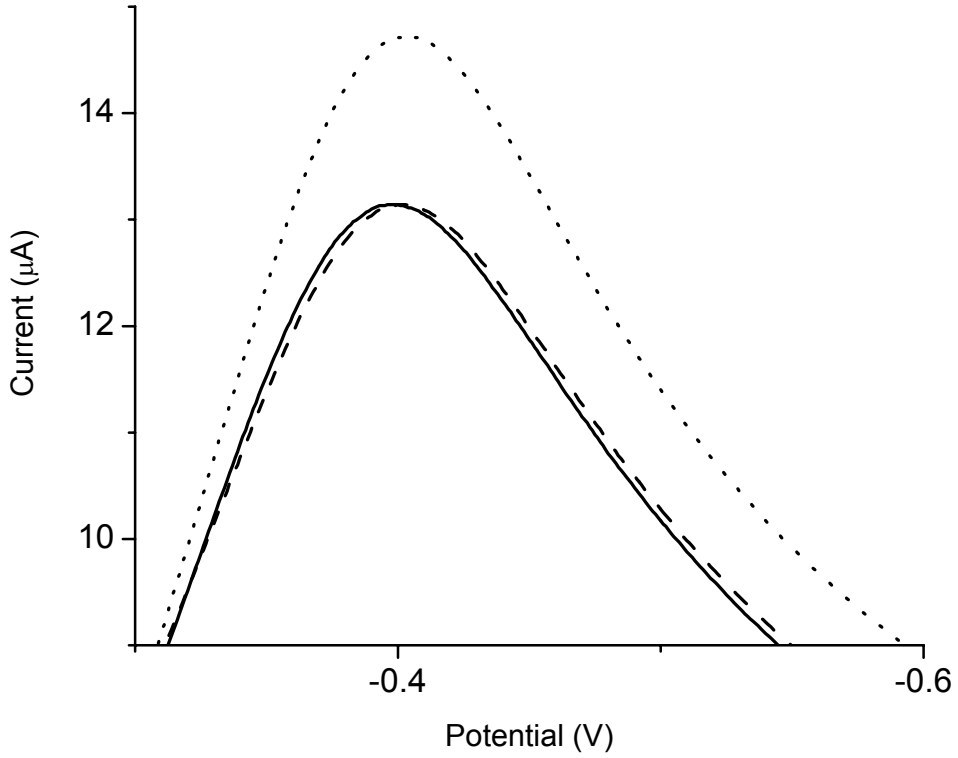

Figure 3.15: Cyclic voltammetry of iNOSoxy/DDAB in ionic liquid saturated with oxygen with 3.30% added D_2O and 20% H_2O (── **),** after an additional 10% D_2O is added (**-----**), followed by an additional 10% H_2O (····). Scan rate = 0.075 V/sec.

3.4 Chapter III Summary and Conclusions

In this chapter, we add supporting evidence that availability of protons is rate-limiting in the catalytic reduction of oxygen and nitric oxide. In the case of the myoglobin-mediated reduction of oxygen, using ionic liquid with 0.01% water is sufficient to drive catalysis, though at levels about half that of aqueous systems with a non-limiting supply of protons. iNOSoxy, on the other hand, did not effectively catalyze reduction of oxygen in this low-water environment. Adding water to each system improves the catalytic efficiency, though the results indicate that each protein requires a different level of available water/protons to bring the catalytic efficiency to levels seen in aqueous media.

Catalytic reduction of NO also shows that a lack of protons in the dry ionic liquid medium will limit the process. Also, the catalytic reduction of NO occurs at significantly lower potentials compared to aqueous systems. Adding controlled levels of water (5-10%) restores protein catalytic reduction of NO to levels seen in aqueous systems.

Isotopic effects prove that it is more the availability of protons than any other property of water that slows down the catalytic reduction of oxygen. Protons are needed in both electron transfer and catalytic reduction and a replacement with analogous deuterons, as expected, inhibited both processes. Addition of H_2O to the system partially restores catalytic efficiency, but the presence of deuterons does not allow the catalysis to occur at the same low energy potentials as a system with pure H_2O added. This points to

a slow exchange of protons for deuterons as a possible cause, which is likely a result of an inability of bulk water to interact with bound, structured D_2O at the protein surface.

3.5 References

1. Zu, X., Lu, Z., Zhang, Z., Schenkman, J.B., and Rusling, J.F. (1999). Electroenzyme-Catalyzed Oxidation of Styrene and cis-β-Methylstyrene Using Thin Films of Cytochrome P450cam and Myoglobin Langmuir *15*, 7372-7377.
2. Nassar, A.-E.F., Zhang, Z., Hu, N., Rusling, J.F., and Kumosinski, T.F. (1997). Proton-Coupled Electron Transfer from Electrodes to Myoglobin in Ordered Biomembrane-like Films. Journal of Physical Chemistry B *101*, 2224-2231.
3. Su, Y.O. (1985). Electrochemistry of metalloporphyrins and their catalytic reduction of oxygen at carbon electrodes. 170 pp.
4. Degrand, C. (1984). Influence of the pH on the catalytic reduction of oxygen to hydrogen peroxide at carbon electrodes modified by an absorbed anthraquinone polymer. Journal of Electroanalytical Chemistry and Interfacial Electrochemistry *169*, 259-268.
5. Bettelheim, A., Kuwana, Theodore (1979). Rotating-ring-disk analysis of iron tetra(N-methylpyridyl)porphyrin in electrocatalysis of oxygen. Anal. Chem *51*, 2257-2260.
6. Marcus, R.A. (1956). The theory of oxidation-reduction reactions involving electron transfer. Journal of Chemical Physics *24*, 966-978.

7. Dreyer, J.L. (1984). Electron Transfer in Biological Systems: An Overview. Experientia *40*, 653-675.

8. Siddarth, P., and Marcus, R.A. (1993). Electron-transfer reactions in proteins: electronic coupling in myoglobin. Journal of Physical Chemistry *97*, 6111 - 6114.

9. Van Dyke, B.R., Saltman, P., and Armstrong, F.A. (1996). Control of Myoglobin Electron-Transfer Rates by the Distal (Nonbound) Histidine Residue. Journal of the American Chemical Society *118*, 3490-3492.

10. Rusling, J.F.N., Alaa Eldin F. (1993). Enhanced electron transfer for myoglobin in surfactant films on electrodes. Journal of the American Chemical Society *115*, 11891-11897.

11. Rusling, J.F., Nassar, Alaa-Eldin F. (1994). Electron Transfer Rates in Electroactive Films from Normal Pulse Voltammetry. Myoglobin-Surfactant Films. Langmuir *10*, 2800-2806.

12. Nassar, A.E.F., Willis, William S.; Rusling, James F. (1995). Electron Transfer from Electrodes to Myoglobin: Facilitated in Surfactant Films and Blocked by Adsorbed Biomacromolecules. Analytical Chemistry *67*, 2386-2392.

13. Bayachou, M., Lin, R., Cho, W., and Farmer, P.J. (1998). Electrochemical Reduction of NO by Myoglobin in Surfactant Film: Characterization and Reactivity of the Nitroxyl (NO-) Adduct. Journal of the American Chemical Society *120*, 9888-9893.

14. Boutros, J., and Bayachou, M. (2004). Myoglobin as an Efficient Electrocatalyst for Nitromethane Reduction. Inorganic Chemistry *43*, 3847-3853.

15. Moser, C.C., Chobot, S.E., Page, C.C., and Dutton, P.L. (2008). Distance metrics for heme protein electron tunneling. Biochimica et Biophysica Acta, Bioenergetics *1777*, 1032-1037.

16. Presswala, L., Matthews, M.E., Atkinson, I., Najjar, O., Gerhardstein, N., Moran, J., Wei, R., and Riga, A.T. (2008). Discovery of bound and unbound waters in crystalline amino acids revealed by thermal analysis. Journal of Thermal Analysis and Calorimetry *93*, 295-300.

17. Lin, J., Balabin, I.A., and Beratan, D.N. (2005). The Nature of Aqueous Tunneling Pathways Between Electron-Transfer Proteins 10.1126/science.1118316. Science *310*, 1311-1313.

CHAPTER IV

FUTURE DIRECTIONS

4.1 Preliminary Results: Full Turnover of iNOSoxy in Ionic Liquids and Production of NO from Substrate L-Arginine with Cofactor Tetrahydrobiopterin

A primary objective of the overall study is to look at elementary steps in the catalytic process, such as charge transfer and catalytic activation of oxygen, under low water, low proton conditions. The culmination point of the research, then, would be to look at how all of the individual steps come together into the complex biocatalytic production of NO from substrate L-arginine in the presence of cofactor tetrahydrobiopterin. In previous sections, we have already discussed that certain elementary steps in this catalytic process are confounded in the near-absence of water and protons, so it may prove difficult to realize the production of NO under these conditions. Many of the preparatory and procedural steps involved in this section have already been outlined in great detail, but a new wrinkle is added with the introduction of substrate L-arginine into the experimental set-up. L-arginine is insoluble in the ionic liquid and cannot be introduced in the same fashion as in earlier aqueous studies[1]. It must be added to the protein-lipid film. This creates a problem with balancing the level of

addition to one that does not change the structure of the film, yet still provides enough substrate to drive catalysis. Using a 200:1 (mol/mol) ratio of L-arginine per heme unit should provide enough substrate to drive a limited reaction, while contributing only about 21% (w/w) to the protein-lipid film.

4.1.1 Experimental

NOS is prepared and purified as mentioned in section 2.3.1.1, where excess glycerol is removed from the system with successive washings. In the case of this particular experimental trial, tetrahydrobiopterin (H_4B) is added to the aqueous dimeric NOS on a 10:1 mol/mole heme basis, and L-arginine is added on a 200:1 mol/mole heme basis, and the system is allowed to equilibrate for four hours. The pyrolytic graphite electrode is prepared by casting 5 μl of 10 mM DDAB[2] and 5 μl of 30 μM iNOSoxy/600 μM H_4B/12 mM L-arginine. The electrode is allowed to dry as described previously**.** To measure and compare the effects of cofactor H_4B and substrate L-arginine, additional electrodes are prepared as above, but without the added cofactor and substrate.

Ionic liquid BMIM BF_4 is dried with 3Å molecular sieves to a water level <0.01%. Ionic liquid is purged with 99.9% purity nitrogen gas for at least 30 min before the experiment and is kept oxygen-free during the experiment, except when oxygen is needed to drive catalysis. Deoxygenated water is added to the ionic liquid as indicated.

4.1.2 Preliminary Results and Discussion

Initial results with iNOSoxy with cofactor and substrate (figure 4.1) show that catalytic current increases after addition of 1.65% water, but at low potential. This indicates that catalysis does not occur to any appreciable degree without water present, and that it is a sluggish process. For comparison, iNOSoxy without cofactor and substrate is also shown.

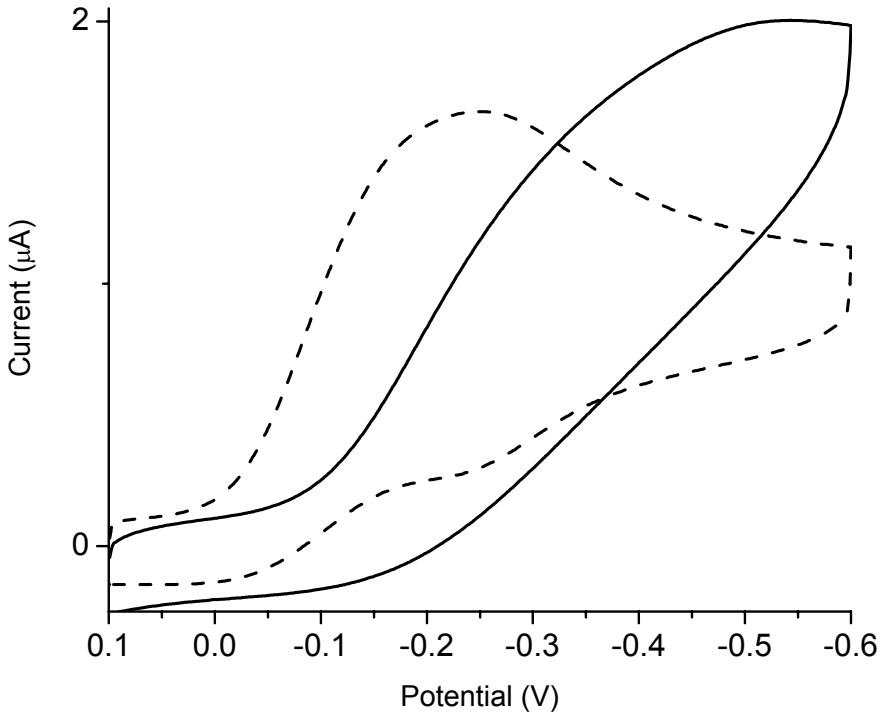

Figure 4.1: iNOSoxy-H_4B-L-arginine electrode in BMIM BF_4 at 1.65% added water (—), vs. iNOSoxy without cofactor and substrate (----) at 1.65% added water.

Figure 4.2 shows the continued increase in peak height as a function of added water. Current in the iNOSoxy sample with substrate and cofactor continues to increase and shift to lower energy with added water, but it is unclear at this stage if the catalytic peak is from production of NO in full turnover, if it is merely catalytic reduction of oxygen, or a combination of both.

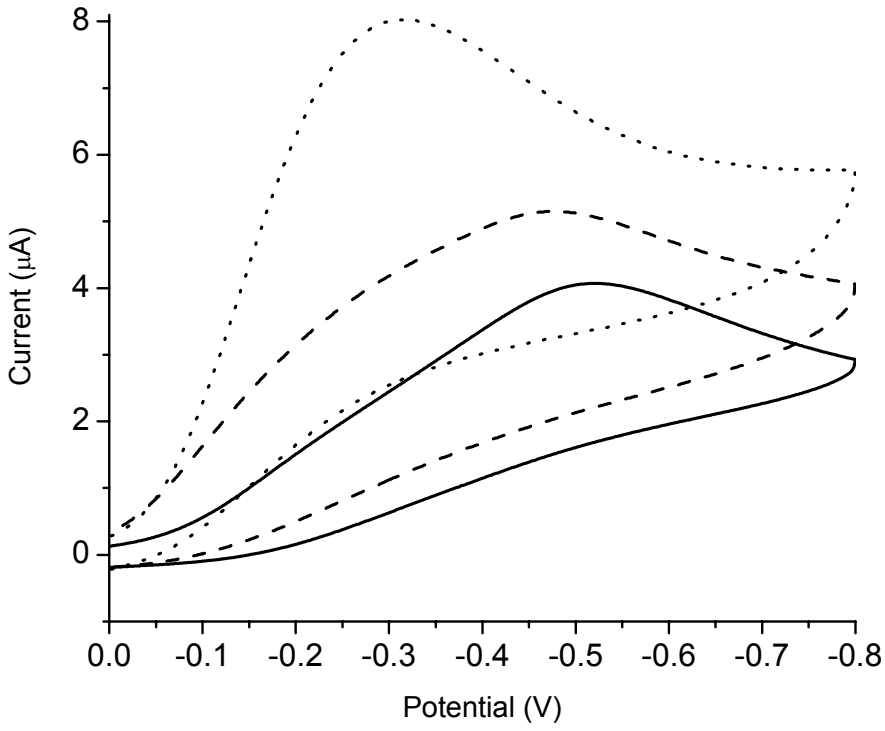

Figure 4.2: iNOSoxy-H4B-L-arginine electrode in BMIM BF_4 at 3.30% added water (—), 5% added water (----), and at 10% added water (····).

Previously, we had worked with concentrations of substrate and co-substrate in excess in order to ensure that any limitations in catalytic reduction are a direct result of the decrease in water/protons. In this study, we have the added variable of substrate L-arginine being in finite supply. As a result, it is currently unclear as to whether the limited catalysis is a result of the water/proton issue being studied or a deficiency of L-arginine. One way to highlight L-arginine as a possible limiting factor is to replace L-arginine with agmatine, a NOS-inhibiting decarboxylated L-arginine analogue that does not support catalytic production of nitric oxide [3, 4].

The results in figure 4.1 indicate a slower catalytic process on the iNOSoxy electrode with added cofactor and substrate as compared to iNOSoxy electrode with added cofactor and substrate. Both cofactor and substrate are documented to support electron transfers[5] and other elementary steps in the NOS catalytic process[6]. Our results show that the presence of water and/or protons is vital for the effect of the cofactor and substrate to take place. There are some aspects of the catalytic peak that need further investigation. Also, the peak potential does not match earlier studies[1] in the NOS-catalyzed production of nitric oxide, yet the peak is also more sluggish than that for simple reduction of oxygen, as was shown in the control NOS-only electrode in figure 4.1. While the Griess assay confirms the presence of limited amounts of NO generated by the catalytic process with added water, uncoupled reduction of oxygen is also a likely cause of catalytic current increase.

At this point, there remain some unanswered questions and there are many opportunities in the future to modify the experimental design. L-arginine supply and availability in the heme pocket is the first and most important modification that comes to mind. It is difficult to interrogate protons as a limiting factor when it is unclear if arginine is also limiting or if the relatively large amounts in the film affects the structure of the film and/or the local response of iNOSoxy in this modified experiment. Experiments with arginine analogues previously mentioned[3, 4] that do not support NOS catalysis are underway to help shed more light on this issue.

4.2 The Catalytic and Redox Properties of Other Significant Metalloproteins Using Ionic Liquids to Simulate Low-Water Environments

Of course, the study of other proton-dependent metalloproteins comes to mind when looking at possibilities for future work in this field. It is of particular interest, because of the nature of the proteins involved and their proton-dependency in their function[7], to study electron transport chain proteins such as NADPH dehydrogenase, cytochrome reductase, and/or cytochrome oxidase, among others.

4.3 References

1. Boutros, J. (2007). Molecular function of nitric oxide synthase (NOS): Direct electrochemical investigation (Cleveland, Ohio: Cleveland State University).

2. Bayachou, M., Lin, R., Cho, W., and Farmer, P.J. (1998). Electrochemical Reduction of NO by Myoglobin in Surfactant Film: Characterization and Reactivity of the Nitroxyl (NO-) Adduct. Journal of the American Chemical Society *120*, 9888-9893.

3. Galea, E., Regunathan, S., Eliopoulos, V., Feinstein, D.L., and Reis, D.J. (1996). Inhibition of mammalian nitric oxide synthases by agmatine, an endogenous polyamine formed by decarboxylation of arginine. Biochemical Journal *316*, 247-249.

4. Komori, Y., Wallace, G.C., and Fukuto, J.M. (1994). Inhibition of purified nitric oxide synthase from rat cerebellum and macrophage by L-arginine analogs Archives of Biochemistry and Biophysics *315*, 213-218.

5. Bayachou, M., and Boutros, J.A. (2004). Direct electron transfer to the oxygenase domain of neuronal nitric oxide synthase (NOS): Exploring unique redox properties of NOS enzymes. Journal of the American Chemical Society *126*, 12722-12723.

6. Alderton, W.K., Cooper, C.E., and Knowles, R.G. (2001). Nitric oxide synthases: Structure, function and inhibition. Biochemical Journal *357*, 593-615.

7. Simon, J., van Spanning, R.J.M., and Richardson, D.J. (2008). The organisation of proton motive and non-proton motive redox loops in prokaryotic respiratory systems. Biochimica et Biophysica Acta (BBA) - Bioenergetics *1777*, 1480-1490.